THE STRUCTURE AND DYNAMICS OF POLYMERS

ADSORBED ONTO SILICA

By

UGO NNENNA ARUA

Bachelor of Science in Chemistry
University of Botswana
Gaborone, Botswana
2010

Submitted to the Faculty of the
Graduate College of the
Oklahoma State University
in partial fulfillment of
the requirements for
the Degree of
DOCTOR OF PHILOSOPHY
May, 2021

THE STRUCTURE AND DYNAMICS OF POLYMERS

ADSORBED ON SILICA

Dissertation Approved:

Dr. Frank D. Blum

Dissertation Adviser

Dr. Darrell K. Berlin

Dr. Sadogopan Krishnan

Dr. Ziad El Rassi

Dr. Elliot Atekwana

ACKNOWLEDGEMENTS

I would like to acknowledge the many people who contributed to the completion of this dissertation. In particular, I would like to thank my advisor Dr. Frank D. Blum. For the many years that he has been my advisor, he has been a great mentor, supporter and teacher. He has taught me to be an independent researcher and has done so with a lot of understanding, humor and kindness. I would also like to thank my advisory committee members, Dr. Krishnan Sadagopan, Dr. Darrel K. Berlin, Dr. Ziad El Rassi, and Dr. Eliot Atekwana for their contributions to this dissertation. I appreciate the time and effort that they put into reading and corrections.

I am grateful to my lab mates, past and present, Dr. Bal Khatiwada, Dr. Charmaine Munro, Dr. Tan Zhang, Dr. Hamid Mortazavian, Dr. Helanka Perera, Dr. Bhishma Sedai, Ishan Niranga, Reza Azarfam, and Joel Coates for their help on very many occasions, their support, suggestions, laughs and for a great group dynamic. I would also like to thank all the faculty and staff members of the Department of Chemistry, Oklahoma State University for being very helpful and friendly.

I would like to thank my friends and family. I am especially grateful to my parents, Dr. Arua E. Arua and Dr. Comfort E. Arua for their love, support, and guidance. They continue to inspire and push me to be better and have made innumerable sacrifices to give me a better life. They also gave me my brothers Eke Nnanna Arua and Awa Enyinnaya Arua who have also been amazing supporters and encouragers. Finally, I would like to thank my Stillwater friends who have brought a lot of joy to me during the writing and researching of this dissertation. I am grateful.

Name: UGO NNENNA ARUA

Date of Degree: MAY, 2021

Title of Study: THE STRUCTURE AND DYNAMICS OF POLYMERS ADSORBED ON SILICA

Major Field: CHEMISTRY

Abstract:

Polymer nano-composites have been studied extentsively due to their large scope of applications. These studies have been undertaken to understand the properties of materials which depend on both of the components, as well as their interfacial properties. In this study, the polymers of interest were poly(lauryl methacrylate), a copolymer – poly(styrene-*r*-methyl methacrylate-d_3), poly(methyl methacrylate), and poly(vinyl pyrrolidone).

The effects of adsorption on poly(lauryl methacrylate) (PLMA), a side-chain crystalline polymer, on silica on its side chain crystallinity were investigated using FTIR and differential scanning calorimetry (DSC) measurements. Adsorption caused a disruption of the side-chain crystallinity in the tightly-bound layer of the polymer without affecting its glass transition temperature. It also changed the packing of the hydrophobic side chains for tightly-bound polymer.

Solid-state deuterium NMR spectroscopy was used to observe the dynamics of bulk and adsorbed poly(styrene-*r*-methyl methacrylate-d_3). The ^{2}H-NMR spectra of adsorbed samples showed significant differences from those of the bulk; decreased segmental mobility of the MMA-d_3 units was clear in all the small adsorbed amounts at all polymer compositions. This work led to the conclusion that methyl methacrylate units preferentially adsorb to the silica surface.

Poly(methyl methacrylate) polymers with different molecular masses were adsorbed on silica and studied using FTIR and temperature modulated DSC. The effect of the surface on the polymer increased with decreasing molecular mass. Lower molecular mass polymers had higher bound fractions indicating that they are more extended on the surface than higher molecular mass polymers. Polymer segments associated with smaller adsorbed amounts showed larger increases in glass transitions and their “loosely-bound” fractions were observed to be more restricted on the surface than those of higher molecular mass polymers

Thermogravimetric analysis (TGA), DSC and FTIR were used to study the thermal behavior of poly(vinyl pyrrolidone) adsorbed on silica. All three of these characterization techniques showed that when adsorbed, PVP showed lower mobility than in the bulk due to attractive hydrogen bonding between the polymer segments and the silica surface.

TABLE OF CONTENTS

Chapter Page

I. INTRODUCTION……..1

II. LITERATURE REVIEW……..8

2.1 Polymer adsorption……...8
2.2 Structure of polymers at the interface……..13
2.3 Glass transition…….….15
2.4 Characterization……...16
2.4.1 Thermogravimetric analysis……..16
2.4.2 Differential scanning calorimetry……..18
2.4.2.1 Temperature modulated differential scanning calorimetry…….19
2.4.2.2 Quasi isothermal differential scanning calorimetry…….....21
2.4.3 Fourier transform infrared spectroscopy…….....23
2.4.3.1 Attenuated total reflectance…….....26
2.4.4 Nuclear magnetic resonance……..27
2.4.4.1 Solid state ^{2}H-NMR……...30
2.5 References……....38

III. DISRUPTIONS IN THE CRYSTALLINITY OF POLY(LAURYL METHACRYLATE) DUE TO ADSORPTION ON SILICA……...48

3.1 Abstract……48
3.2 Introduction……..49
3.3 Experimental……51
3.4 Results……..52
3.5 Discussion……62
3.6 Conclusions……..69
3.7 References……69

IV. DYNAMICS OF METHYL METHACRYLATE SEGMENTS IN POLY(STYRENE-CO-METHYL METHACRYLATE) IN BULK AND AT LOW ADSORBED AMOUNTS ON SILICA……...76

4.1 Abstract…….76
4.2 Introduction……...77
4.3 Experimental…….79
4.4 Results……...81
4.5 Discussion…….95
4.6 Conclusions……..99
4.7 References…….....100

V. THE GLASS TRANSITION OF "LOOSELY BOUND" PMMA ADSORBED ON SILICA IS MOLECULAR MASS DEPENDENT……105

5.1 Abstract……105
5.2 Introduction……..106
5.3 Experimental……...…….108
5.4 Results……..112
5.5 Discussion……120
5.6 Conclusions……..124
5.7 References……125

VI. ADSORPTION OF POLY(VINYL PYRROLIDONE) ON SILICA……...132

6.1 Abstract……132
6.2 Introduction……..133
6.3 Experimental……134
6.4 Results……..136
6.5 Discussion……141
6.6 Conclusions……..144
6.7 References……145

APPENDICES……...151

LIST OF TABLES

Table Page

CHAPTER III

1. Bound fractions of adsorbed PLMA on silica……..……..56

2. CH_2 stretching frequencies of bulk and adsorbed PLMA…….……57

3. Calorimetric results for adsorbed samples of PLMA…….……...61

4. Thermal properties of bulk PLMA and PLMA composites…….……62

5. ΔC_p for bulk and adsorbed samples…….……..67

CHAPTER IV

1. The copolymer compositions, weight average molar masses (M_w) and polydispersity inidices (PD) of the synthesized polymers…….……...80

CHAPTER V

1. Molecular masses and tacticities of synthesized PMMA polymers from GPC and 1H-NMR……110

LIST OF FIGURES

Figure Page

CHAPTER II

1. A typical high-affinity polymer adsorption isotherm……..……..11

2. Adsorption of polymer on a surface showing loops, trains and tails……13

3. Adsorbed polymer; tightly bound, loosely bound and mobile……...……..14

4. Block diagram of a thermobalance……...……17

5. Typical modulated temperature profile vs. time in TMDSC…..…….21

6. Mode of operating quasi-isothermal DSC……..…….22

7. Quasi-isothermal DSC experiment……..……....23

8. Schematic diagram of the Michaelson interferometer……..……...25

9. Interaction of light with matter……..……..26

10. Schematic diagram of the penetration of light into the sample using ATR.27

11. The behavior of nuclear spin in the presence of a magnetic field…...……29

12. Quantized energies of nuclei in a magnetic field…...…….30

13. Energy level diagram for a spin of I = 1……...……..31

14. Deuterium NMR spectrum of a single crystal with only one C-D bond orientation…….……..32

15. (a)A histogram of the lines for the C-D bond orientation. (b) Pake powder pattern (both transitions crosshatched…….……...33

Figure

16. NMR lineshapes for different kinds of motions associated with functional groups……..……35

17. Quadrupole echo pulse sequence……36

CHAPTER III

1. FTIR spectra of Cab-O-Sil M5P silica and PLMA-silica in the silanol region. (b) FTIR spectra of bulk and adsorbed PLMA samples in the 1760-1660 cm^{-1} region…..…….54

2. Fitting of the FTIR-ATR carbonyl peak with free and bound components for the 0.74 mg/m^2 adsorbed amount sample…….……...56

3. FTIR spectra of PLMA in bulk and different adsorbed amounts on silica (in mg/m^2) with the neighboring silica peaks subtracted in the 770-700 cm^{-1} range. (b) FTIR spectrum of only 0.74 mg/m^2 bound amount in the 770-700 cm^{-1} range…….. 58

4. (a) DSC thermograms of bulk and adsorbed PLMA samples (mg/m^2) (b) Derivative heat flow rate curves of the bulk polymer and adsorbed polymer samples in the glass transition region…….…….. 60

CHAPTER IV

1. Experimental (solid) and simulated (dashed) ^{2}H-NMR quadrupole echo spectra for bulk samples of A) PMMA-d_3, B) PS-*r*-PMMA-d_3 71% MMA-d_3, C) PS-*r*-PMMA-d_3 50% MMA-d_3, D) PS-*r*-PMMA-d_3 26% MMA-d_3, and E) PS-*r*-PMMA-d_3 10% MMA-d_3 as a function of temperature.....82

2. Distributions of jump rates used to fit the experimental spectra of bulk homo- and copolymer.……84

3. ^{2}H-NMR quadrupole echo spectra for bulk and adsorbed (2.12 mg/m^2 and 1.02 mg/m^2) PMMA-d_3 samples as a function of temperature…...……85

4. ^{2}H-NMR quadrupole echo spectra for bulk and adsorbed (1.79 mg/m^2 and 1.00 mg/m^2) PS-*r*-PMMA-d_3 71% MMA-d_3 samples as a function of temperature……..86

5. ^{2}H-NMR quadrupole echo spectra for bulk and adsorbed (1.89 mg/m^2 and 0.95 mg/m^2) PS-*r*-PMMA-d$_3$ 51% MMA-d$_3$ samples as a function of temperature……...……...87

6. ^{2}H-NMR quadrupole echo spectra for bulk and adsorbed (2 mg/m^2 and 0.98 mg/m^2) PS-r-PMMA-d$_3$ 26% MMA-d$_3$ samples as a function of temperature……..89

7. ^{2}H-NMR quadrupole echo spectra for bulk and adsorbed (2.24 mg/m^2 and 0.96 mg/m^2) PS-*r*-PMMA-d$_3$ 10% MMA-d$_3$ samples as a function of temperature……..90

8. Distributions of jump rates used to fit the experimental spectra of adsorbed (~ 2 mg/m^2) homo- and copolymers…...…….91

9. Distributions of jump rates used to fit the experimental spectra of adsorbed (~ 1 mg/m^2) homo- and copolymers……...…….92

10. ^{2}H-NMR quadrupole echo spectra of bulk and adsorbed (~2 mg/m^2 and ~1 mg/m^2) of PMMA-d$_3$ and PS-*r*-PMMA-d$_3$ copolymers as a function of the polymer composition and adsorbed amount at 160 ºC…...……93

11. <log *k*> of the bulk (●) and adsorbed, 2 mg/m^2 (○) and 1 mg/m^2 (×), homo- and copolymers as a function of temperature for different polymer compositions….....……95

CHAPTER V

1. (a) FTIR spectra of PMMA (4990 g/mol) adsorbed samples (b) FTIR spectra of PMMA (4990 g/mol) adsorbed samples in the 1550 to 1800 cm-1 region……..……112

2. FTIR spectra of adsorbed PMMA on silica (Cab-O-Sil M5) as a function of molecular mass at different adsorbed amounts (a) 0.5 mg/m2 and (b) 1.5 mg/m2…….……...114

3. Bound fraction of carbonyl groups as a function of molecular mass for (a) M5 silica (200 m2/g) and (b) EH-5 silica (380 m2/g) at 0.5 and 1.5 mg/m2…….....……...115

4. Derivative heat flow rate curves of the bulk polymer (4990 g/mol) and adsorbed polymer samples (on 200 m2/g silica) in the glass transition region…….116

5. Derivative heat flow rate curves of the bulk polymer (20400 g/mol) and adsorbed polymer samples (on 200 m2/mg silica) in the glass transition region……..117

6. Derivative heat flow rate curves of the bulk polymer (38800 g/mol) and adsorbed polymer samples (on 200 m2/g silica) in the glass transition region……..118

7. Derivative heat flow rate curves of the bulk polymer (181000 g/mol) and adsorbed polymer samples (on 200 m2/g) in the glass transition region…….119

8. Schematic illustration of high molecular mass and low molecular mass PMMA adsorbed on silica…….124

CHAPTER VI

1. Decomposition profiles of bulk and adsorbed PVP obtained via thermogravimetric analysis……...……137

2. FTIR spectra of adsorbed PVP samples in the (a) isolated silanol group region (4000 – 3400 cm^{-1}) and the (b) carbonyl group region (1800 to 1550 c..……..138

3. (a) Fitting of PVP adsorbed sample (0.49 mg/m^2) into peaks corresponding to free and bound carbonyl peaks (b) plot of relationship between adsorbed amount and ratio of intensities relating free to bound carbonyl groups…….140

4. Derivative reversing heat flow curves of bulk and adsorbed PVP…141

CHAPTER I

INTRODUCTION

The ubiquitous use of polymers in modern day society has contributed to the need to understand and tailor their properties and characteristics. Polymers are large molecules that are made from smaller molecules (called monomers) through covalent bonding.[1] The monomers of which they are comprised dictate the final properties of the polymer. The large number of monomers available means that there are many potential polymers possible with properties that can be customized depending on the applications for which they are intended.[2,3] The glass transition is one of most important and most investigated of a polymer's properties; it is the temperature at which a polymer goes from being glassy (hard, brittle) to being rubbery (soft, flexible) and determines the applications for which the polymer can be used.[1,4]

A number of studies have focused on understanding the factors that affect the glass transition of a polymer. Polymer tacticity (local stereochemistry) is one such factor. The glass transition temperatures of vinyl polymers have been found to vary with tacticity if neither of the dissimilar constituents is hydrogen.[5] The effect of tacticity has also been observed in poly(n-alkyl methacrylate) polymers where a difference in tacticity

can result in an 80 °C change in the glass transition.[6] The presence and lengths of side chains can also have a significant impact on the glass transition. In poly(n-alkyl methacrylates), the glass transition is seen to decrease with increasing chain length as a result of internal plasticization.[7] Polymer crystallinity is another such factor. The crystalline regions are found to constrain the amorphous phase and thus influence the glass transition dynamics. This has been seen in poly (L-lactic acid),[8] copoly(γ,DL-glutamate)s,[9] poly(lauryl methacrylate),[10] poly(L-lysine)[11] and N-alkylated poly(*p*-benzamide)[12] polymers among others.

Polymers are often used in composite materials which consist of the polymeric material and an inorganic filler material used to reinforce the polymer, which result in improved properties.[4,13] Carbon,[14-16] layered silicates,[17] and nanoparticles such as silica, titania[18] and alumina have all been used as nanofillers. Studies have shown that polymers in these systems can have glass transitions different from those in the bulk.[19-21] The adsorption of polymers onto the surfaces of such filler materials can result in either an increase or decrease in the T_g depending, among other things, on the type of interaction present between the polymer and the filler.[20,22] Changes in the properties of polymers in these nanocomposite systems are due to the modification of the structure and dynamics of polymer near the particle surface. The large surface area of nanofillers makes it so that this interphase of polymer contributes greatly to the properties of the whole composite material.[13]

Great strides have been made towards understanding the dynamics of polymers in the glass transition region under different conditions, but there is still much to learn as the glass transition of polymers remains a relatively poorly understood phenomenon.[23]

Fortunately, technological advances in characterization techniques have allowed for the determination of more information about polymers at the interface. A number of techniques can be used to obtain information about different aspects of the polymer. These techniques include ellipsometry,[24] dielectric relaxation,[25] x-ray reflectivity,[26] x-ray diffraction (XRD),[27] electron paramagnetic resonance (EPR),[28] NMR[29] and calorimetry,[30] among others.

This dissertation aims to, using the techniques highlighted, determine the impact of the structure of the polymer on its adsorption onto silica, and conversely, to determine how adsorption changes the properties of the polymers. Different polymer-composite systems have been studied. The first study determines how the crystallinity of a long side chain containing polymer, poly(lauryl methacrylate) was affected by its adsorption. The properties of poly(methyl methacrylate) in bulk and on silica were probed. Related to this, the effect of polymer composition and adsorption on a poly(methyl methacrylate)-polystyrene copolymer were studied. The methyl methacrylate units were deuterated and their dynamics were observed using solid-state NMR in combination with FTIR and DSC. Lastly, poly(vinyl pyrrolidone) adsorbed on silica was studied using quasi-isothermal DSC and the behaviors were modelled using various models. These studies aim to shed light on the relationship between polymer dynamics upon adsorption and polymer composition.

References

(1) Erber, M.; Tress, M.; Eichhorn, K.-J.: Glass transition of polymers with different architectures in the confinement of nanoscopic films. In *Ellipsometry of Functional Organic Surfaces and Films*; Hinrichs, K., Eichhorn, K.-J., Eds.; Springer Berlin Heidelberg: Berlin, Heidelberg, 2014; pp 63-78.

(2) Li, H.; Lee, T.; Dziubla, T.; Pi, F.; Guo, S.; Xu, J.; Li, C.; Haque, F.; Liang, X.-J.; Guo, P. RNA as a stable polymer to build controllable and defined nanostructures for material and biomedical applications. *Nano Today* **2015**, *10*, 631-655.

(3) Lee, C. C.; MacKay, J. A.; Fréchet, J. M. J.; Szoka, F. C. Designing dendrimers for biological applications. *Nat. Biotechnol.* **2005**, *23*, 1517-1526.

(4) Stevenson, C. S.; Curro, J. G.; McCoy, J. D. The glass transition temperature of thin films: A molecular dynamics study for a bead-spring model. *J. Chem. Phys.* **2017**, *146*, 203322.

(5) Karasz, F.; Bair, H.; O'reilly, J. Thermal properties of atactic and isotactic polystyrene. *J. Phys. Chem.* **1965**, *69*, 2657-2667.

(6) Goode, W.; Owens, F.; Fellmann, R.; Snyder, W.; Moore, J. Crystalline acrylic polymers. I. Stereospecific anionic polymerization of methyl methacrylate. *J. Polym. Sci., Part A: Polym. Chem.* **1960**, *46*, 317-331.

(7) Rogers, S.; Mandelkern, L. Glass transitions of the poly-(n-alkyl methacrylates). *J. Phys. Chem.* **1957**, *61*, 985-991.

(8) Mano, J. F.; Gómez Ribelles, J. L.; Alves, N. M.; Salmerón Sanchez, M. Glass transition dynamics and structural relaxation of PLLA studied by DSC: Influence of crystallinity. *Polymer* **2005**, *46*, 8258-8265.

(9) Morillo, M.; Martínez de Ilarduya, A.; Muñoz-Guerra, S. Copoly(γ,dl-glutamate)s containing short and long linear alkyl side chains. *Polymer* **2003**, *44*, 7557-7564.

(10) Hempel, E.; Huth, H.; Beiner, M. Interrelation between side chain crystallization and dynamic glass transitions in higher poly(n-alkyl methacrylates). *Thermochim. Acta* **2003**, *403*, 105-114.

(11) Krikorian, V.; Kurian, M.; Galvin, M. E.; Nowak, A. P.; Deming, T. J.; Pochan, D. J. Polypeptide-based nanocomposite: Structure and properties of poly(L-lysine)/Na+-montmorillonite. *J. Polym. Sci., Part B: Polym. Phys.* **2002**, *40*, 2579-2586.

(12) Shi, H.; Zhao, Y.; Zhang, X.; Zhou, Y.; Xu, Y.; Zhou, S.; Wang, D.; Han, C. C.; Xu, D. Packing mode and conformational transition of alkyl side chains in N-alkylated poly(p-benzamide) comb-like polymer. *Polymer* **2004**, *45*, 6299-6307.

(13) Sargsyan, A.; Tonoyan, A.; Davtyan, S.; Schick, C. The amount of immobilized polymer in PMMA SiO2 nanocomposites determined from calorimetric data. *Eur. Polym. J.* **2007**, *43*, 3113-3127.

(14) Chen, G.; Wu, C.; Weng, W.; Wu, D.; Yan, W. Preparation of polystyrene/graphite nanosheet composite. *Polymer* **2003**, *44*, 1781-1784.

(15) Kotsilkova, R.; Nesheva, D.; Nedkov, I.; Krusteva, E.; Stavrev, S. Rheological, electrical, and microwave properties of polymers with nanosized carbon particles. *J. Appl. Polym. Sci.* **2004**, *92*, 2220-2227.

(16) Thostenson, E. T.; Ren, Z.; Chou, T.-W. Advances in the science and technology of carbon nanotubes and their composites: a review. *Compos. Sci. Technol.* **2001**, *61*, 1899-1912.

(17) Alexandre, M.; Dubois, P. Polymer-layered silicate nanocomposites: preparation, properties and uses of a new class of materials. *Mater. Sci. Eng., R* **2000**, *28*, 1-63.

(18) Mark, J. E. Ceramic-reinforced polymers and polymer-modified ceramics. *Polym. Eng. Sci.* **1996**, *36*, 2905-2920.

(19) Blum, F. D.; Young, E. N.; Smith, G.; Sitton, O. C. Thermal analysis of adsorbed poly(methyl methacrylate) on silica. *Langmuir* **2006**, *22*, 4741-4744.

(20) Kabomo, M. T.; Blum, F. D.; Kulkeratiyut, S.; Kulkeratiyut, S.; Krisanangkura, P. Effects of molecular mass and surface treatment on adsorbed poly(methyl methacrylate) on silica. *J. Polym. Sci., Part B: Polym. Phys.* **2008**, *46*, 649-658.

(21) Keddie, J. L.; Jones, R. A. L.; Cory, R. A. Size-dependent depression of the glass transition temperature in polymer films. *Europhys. Lett.* **1994**, *27*, 59.

(22) Mataz, A.; Gregory, B. M. Effects of confinement on material behaviour at the nanometre size scale. *J. Phys.: Condens. Matter* **2005**, *17*, R461.

(23) Dudognon, E.; Bernès, A.; Lacabanne, C. Nature of molecular mobility through the glass transition in poly(n-alkyl methacrylates): a study by dielectric spectroscopies. *J. Macromol. Sci. Part B Phys.* **2004**, *43*, 591-604.

(24) Keddie, J. L.; Jones, R. A. L.; Cory, R. A. Interface and surface effects on the glass-transition temperature in thin polymer films. *Faraday Discuss.* **1994**, *98*, 219-230.

(25) Fukao, K.; Miyamoto, Y. Glass transition temperature and dynamics of α-process in thin polymer films. *Europhys. Lett.* **1999**, *46*, 649.

(26) Wallace, W.; Van Zanten, J.; Wu, W. Influence of an impenetrable interface on a polymer glass-transition temperature. *Phys. Rev. E* **1995**, *52*, R3329.

(27) Zhang, K.; Gui, Z.; Chen, D.; Jiang, M. Synthesis of small polymeric nanoparticles sized below 10 nm viapolymerization of a cross-linker in a glassy polymer matrix. *Chem. Commun.* **2009**, 6234-6236.

(28) Robb, I. D.; Smith, R. Adsorption of polymers at the solid-liquid interface: a comparison of the e.p.r. and i.r. techniques. *Polymer* **1977**, *18*, 500-504.

(29) Metin, B., Okuom, M., Blum, F. Dynamics of adsorbed PMA-d3 - effect of substrate. *Polym. Prepr.* **2008**, *49*.

(30) Porter, C. E.; Blum, F. D. Thermal characterization of PMMA thin films using modulated differential scanning calorimetry. *Macromolecules* **2000**, *33*, 7016-7020.

CHAPTER II

LITERATURE REVIEW

2.1. Polymer adsorption

Polymer composites are often used in multicomponent materials including polymer blends, plasticized polymers and adsorbed polymers.[1] These materials are often found to have superior properties to their corresponding bulk polymers.[2] How they perform in different applications depends on their properties and the interactions of these components, particularly at the interfaces, where they come into contact.[3] These materials combine the advantages of inorganic materials like rigidity and thermal stability, with those of organic polymers such as flexibility and ductility.[3] This is especially true of nanocomposites, where the small size of fillers leads to a dramatic increase in interfacial area and polymer properties.[4] An understanding of the dynamics of these materials is important for the improvement of properties and for the development of novel materials. Of particular interest is how polymers act at the interfaces in adsorbed polymer systems. The behavior of polymers at interfaces has been studied quite extensively[5] and will be discussed.

Adsorption is defined as an increase in the concentration of a solute in the interfacial region.[5] When there is a chemical bond involved in adsorption, it is called chemisorption. Physisorption involves only physical interactions between the solute and the sorbent. Polymer adsorption is seen in a number of industrial applications such as mineral benefication, where polymers are added for the depression, flocculation, or dispersion of minerals.[6] An important parameter in adsorption is the adsorbed amount which can be defined as the amount of polymer in contact with the surface.[5]

The Langmuir adsorption isotherm which was developed in 1915 by Irving Langmuir can be used to describe the adsorption of polymers from solution onto surfaces.[7] A statistical derivation is done by Adamson and Gast and is described below.[8] The total number of sites for adsorption, S_0, is given by the following equation.

$$S_0 = S_1 + S_2 \tag{1}$$

where S_1 is the number of unoccupied sites and S_2 is the number of occupied sites. If the rate of adsorption is proportional to the number of unoccupied sites, S_1, and the pressure of the gas and the rate of desorption is proportional to the number of occupied sites, then at equilibrium, the rates of adsorption and desorption are equal yielding the following expression.

$$k_1 S_1 p = k_1 p(S_0 - S_2) = k_2 S_2 \tag{2}$$

Dividing the above expression by S_0 yields the following expression which constitutes the Langmuir adsorption isotherm.

$$\theta = \frac{pb}{1 + pb} \tag{3}$$

where $b = K_1/K_2$ is called the Langmuir constant and θ is the fraction of surface covered and is equal to S_2/S_0. The Langmuir isotherm can be used to describe the adsorption of polymers from solution onto the surface of a substrate and can be expressed in *mg of polymer adsorbed per* m^2 of the surface.

A typical adsorption isotherm for a monodisperse polymer is shown in Figure 1 below. Typically, adsorption occurs at very low concentrations below 1 g m^{-3}. For higher concentrations, one often observes plateau which indicates the saturation of the surface. The isotherm shown in Figure 1 is typical of a high-affinity polymer-surface isotherm. As the polydispersity of the polymer increases, the plateau becomes less well-defined and more rounded. The plateau adsorbed amount can reach values of a few mg/m^2 and is a function of the molecular mass, i.e. higher molecular masses typically give higher plateau values.[5]

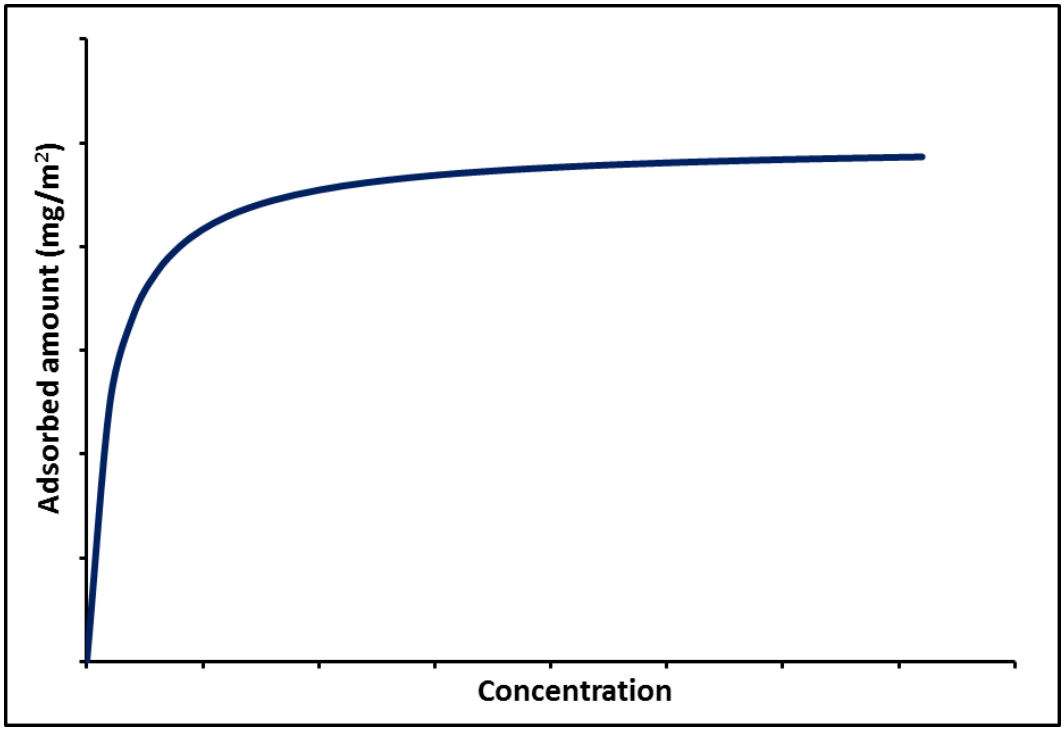

Figure 1. A typical high-affinity polymer adsorption isotherm.

A number of factors affect how polymers adsorb onto surfaces.[6] The first factor is the nature of the adsorbent. The characteristics of the solid surface (surface charge, degree of solvation) can be affected by the solvent properties and temperature of the system. A commonly used surface is that of silica. Nanosilica powder, for example, has a very large surface area and a smooth non-porous surface for strong physical contact making it ideal for use as an adsorbent.[9] Solubility of the adsorbent is also an important factor as dissolution may result in detachment. In addition to the adsorbent chemical properties, the physical properties such as porosity and particle size also play significant roles in adsorption. The second factor is the chemical nature of the polymer relative to the solid surface. This is highlighted by the observation that a polar functional group will interact favorably with a hydrophilic site. The molecular mass of the polymer is the third

factor in adsorption. For non-porous adsorbents, polymer adsorption increases with molecular mass. For a good solvent, there is a weak dependence of adsorbed amount on molecular mass, while a poor solvent shows a square root dependence. The behavior of a polymer in the bulk or at the interface depends on the polymer solvent interaction which can be defined by the Flory Huggins parameter.[6] In general, there is a decrease in adsorption with an increase in solvent compatibility although the temperature dependence may vary. The effect of temperature on the solubility of the polymer and the state of solvation of the surface and the polymer play a significant role in polymer adsorption.

Adsorption of polymers on a solid surface results in a loss of conformational entropy for the polymer. Localization at the solid surface also means a loss in translational entropy. At the same time, adsorption may be followed by the displacement of many small molecules from the surface resulting in a net positive entropy.[6] The favorable adsorption energy for a polymer segment over a solvent molecule can be characterized by a dimensionless energy parameter, χ_s which is described by equation 4 below.

$$\chi = \frac{(U_{1a} - U_{2a})}{k_B T} \tag{4}$$

where U_{ia} is the adsorption energy of species *I*, *1* being solvent and *2* a polymer segment. A positive value of χ provides a driving force for polymer adsorption.[10]

2.2. Structure of polymers at the interface

The adsorption of polymers results in a change in their shape. The most typically used description of polymer conformation at an adsorbing interface was first proposed by Jenkel and Rumbach.[11] It is described in terms of 3 sub-chains illustrated in Figure 2 and consists of trains which have all their segments in contact with the substrate, loops have no contacts with the surface and connect two trains and tails which are non-adsorbing chain ends.[5]

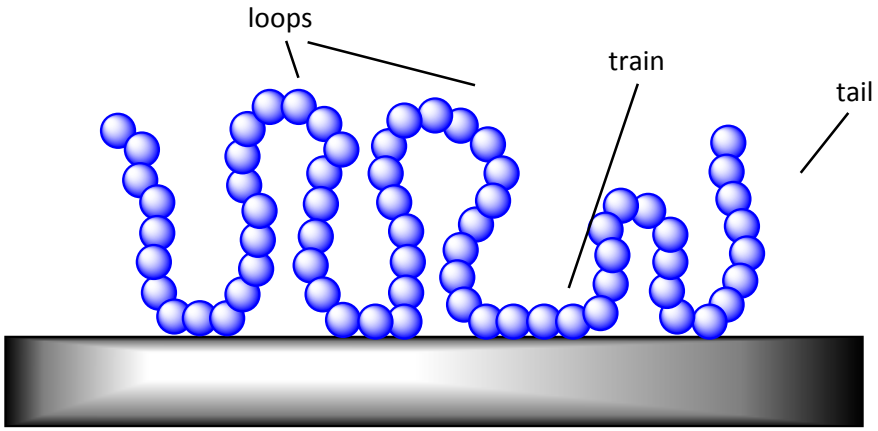

Figure 2. Adsorption of polymer on a surface showing loops, trains and tails.

The behavior of polymers at interfaces has been studied for quite some time as have the impact of the surface on polymers.[5] In some cases, adsorption on the surface results in a significant difference in the segmental dynamics and glass transition of the polymer.[12] In other cases, despite the evidence of bound polymer, the glass transition is largely unaffected.[13] Generally, the properties of surface bound polymers have been shown to be different from those of bulk polymers.[2] The increases in glass transition observed can be due to interaction of the polymer with attractive surfaces.[14-16] On the

other hand, in the absence of strong interactions, there is sometimes a reduction of glass transition.[17]

It has been shown that there are distinct regions in adsorbed polymers where there is a positive interaction.[16] One can describe regions or sections of the adsorbed polymer according to the distance from the surface.[18] The layer closest to the surface is described as *tightly bound* and has reduced mobility mainly due to trains which are directly attached to the surface. Studies have shown that this layer of adsorbed polymer is most affected by the surface and has significantly higher glass transition temperatures due to hydrogen bonding between surface silanols and carbonyl groups.[18-22] The layer above the tightly bound layer is called the *loosely bound* polymer and consists of loops; this layer of polymer shows only a slightly increased glass transition temperature relative to the bulk and is sensitive to the adsorbed amount. The polymer at the air interface is called the mobile layer. This polymer is thought to be more mobile than bulk polymer. Though it has not been observed for many polymers, it has been seen for PVAc with a glass transition temperature slightly less than that of the bulk polymer.[23] These layers are illustrated in Figure 3 below.

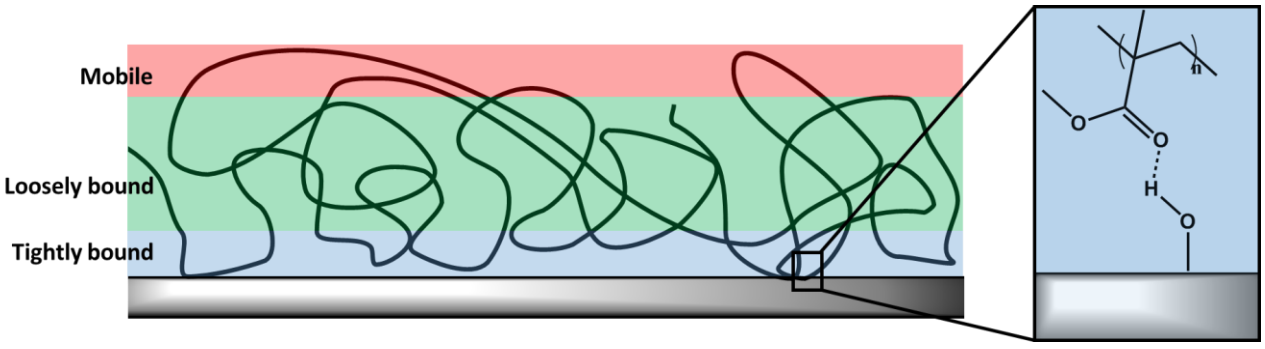

Figure 3. Adsorbed polymer; tightly bound, loosely bound and mobile

2.3. Glass transition

The glass transition temperature is the temperature at which an amorphous polymer, when cooled in the liquid (rubbery state), transitions to the solid state (glassy) without undergoing crystallization.[24] It has also been described as a second order transition that originates from kinetic limitations on the rates of internal adjustments caused by changes in temperature. A number of factors affect the glass transition temperature. Molecular mass is one factor that has an impact on the glass transition of amorphous polymers.[24] The relationship between molecular mass and the glass transition temperature is given by the equation (5).[25-28]

$$T_g = T_{g\infty} - \frac{K}{M_n} \tag{5}$$

where T_g is the glass transition temperature observed for a polymer with a molecular mass M_n, $T_{g\infty}$ is the glass transition temperature when the polymer molecular mass is infinite. K is a constant whose units are K mol g^{-1}. The thermal properties of polymers are affected by chemical crosslinking, the main chain rigidity and crosslinking density.[29] Stereochemistry can be a factor in the glass transition of polymers. This is illustrated clearly in the difference between isotactic and syndiotactic poly(methyl methacrylate). Syndiotactic PMMA has a glass transition about 80 degrees higher than that of isotactic PMMA.[30-32] Larger differences are seen between syndiotactic and isotactic polymers of the same chemical species in the lower members of the poly(n-alkyl methacrylate) series. As the size of the alkyl group attached to the ester increases, the differences in temperature between the glass transitions of syndio- and isotactic polymers decrease. On

the other hand, other polymers show little difference between the syndiotactic and isotactic polymers. This is the case for polystyrene and polypropylene.[30]

2.4. Characterization

There are a number of techniques that can be used to characterize polymers on the surface. Adsorbed polymers present a unique challenge due to how thin the interfacial layer is.[33] Fortunately, there are still some techniques that can be used to obtain a picture of what is happening at the surface. The methods used for characterization include ellipsometry,[14] neutron reflectometry,[34] thermal analysis,[35] electrophoresis[36,37] FTIR[38,39] and NMR[40-42] to name a few. The characterization techniques most relevant to this dissertation are outlined as follows.

2.4.1. Thermogravimetric analysis

Thermogravimetric analysis (TGA) is a technique that is used to measure the mass of a material as the temperature changes under a controlled temperature program in a controlled environment.[43] A number of important thermal events can cause changes in sample mass and these include desorption, adsorption, sublimation, vaporization, oxidation, reduction, and decomposition.[44] This type of analysis is typically carried out between ambient temperatures and, say 1000 °C and using either inert (nitrogen, argon, helium) or oxidative (oxygen, air) gases.

The core of the TGA is the thermobalance which measures mass as a function of temperature and time[45] and consists of an electronic microbalance, a furnace, temperature

controller, and a computer to simultaneously record output from these devices as illustrated in Figure 4.[44]

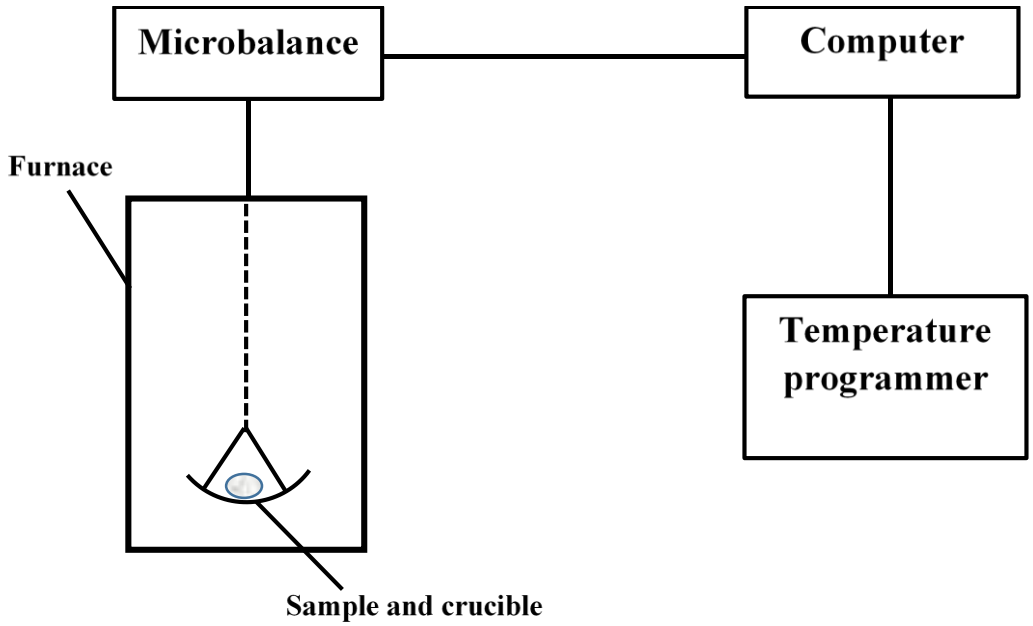

Figure 4. Block diagram of a thermobalance[44]

TGA has been used to study the pyrolysis of polymers at constant heating rates[46-49] allowing the thermal stability of polymers to be determined. The decomposition processes are generally free-radical processes grouped into three categories: random scission, unzipping, side group elimination.[48] In addition, TGA is often used to obtain quantitative information about the compositions of polymeric composites since the components of such materials can be separated by decomposition temperature. Inorganic additives are typically stable at very high temperatures. A TGA scan of most organic polymer composites would typically show a mass loss below 300 °C due to volatile components such as water, and monomer. Mass loss between 300 and 550 °C would be attributed to polymer degradation while the residues would be associated with inorganic

compounds such as silica.[45] This method provides an accurate way to determine the proportion of polymer present in polymer composites sometimes denoted as the adsorbed amount. This quantity can be calculated using equation (6).

$$AA\left(\frac{mg}{m^2}\right) = \frac{\Delta m}{R \times SA} \quad (6)$$

where *AA* is the adsorbed polymer amount in milligrams per m^2, Δm is the mass loss due to the polymer, *R* is the mass of the inorganic residue and *SA* is the specific surface area of the substrate.

2.4.2. Differential scanning calorimetry

Differential scanning calorimetry (DSC) is widely applied in polymer science. It can be used to determine the melting, crystallization and their associated enthalpy and entropy changes. In addition, it is used for the characterization of the glass transition temperature.[50] DSC is a technique in which the heat flow difference between a sample and a reference is measured as a function of temperature under a controlled temperature program.[51] DSC has also been used in the pharmaceutical field as well as in inorganic and organic chemistry. It is used in particular for the determination of the glass transition temperature, melting and crystallization, as well as heats of reaction. In addition to its other benefits, DSC can be used for small sample amounts as only milligram quantities are needed for analysis.

There are two types of DSC instruments; heat flux and power compensation. Heat flux DSC consists of a cell with sample and reference holders which are separated by a bridge which acts as a heat leak and are also surrounded by a block that is housed in a

constant-body temperature body. The block houses the heater, sensors, and holders. The differential behavior of the sample and reference is used to determine the thermal properties of the sample. There is a temperature sensor in the base of each platform. Power compensation DSC, on the other hand, has two separate and identical holders each with its own heater and sensor. The cells are heated at a constant linear rate and the signal is returned from the sensors to the programmer's signal. The temperature difference caused by lag due to a difference in heat capacity is measured.[45]

2.4.2.1. Temperature modulated differential scanning calorimetry

Temperature modulated differential scanning calorimetry (TMDSC) is an extension of DSC where the linear or isothermal heating program is modulated by some form of perturbation. The simplest modulation possible is described by equation (7) below and illustrated in Figure 5.[52] It was introduced by Reading in 1993 and is now known to be very powerful thermal analysis technique.[53,54] The periodic temperature perturbation is superimposed on a linear heating or cooling and takes place around a fixed temperature.[55]

$$Temperature = T_0 + bt + Bsin(\omega t) \tag{7}$$

where T_0 is the starting temperature, ω is the frequency, b is the heating rate and B is the amplitude of temperature modulation. Assuming that the temperature modulation is small and that over the interval of the modulation the response of the rate of the kinetic process to temperature is linear, the equation (7) above can be rewritten as follows:[52]

$$\frac{dQ}{dt} = C_{p,t}(b + B\omega\cos(\omega t)) + f'(t,T) + Csin(\omega t) \tag{8}$$

where $f'(t,T)$ is the average underlying kinetic function once the effect of the sine wave modulation has been subtracted, C is the amplitude of the kinetic response to the sine wave modulation and $(b + B\omega cos(\omega t))$ is the measured quantity dT/dt. Equation (8) above shows that the heat flow signal contains a cyclic component that depends on the value of B, ω and C. The cyclic response of the sample can be separated from its response to the underlying heating rate and these two signals can be separately quantified.[52] This is the most common TMDSC analysis: the separation of the total heat flow into reversing and non-reversing componets.[56] The reversing component of the heat flow is from the amplitude of the first harmonic of the heat flow using a Fourier transform of the data. The division of this by the amplitude of the applied heating rate gives the reversing component of the apparent heat capacity.

The advantage that TMDSC has over standard DSC is that it has improved resolution and sensitivity and can be used to separate overlapping phenomena. This method can be used to separate the total heat flow or apparent heat capacity into reversing and non-reversing components[52,54,56] The accuracy of glass transition temperatures can be affected by complex thermal histories.[57] The T_g depends on many parameters such as the chemical nature of the polymer, its thermal history, different residual stresses. These effects appear in the total heat flow signal from differential scanning calorimetry.[57] The heat flow signal of the total heat flow is very complex. However, using the differential of heat capacity signal can be used to obtain them accurately and simply.

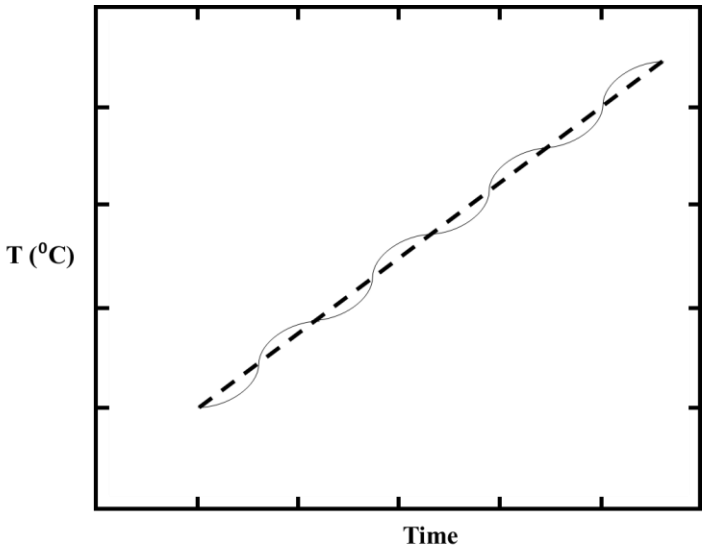

Figure 5. Typical modulated temperature profile vs. time in TMDSC. The dashed line shows the underlying heating rate.

2.4.2.2. Quasi- isothermal differential scanning calorimetry

The mode of modulation of DSC can be varied. One variation of TMDSC is quasi-isothermal MDSC which was developed shortly after TMDSC.[58,59] The underlying heating rate <*q*> is equal to zero, keeping a constant average temperature, T_0 as shown in Figure 6. The modulation amplitude can be varied so that truly isothermal calorimetry of reversible processes at chosen frequencies is possible by extrapolation to zero amplitude.[60] The quasi isothermal mode, which occurs when the average scanning rate is equal to zero, allows the heat capacity of the polymer to be determined with close to equilibrium conditions. These types of experiments allow the measurement of heat capacity in a reproducible manner.

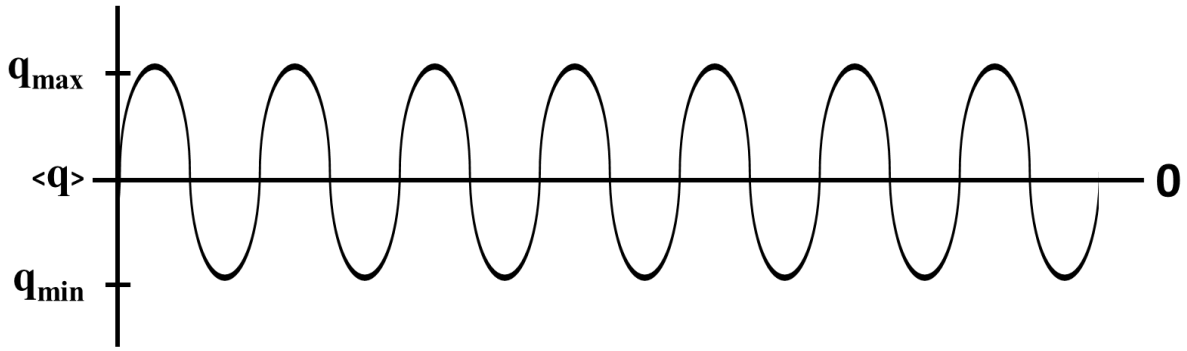

Figure 6. Mode of operating quasi-isothermal DSC

Non-zero values of <q> can be used to exclude repeated, reversing or reversible recrystallization or remelting.[60] The measurement of heat capacity under these practically isothermal conditions can be made using the oscillating temperature T_s and temperature difference ΔT assuming heat capacity is constant over the amplitude of temperature oscillation.[59]

$$(C_s - C_r) = \frac{A_\Delta}{A_{Ts}} \sqrt{\left(\frac{K}{\omega}\right)^2 + {C_r}^2} \qquad (9)$$

where C_s and C_r are the specific heat capacities of the sample and reference, K is Newton's law constant in J/s K, ω is the modulation, and A_Δ and A_{Ts} is the maximum amplitude of the temperature difference and modulated temperature, respectively.

In a quasi-isothermal experiment, a sample is typically heated in intervals, often 10 °C. A sinusoidal modulation is applied so that the average temperature of the sample doesn't change by a significant amount.[61] An example of a heat capacity profile is shown in Figure 7. Following the measurement at one temperature, the sample is heated to the

next temperature. The temperature is increased step-wise and the cycle is repeated to obtain heat capacities at different temperatures.

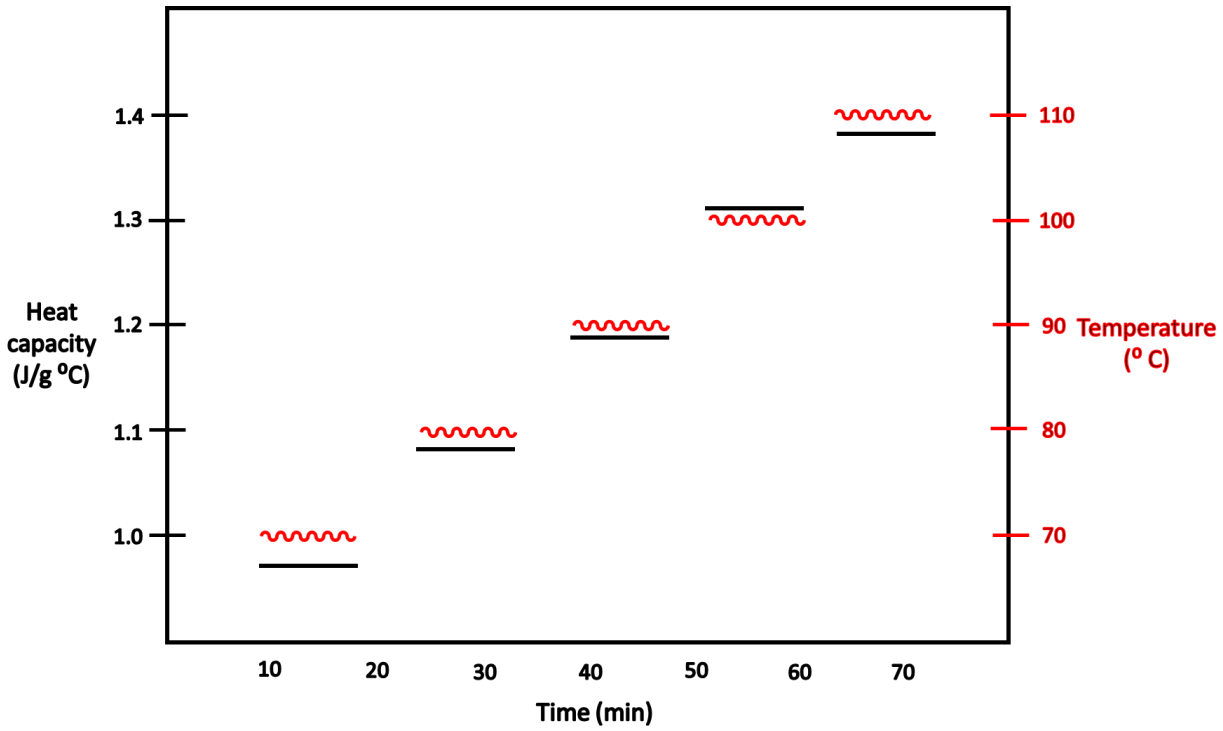

Figure 7. Quasi-isothermal DSC experiment

2.4.3. Fourier transform infrared spectroscopy

Infrared spectroscopy is a commonly used spectroscopic tool for polymer characterization. It is a rapid and sensitive technique which has sampling techniques that are simple and non-destructive. For a given molecule, vibrational modes may give rise to resonant infrared absorption of electromagnetic radiation only when the transition is induced by the interaction of the electric vector of the incident beam with the electric dipole of the molecule. Vibrational frequencies for IR are usually reported in

wavenumbers (cm^{-1}). According to equation (10), wavenumbers are directly proportional to the energy and vibrational frequency of the molecule.

$$\Delta E = hc\nu \ (cm^{-1}) \tag{10}$$

where ΔE_{vib} is the vibrational energy level separation, h is Planck's constant and c is the speed of light. The typical IR region extends from 4000 cm^{-1} to 300 cm^{-1}. The vibrational frequencies of a molecule depend on the nature of the motion and the mass of atoms, geometric arrangements, and the nature of chemical bonding. The vibrational frequency of a stretching mode of a diatomic molecule can be calculated using equation (11) below.

$$\nu \ (cm^{-1}) = \left[k_f \frac{[M_A + M_B]}{M_A M_B} \right]^{1/2} \tag{11}$$

where k_f is the force constant or bond stiffness, M_A and M_B are the masses of the two atoms. The force constant is inversely proportional to the bond length and atom electronegativity as shown in the expression below.

$$k_f \propto N_b \left[\frac{X_A X_B}{d^2} \right]^{3/4} \tag{12}$$

where N_b is the bond order, d is the bond length and X_A and X_B are the electronegativities of atoms A and B, respectively. Increasing the bond stiffness increases the frequency of vibration.[62] The vibrational spectra of diatomic molecules shows only one observable mode. Complex molecules such as polymers would have much more complicated vibrational spectra.

Fourier transform infrared spectroscopy uses the Michaelson interferometer illustrated in Figure 8 as the multiplex optical device. This device can measure spectral information about the intensities at individual frequencies while at the same time measuring the intensities of all frequencies simultaneously using a single detector.[63]

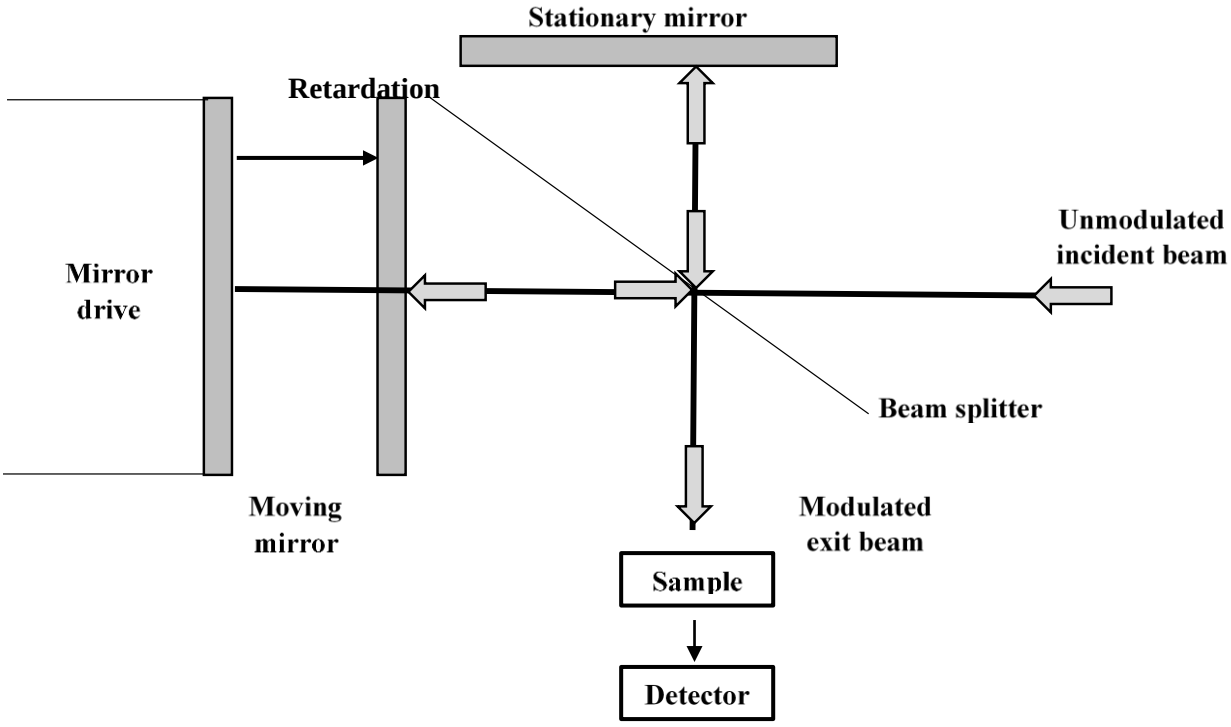

Figure 8. Schematic diagram of the Michaelson interferometer

The Michaelson interferometer works as follows. One arm of the interferometer contains a stationary plane mirror and another arm has a movable mirror. A beam splitter bisects the two arms and divides the source beam into two equal beams that traverse the two arms of the interferometer. These two beams travel down the arms of the interferometer and are reflected back to the beam splitter where they recombine. This beam is then reflected to the detector. All wavelengths of radiation striking the beam splitter after reflection produce an interferogram which is then Fourier transformed.[64]

2.4.3.1. Attenuated total reflectance

IR rays, when they encounter a surface are either reflected, absorbed, transmitted or scattered. Any of these rays can be used to obtain a spectrum of the sample.

$$I_0 = I_T + I_R + I_S + I_A \tag{13}$$

where I_0 is the intensity of the incident ray, I_R is the intensity of the reflected ray, I_S is the intensity of scattered radiation and I_T is the intensity of transmitted radiation.[65]

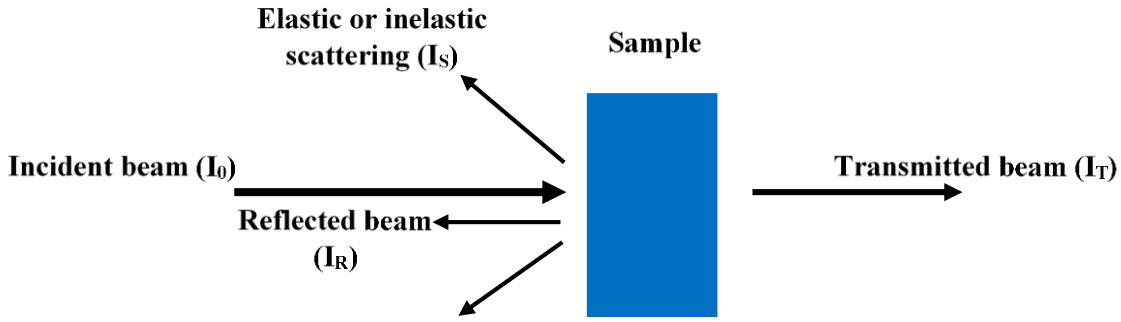

Figure 9. Interaction of light with matter.

Reflected, absorbed, transmitted and scattered light can all be used for sampling. The most commonly used method is transmission spectroscopy which is advantageous in that it has ease of quantification and gives spectra with high signal to noise ratios. ATR is an alternative sampling method which involves the use of a crystal with a high refractive index and low IR absorption in the IR region of interest. The depth of penetration depends on a number of factors including the angle of incidence and the refractive index and can be calculated using equation (14).

$$d_p = \frac{\lambda}{2\pi n_1 \left(sin\,^2\theta - n_{21}^2\right)^{1/2}} \tag{14}$$

where λ is the wavelength of the radiation in air, θ is the angle of incidence, n_1 is the refractive index of the ATR crystal, and n_{21} is the ratio of the refractive index of the sample to that of the ATR crystal. The penetration depth is defined as the distance required for the electric field amplitude to fall to e^{-1} of its value at the surface.[64] This is shown in Figure 10.

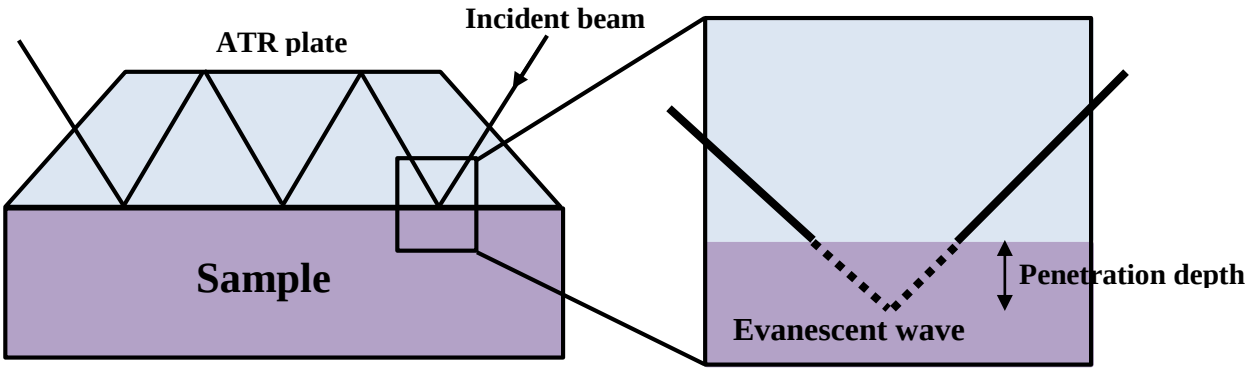

Figure 10. Schematic diagram of the penetration of light into the sample using ATR

2.4.4. Nuclear magnetic resonance

All atomic nuclei possess a fundamental property called nuclear spin, *I*, which has values of 1/2, 1, 3/2, etc. in units of h/2π.[66] Only atomic nuclei with odd numbers of protons or neutrons have a nonzero spin; nuclei with I = 0 have no spin angular momentum and thus have no magnetic moment and cannot be studied using NMR.[66,67] Spin active nuclei behave as if they were spinning on their axes creating a magnetic moment, μ, which aligns in a magnetic field. The nuclear magnetic moment, μ, is given by equation.

$$\mu = \frac{\gamma I h}{2\pi} \qquad (15)$$

where h is Planck's constant, and γ is the gyromagnetic ratio, a constant specific to nuclei.[66]

In the absence of a magnetic field, the orientations of magnetic dipoles are random. When atomic nuclei with nuclear magnetic moments are placed in a uniform magnetic field, B_0, the magnetic moments orient themselves in specific allowed orientations. A nucleus of spin I has $(2I+1)$ possible orientations which are characterized by magnetic quantum numbers. These orientations are determined as shown in Figure 11 (b) and precess with a characteristic frequency call the Larmour frequency which is proportional to the applied magnetic field and is given by:[67,68]

$$\omega_0 = \gamma B_0 \tag{16}$$

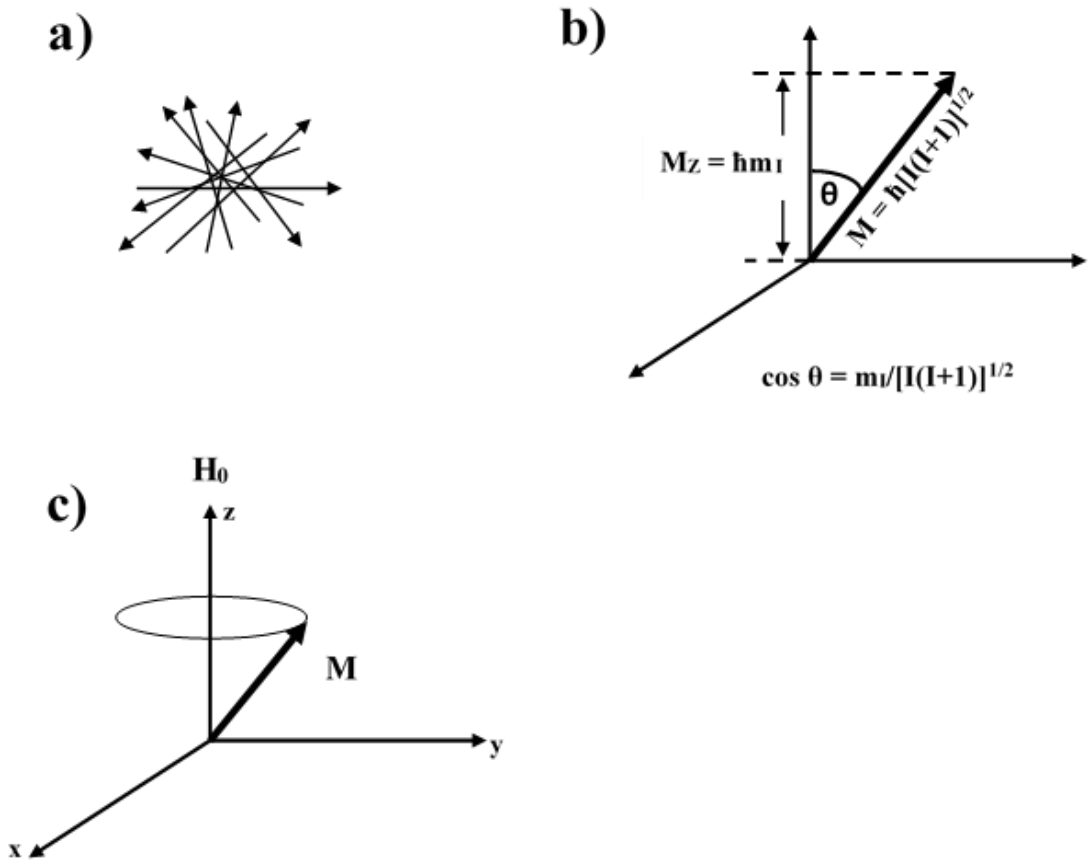

Figure 11. The behavior of nuclear spin in the presence of a magnetic field. (a) Initially the orientation of the spin dipoles is random. (b) The spin dipoles are exposed to a homogeneous magnetic field, where m_I = I, I-1, …., -I. (c) The magnetic moment precesses about the magnetic field at the Larmor frequency.[67,68]

For a nucleus with spin *I*, there are *2I+1* nuclear energy states as shown in Figure 12. Nuclei can be induced into a higher energy state by the absorption of a radiofrequency pulse with the appropriate frequency and strength, $\Delta E = h\nu$.[67]

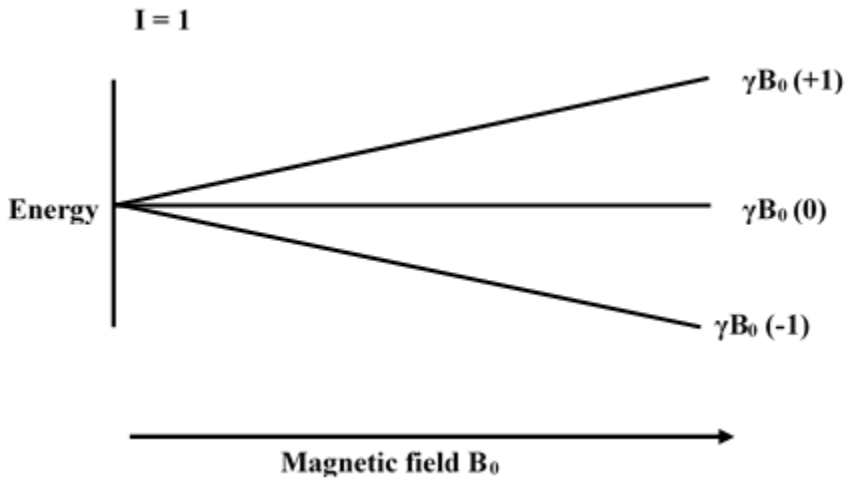

Figure 12. Quantized energies of nuclei in a magnetic field.

2.4.4.1. ^{2}H-NMR solid state

Solid state ^{2}H-NMR is a valuable technique for the characterization of non-crystalline or amorphous materials such as polymers and their composites.[69] This technique is somewhat unique in that it can give both structural and dynamic information at a molecularly resolved level through site-specific ^{2}H labels. In the presence of a magnetic field, deuterium which has a spin of 1, has three quantized energy levels, +1, 0, -1, shown in Figure 12. The deuterium nucleus (like other $I \geq 1$ nuclei) is quadrupolar meaning that it has a non-spherical charge distribution at the nucleus.[70,71] The interaction of this quadrupole moment with the electric field gradient tensor at the nucleus causes a perturbation of the Zeeman splitting.[72] This perturbation dwarfs other NMR nuclear spin interactions such as dipole dipole interactions and chemical shift anisotrophy.[73,74]

$$H_{total} = H_{Zeeman} + H_{quadrupolar} + H_{dipolar} + H_{CSA} \qquad (17)$$

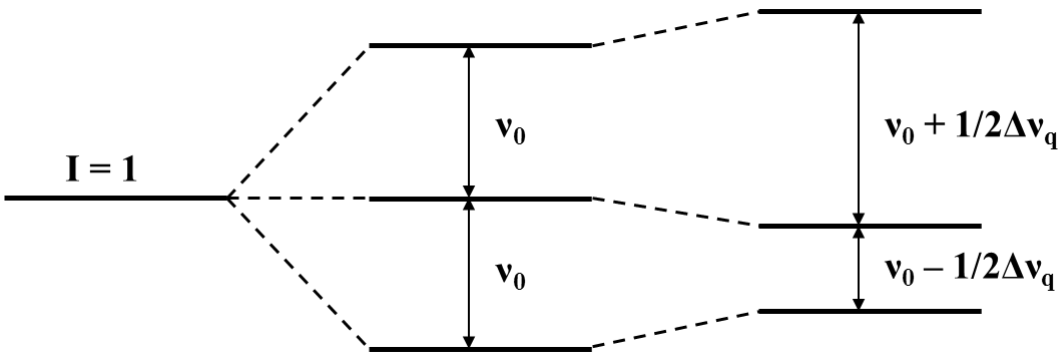

Figure 13. Energy level diagram for a spin of I = 1[72]

Given selection rules of $\Delta m = \pm 1$, there are two allowed transitions for spin ½ nuclei in a magnetic field. The NMR experiment involves causing transitions between these levels by applying energy in the radiofrequency range. This is shown in the Figure 12. For a single crystal with only one C-D bond, the deuterium NMR spectrum would consist of two equally spaced lines about the zero frequency. The separation of these two lines is given by the following equation.[74,75]

$$\omega = \omega_0 \pm \delta(3cos^2\theta - 1 - \eta sin^2\theta\ cos2\varphi) \qquad (18)$$

where $\delta = 3e^2qQ/8\hbar$, where $e^2qQ/\hbar$ is the quadrupole coupling constant, and ω_0 is the Zeeman frequency. The quantity η is the asymmetry parameter, which is usually zero for C-D bonds with axially symmetric electric field gradient tensors. The axis of the electric field gradient tensor is typically along the C-D bond direction. The polar angles θ and φ specify the orientation of the magnetic field with respect to the principal axis system of the electric field gradient tensor. For $\eta = 0$, the NMR frequencies of the transitions are as follows.[74]

$$\omega = \omega_0 \pm \delta(3cos^2\theta - 1) \qquad (19)$$

Thus, the frequencies of the NMR resonances depend on the angles that the C-D bond makes with the external magnetic field. For a single crystal or an oriented system rotated in the magnetic field, different resonances would be obtained for each orientation. Polymers rarely exist as single crystals and typically would yield a powder line shape. This line shape is due to the various C-D bond orientations with respect to the magnetic field.[74]

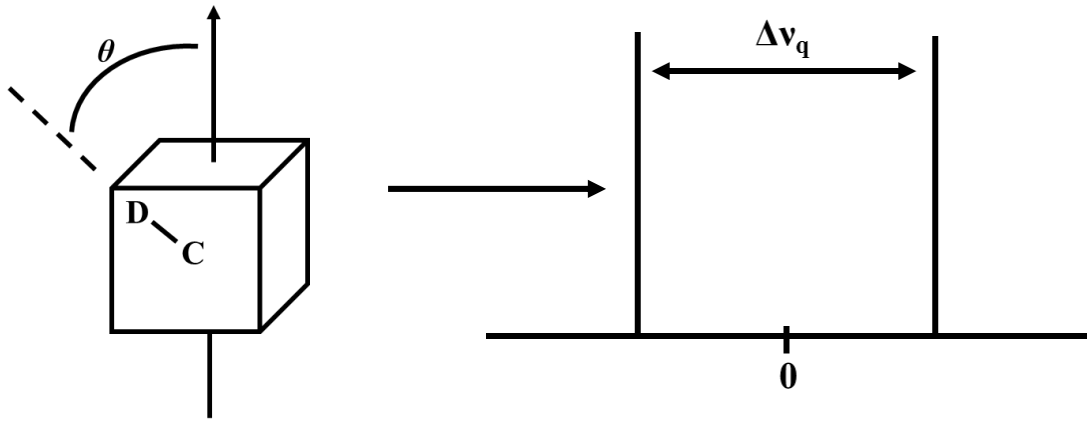

Figure 14. Deuterium NMR spectrum of a single crystal with only one C-D bond orientation

$$\Delta\nu_q = \frac{3}{4}\left(\frac{e^2qQ}{h}\right)(3cos^2\theta - 1) \qquad (20)$$

where $\frac{e^2qQ}{h}$ is the quadrupole coupling constant (QCC), and θ is the angle between the C-D bond and the external magnetic field, B_0. Rotation of the crystal in the magnetic field would cause the two lines to change while molecular motion averages the line positions.[72]

Polymers are typically analyzed as powders, the powder average results in a Pake pattern where the line shape from one transition is cross hatched.

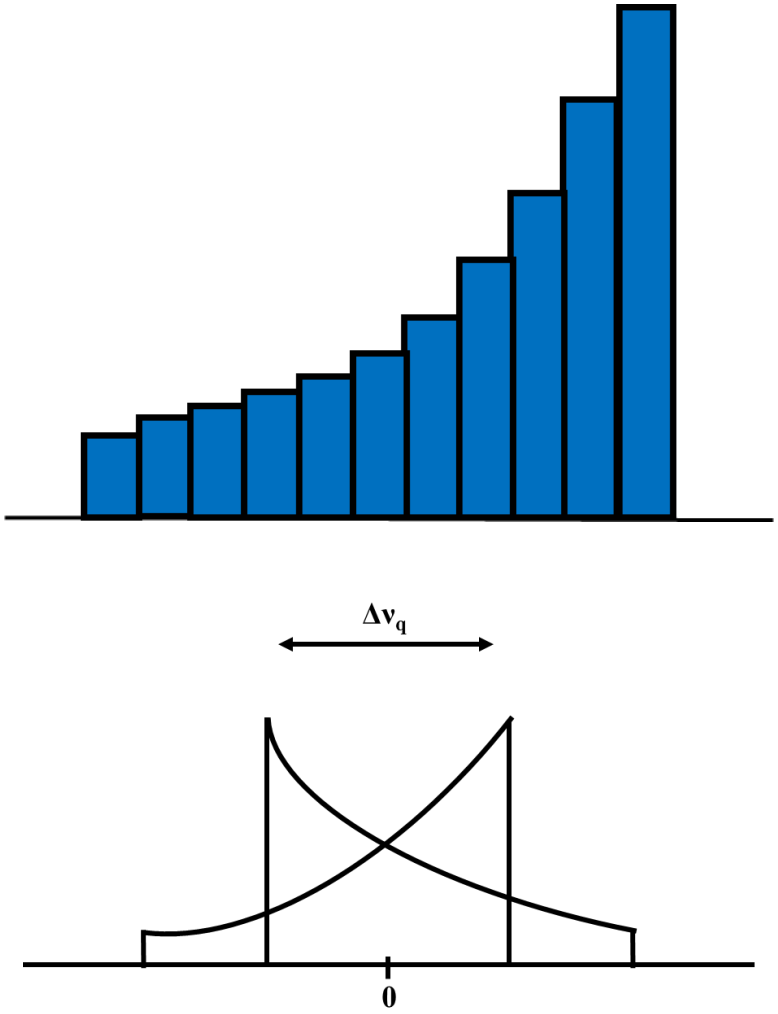

Figure 15. (a)A histogram of the lines for the C-D bond orientation. (b) Pake powder pattern (both transitions crosshatched.

Molecular motion results in the averaging of line shapes in ways that are specific to types of motion.[75] The following figures show some ways in which motions can be

averaged for different types of bonds. For example, in ^{2}H solid-state NMR, the static C-D bond forms part of a methyl group; rotation of the methyl group causes the line shape to collapse by a factor of $\frac{1}{2}(3\cos\phi^2 - 1)$ where φ is the angle the C-D bond makes with the rotation axis.[72,74]

Static C-D

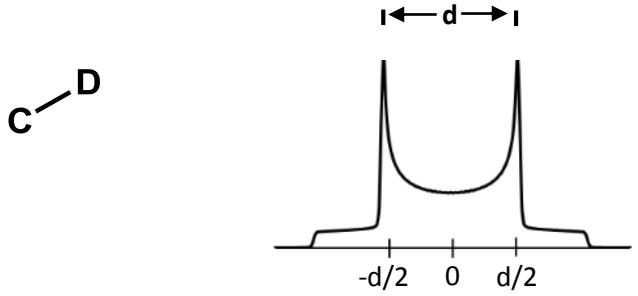

Rotating methyl

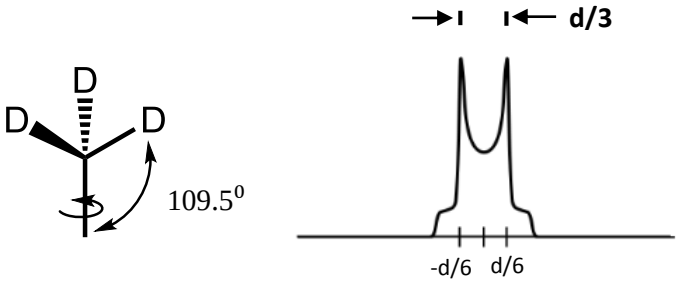

180° phenyl ring flip

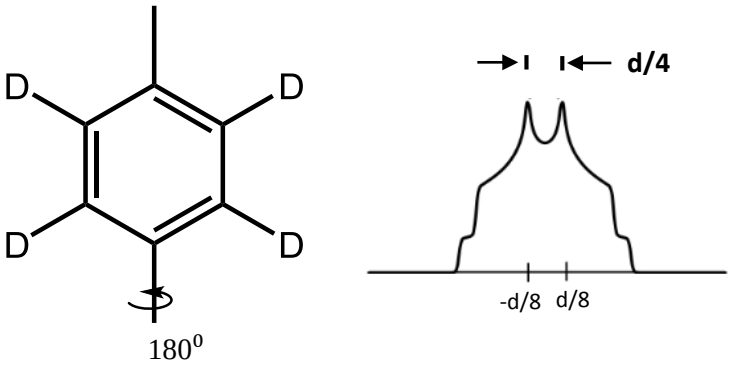

Free diffusion of

phenyl ring

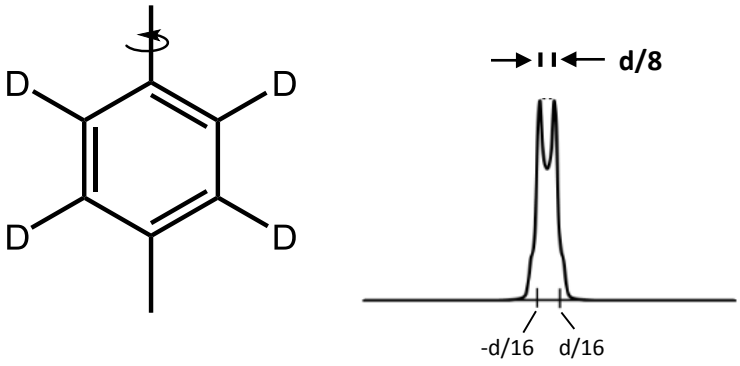

Figure 16. ^{2}H-NMR lineshapes for some different kinds of motions associated with functional groups.[72]

The spectra of amorphous materials are typically quite broad and of low intensity, making them difficult to measure. For these samples, the free induction decay is quite short and is partially obscured by the spectrometer dead time meaning that a lot of information is lost.[76,77] To partially avoid this problem, a quadrupole echo pulse sequence can be used to avoid receiver overload and probe ring down after the rf pulses.[78] However, during this time other things can affect the spectra and these need to be minimized.

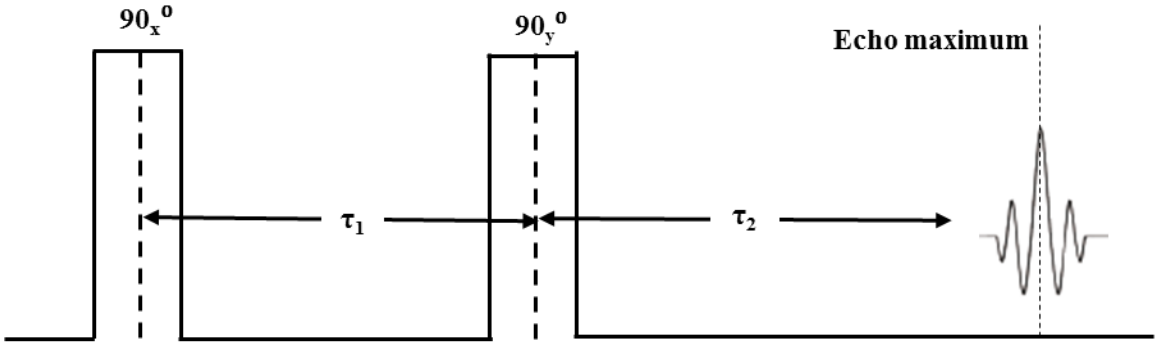

Figure 17. Quadrupole echo pulse sequence.[74,78]

A typical quadrupole echo pulse sequence is shown in Figure 17. There are two 90° rf pulses with phases that differ by 90° (i.e. an X and Y pulse) which are separated by a time, τ. The first pulse produces a free induction decay and is followed by the second pulse which refocuses the magnetization so that an echo takes place at $t = 2\tau$. It is important that the τ be long enough so that the receiver recovers from the rf pulses. The magnetization is sampled and beginning at the peak of the echo, the FID is Fourier transformed to give a spectrum.[72,78]

The description of rotational motion by a specific model can be carried out for NMR techniques and the experimental data can be fit to the model by adjusting parameters that represent the rates and detailed trajectories of motion.[79] One method that can be used to great effect is EXPRESS (*Ex*change *P*rogram for *Re*laxing *S*pin *S*ystems) which is an interface for simulating the effects of motion on a variety of pulsed NMR experiments. This code was written by the Vold-Hoatson research group in MATLAB, and is platform-independent and easy to modify. EXPRESS simulates NMR line shapes and relaxation times by solving the stochastic Liouville equation for the spin density matrix. Motion is described as discrete Markovian jumps.[79]

Deuterium is a nucleus that is particularly well suited to the study of polymer dynamics. The reasons are as follows. Firstly, it is a nucleus dominated by the quadrupole interaction with the electric field gradient at the deuteron site making it suitable for use in monitoring the orientation of individual C-H bond directions.[69,70] Different types of motion can be distinguished via the analysis of ^{2}H line shapes. Motional heterogeneity can be detected and the signals from the mobile and rigid fractions can be separated easily.[73,80] Selective deuteration allows the mobility of different components in various types of systems to be determined. The variety in the types of systems that have been studied is quite striking. Solid state deuterium NMR lineshapes have been used to study the dynamics of deuterated plasticizers in the tightly bound region of adsorbed polymers.[1] It has been used as a sensitive probe of the structure of liquid crystals and has shown the effect of agitation on these systems.[81] Adsorbed peptides have also been studied using this technique[82] as has the RNA of a 29 nucleotide HIV-1 virus.[83]

References

(1) Hetayothin, B.; Cabaniss, R. A.; Blum, F. D. Does plasticizer penetrate tightly bound polymer in adsorbed poly(vinyl acetate) on silica? *Macromolecules* **2017**, *50*, 2092-2102.

(2) Mataz, A.; Gregory, B. M. Effects of confinement on material behaviour at the nanometre size scale. *J. Phys.: Condens. Matter* **2005**, *17*, R461.

(3) Zou, H.; Wu, S.; Shen, J. Polymer/silica nanocomposites: preparation, characterization, properties, and applications. *Chem. Rev.* **2008**, *108*, 3893-3957.

(4) Balazs, A. C.; Emrick, T.; Russell, T. P. Nanoparticle polymer composites: where two small worlds meet. *Science* **2006**, *314*, 1107-1110.

(5) Fleer, G.; Stuart, M. C.; Scheutjens, J.; Cosgrove, T.; Vincent, B.: *Polymers at interfaces*; Chapman & Hall: London, 1993.

(6) Lee, L.-T.; Somasundaran, P. Adsorption of polyacrylamide on oxide minerals. *Langmuir* **1989**, *5*, 854-860.

(7) Langmuir, I. The adsorption of gases on plane surfaces of glass, mica and platinum. *J. Am. Chem. Soc.* **1918**, *40*, 1361-1403.

(8) Adamson, A. W.; Gast, A. P.: *Physical chemistry of surfaces*; John Wiley & Sons: New York, 1997.

(9) Kim, S. H.; Ahn, S. H.; Hirai, T. Crystallization kinetics and nucleation activity of silica nanoparticle-filled poly(ethylene 2,6-naphthalate). *Polymer* **2003**, *44*, 5625-5634.

(10) Jones, R. A. L.: *Polymers at surfaces and interfaces*; Cambridge University Press: Cambridge, 1999.

(11) Jenckel, E. R., B. Adsorption of high polymers. *Z. Elektrochem. Angew. Phys. Chem.* **1951**, *55*, 612.

(12) Bansal, A.; Yang, H.; Li, C.; Benicewicz, B. C.; Kumar, S. K.; Schadler, L. S. Controlling the thermomechanical properties of polymer nanocomposites by tailoring the polymer–particle interface. *J. Polym. Sci., Part B: Polym. Phys.* **2006**, *44*, 2944-2950.

(13) Vieweg, S.; Unger, R.; Heinrich, G.; Donth, E. Comparison of dynamic shear properties of styrene–butadiene vulcanizates filled with carbon black or polymeric fillers. *J. Appl. Polym. Sci.* **1999**, *73*, 495-503.

(14) Keddie, J. L.; Jones, R. A. L.; Cory, R. A. Interface and surface effects on the glass-transition temperature in thin polymer films. *Faraday Discuss.* **1994**, *98*, 219-230.

(15) Porter, C. E.; Blum, F. D. Thermal characterization of PMMA thin films using modulated differential scanning calorimetry. *Macromolecules* **2000**, *33*, 7016-7020.

(16) Blum, F. D.; Young, E. N.; Smith, G.; Sitton, O. C. Thermal analysis of adsorbed poly(methyl methacrylate) on silica. *Langmuir* **2006**, *22*, 4741-4744.

(17) Metin, B.; Blum, F. D. Segmental dynamics in poly(methyl acrylate) on silica: effect of surface treatment. *Langmuir* **2010**, *26*, 5226-5231.

(18) Mortazavian, H.; Fennell, C. J.; Blum, F. D. Structure of the interfacial region in adsorbed poly(vinyl acetate) on silica. *Macromolecules* **2016**, *49*, 298-307.

(19) Berquier, J.-M.; Arribart, H. Attenuated total reflection Fourier transform infrared spectroscopy study of poly (methyl methacrylate) adsorption on a silica thin film: polymer/surface interactions. *Langmuir* **1998**, *14*, 3716-3719.

(20) Fontana, B. J.; Thomas, J. R. The configuration of adsorbed alkyl methacrylate polymers by infrared and sedimentation studies. *J. Phys. Chem.* **1961**, *65*, 480-487.

(21) Soga, I.; Granick, S. Segmental orientations of trains versus loops and tails: the adsorbed polymethylmethacrylate system when the surface coverage is incomplete. *Colloids Surf., A* **2000**, *170*, 113-117.

(22) Khatiwada, B. K.; Hetayothin, B.; Blum, F. D. Thermal properties of PMMA on silica using temperature-modulated differential scanning calorimetry. *Macromol. Symp.* **2013**, *327*, 20-28.

(23) Blum, F. D.; Xu, G.; Liang, M.; Wade, C. G. Dynamics of poly (vinyl acetate) in bulk and on silica. *Macromolecules* **1996**, *29*, 8740-8745.

(24) Blanchard, L.-P.; Hesse, J.; Malhotra, S. L. Effect of molecular weight on glass transition by differential scanning calorimetry. *Can. J. Chem.* **1974**, *52*, 3170-3175.

(25) Fox, T. G.; Flory, P. J. The glass temperature and related properties of polystyrene. Influence of molecular weight. *J. Polym. Sci.* **1954**, *14*, 315-319.

(26) Fox, T. G.; Loshaek, S. Influence of molecular weight and degree of crosslinking on the specific volume and glass temperature of polymers. *J. Polym. Sci.* **1955**, *15*, 371-390.

(27) Jr., T. G. F.; Flory, P. J. Second-order transition temperatures and related properties of polystyrene. I. Influence of molecular weight. *J. Appl. Phys.* **1950**, *21*, 581-591.

(28) Buera, M. D. P.; Levi, G.; Karel, M. Glass transition in poly (vinylpyrrolidone): effect of molecular weight and diluents. *Biotechnol. Prog.* **1992**, *8*, 144-148.

(29) Krumova, M.; López, D.; Benavente, R.; Mijangos, C.; Pereña, J. M. Effect of crosslinking on the mechanical and thermal properties of poly(vinyl alcohol). *Polymer* **2000**, *41*, 9265-9272.

(30) Shetter, J. A. Effect of stereoregularity on the glass temperatures of a series of polyacrylates and polymethacrylates. *J. Polym. Sci., Part B: Polym. Lett.* **1963**, *1*, 209-213.

(31) Ute, K.; Miyatake, N.; Hatada, K. Glass transition temperature and melting temperature of uniform isotactic and syndiotactic poly(methyl methacrylate)s from 13mer to 50mer. *Polymer* **1995**, *36*, 1415-1419.

(32) Karasz, F.; MacKnight, W. The influence of stereoregularity on the glass transition temperatures of vinyl polymers. *Macromolecules* **1968**, *1*, 537-540.

(33) Blum, F. D.; Krisanangkura, P. Comparison of differential scanning calorimetry, FTIR, and NMR to measurements of adsorbed polymers. *Thermochim. Acta* **2009**, *492*, 55-60.

(34) Wu, W.-l.; van Zanten, J. H.; Orts, W. J. Film thickness dependent thermal expansion in ultrathin poly(methyl methacrylate) films on silicon. *Macromolecules* **1995**, *28*, 771-774.

(35) Fryer, D. S.; Nealey, P. F.; de Pablo, J. J. Thermal probe measurements of the glass transition temperature for ultrathin polymer films as a function of thickness. *Macromolecules* **2000**, *33*, 6439-6447.

(36) Joppien, G. R. Characterization of adsorbed polymers at the charged silica aqueous electrolyte interface. *J. Phys. Chem.* **1978**, *82*, 2210-2215.

(37) Koopal, L. K.; Lyklema, J. Characterization of adsorbed polymers from double layer experiments: The effect of acetate groups in polyvinyl alcohol on its adsorption on silver iodide. *J. Electroanal. Chem. Interfacial Electrochem.* **1979**, *100*, 895-912.

(38) Maddumaarachchi, M.; Blum, F. D. Thermal analysis and FT-IR studies of adsorbed poly(ethylene-stat-vinyl acetate) on silica. *J. Polym. Sci., Part B: Polym. Phys.* **2014**, *52*, 727-736.

(39) Krisanangkura, P.; Packard, A. M.; Burgher, J.; Blum, F. D. Bound fractions of methacrylate polymers adsorbed on silica using FTIR. *J. Polym. Sci., Part B: Polym. Phys.* **2010**, *48*, 1911-1918.

(40) Metin, B., Okuom, M., Blum, F. Dynamics of adsorbed PMA-d3 - effect of substrate. *Polym. Prepr.* **2008**, *49*.

(41) Nambiar, R. R.; Blum, F. D. Segmental dynamics of bulk poly (vinyl acetate)-d 3 by solid-state 2H NMR: effect of small molecule plasticizer. *Macromolecules* **2008**, *41*, 9837-9845.

(42) Cosgrove, T.; Fergie-Woods, J. W. On the kinetics and reversibility of polymer adsorption. *Colloids Surf.* **1987**, *25*, 91-99.

(43) Earnest, C. M.: *Compositional analysis by thermogravimetry*; ASTM International, 1988; Vol. 997.

(44) Hatakeyama, T.; Quinn, F.: *Thermal analysis: fundamentals and applications to polymer science*; John Wiley & Sons: West Sussex, 1999.

(45) Menczel, J. D.; Prime, R. B.; Gallagher, P. K.; Judovits, L.; Bair, H. E.; Reading, M.; Swier, S.; Vyazovkin, S.; Riga, A.; Akinay, A. E.: Differential scanning calorimetry (DSC). In *Thermal Analysis of Polymers: Fundamentals and Applications*; Menczel, J. D., Prime, R. B., Eds.; John Wiley & Sons: New Jersey, 2009.

(46) Salam, L. A.; Matthews, R. D.; Robertson, H. Pyrolysis of poly-methyl methacrylate (PMMA) binder in thermoelectric green tapes made by the tape casting method. *J. Eur. Ceram. Soc.* **2000**, *20*, 335-345.

(47) Ganesh, K.; Latha, R.; Kishore, K.; George, B.; Ninan, K. Stabilization of thermal degradation of poly (methyl methacrylate) by polysulfide polymers. *J. Appl. Polym. Sci.* **1997**, *66*, 2149-2156.

(48) Soudais, Y.; Moga, L.; Blazek, J.; Lemort, F. Coupled DTA–TGA–FT-IR investigation of pyrolytic decomposition of EVA, PVC and cellulose. *J. Anal. Appl. Pyrolysis* **2007**, *78*, 46-57.

(49) Marcilla, A.; Beltrán, M. Thermogravimetric kinetic study of poly(vinyl chloride) pyrolysis. *Polym. Degrad. Stab.* **1995**, *48*, 219-229.

(50) Schick, C. Differential scanning calorimetry (DSC) of semicrystalline polymers. *Anal. Bioanal. Chem.* **2009**, *395*, 1589-1611.

(51) Standard Terminology Relating to Thermal Analysis and Rheology. ASTM International, 2016.

(52) Reading, M.; Luget, A.; Wilson, R. Modulated differential scanning calorimetry. *Thermochim. Acta* **1994**, *238*, 295-307.

(53) Gill, P. S.; Sauerbrunn, S. R.; Reading, M. Modulated differential scanning calorimetry. *J. Therm. Anal.* **1993**, *40*, 931-939.

(54) Ribeiro, M.; Grolier, J.-P. E. Temperature modulated DSC for the investigation of polymer materials: a brief account of recent studies. *J. Therm. Anal. Calorim.* **1999**, *57*, 253-263.

(55) Righetti, M. C. Crystallization of polymers investigated by temperature-modulated DSC. *Materials* **2017**, *10*, 442.

(56) Simon, S. L. Temperature-modulated differential scanning calorimetry: theory and application. *Thermochim. Acta* **2001**, *374*, 55-71.

(57) Hourston, D. J.; Song, M.; Pollock, H. M.; Hammiche, A. Modulated differential scanning calorimetry. *J. Therm. Anal.* **1997**, *49*, 209-218.

(58) Boller, A.; Jin, Y.; Wunderlich, B. Heat capacity measurement by modulated DSC at constant temperature. *J. Therm. Anal.* **1994**, *42*, 307-330.

(59) Wunderlich, B.; Jin, Y.; Boller, A. Mathematical description of differential scanning calorimetry based on periodic temperature modulation. *Thermochim. Acta* **1994**, *238*, 277-293.

(60) Wunderlich, B.: Quasi-isothermal temperature-modulated differential scanning calorimetry (TMDSC) for the separation of reversible and irreversible

thermodynamic changes in glass transition and melting ranges of flexible macromolecules. In *Pure Appl. Chem.*, 2009; Vol. 81; pp 1931.

(61) Verdonck, E.; Schaap, K.; Thomas, L. C. A discussion of the principles and applications of Modulated Temperature DSC (MTDSC). *Int. J. Pharm.* **1999**, *192*, 3-20.

(62) Koenig, J. L.: Chapter 2 - Vibrational spectroscopy of polymers. In *Spectroscopy of Polymers (Second Edition)*; Koenig, J. L., Ed.; Elsevier Science: New York, 1999; pp 35-76.

(63) Faires, L. M. Fourier transforms for analytical atomic spectroscopy. *Anal. Chem.* **1986**, *58*, 1023A-1034A.

(64) Koenig, J. L.: Chapter 3 - Experimental IR spectroscopy of polymers. In *Spectroscopy of Polymers (Second Edition)*; Koenig, J. L., Ed.; Elsevier Science: New York, 1999; pp 77-145.

(65) Urban, M. W.: *Attenuated total reflectance spectroscopy of polymers: theory and practice*; American Chemical Society: Washington, 1996.

(66) Kitayama, T.; Hatada, K.: *NMR Spectroscopy of Polymers*; Springer Science & Business Media: Berlin, 2004.

(67) Koenig, J. L.: Chapter 6 - High resolution NMR spectroscopy of polymers in solution. In *Spectroscopy of Polymers (Second Edition)*; Koenig, J. L., Ed.; Elsevier Science: New York, 1999; pp 255-313.

(68) Harris, R. K.: *Nuclear magnetic resonance spectroscopy*; Longman Scientific & Technical: Essex, 1986.

(69) Brown, M. F.; Lope-Piedrafita, S.; Martinez, G. V.; Petrache, H. I.: Solid-State Deuterium NMR Spectroscopy of Membranes. In *Modern Magnetic Resonance*; Webb, G. A., Ed.; Springer Netherlands: Dordrecht, 2006; pp 249-260.

(70) Silvestri, R. L.; Koenig, J. L. Applications of nuclear magnetic resonance spectrometry to solid polymers. *Anal. Chim. Acta* **1993**, *283*, 997-1005.

(71) Spiess, H. W. NMR methods for solid polymers. *Annu. Rev. Mater. Sci.* **1991**, *21*, 131-158.

(72) Jelinski, L. W. Solid state deuterium nmr studies of polymer chain dynamics. *Annu. Rev. Mater. Sci.* **1985**, *15*, 359-377.

(73) Hiraoki, T.; Kitazawa, S.; Tsutsumi, A. Local dynamics in polypeptides studied by solid state 2H NMR: side chain dynamics of poly(γ-benzyl l-glutamate) and racemic poly(γ-benzyl glutamate). *Annu. Rep. NMR Spectrosc.* **2004**, *53*, 297-339.

(74) Jelinski, L. W.: Deuterium NMR of solid polymers. In *High Resolution NMR Spectroscopy of Synthetic Polymers in Bulk*; Komoroski, R. A., Ed.; VCH Verlagsgesellschaft: Deerfield beach, 1986; pp 335-364.

(75) Spiess, H. W. Pulsed deuteron NMR investigations of structure and dynamics of solid polymers. *J. Mol. Struct.* **1983**, *111*, 119-133.

(76) Boden, N.; Clark, L. D.; Hanlon, S. M.; Mortimer, M. Deuterium nuclear magnetic resonance spin echo spectroscopy in molecular crystals. *Faraday Symp. Chem. Soc.* **1978**, *13*, 109-123.

(77) Davis, J. H.; Jeffrey, K. R.; Bloom, M.; Valic, M. I.; Higgs, T. P. Quadrupolar echo deuteron magnetic resonance spectroscopy in ordered hydrocarbon chains. *Chem. Phys. Lett.* **1976**, *42*, 390-394.

(78) Griffin, R. G. [8] Solid state nuclear magnetic resonance of lipid bilayers. *Methods Enzymol.* **1981**, *72*, 108-174.

(79) Vold, R. L.; Hoatson, G. L. Effects of jump dynamics on solid state nuclear magnetic resonance line shapes and spin relaxation times. *J. Magn. Reson.* **2009**, *198*, 57-72.

(80) Spiess, H. W. Molecular dynamics of solid polymers as revealed by deuteron NMR. *Colloid Polym. Sci.* **1983**, *261*, 193-209.

(81) Blum, F. D.; Franses, E. I.; Rose, K. D.; Bryant, R. G.; Miller, W. G. Structure and dynamics in lamellar liquid crystals. Effect of agitation and aging on deuterium NMR line shapes. *Langmuir* **1987**, *3*, 448-452.

(82) Li, K.; Emani, P. S.; Ash, J.; Groves, M.; Drobny, G. P. A study of phenylalanine side-chain dynamics in surface-adsorbed peptides using solid-state deuterium NMR and rotamer library statistics. *J. Am. Chem. Soc.* **2014**, *136*, 11402-11411.

(83) Huang, W.; Emani, P. S.; Varani, G.; Drobny, G. P. Ultraslow domain motions in HIV-1 TAR RNA revealed by solid-state deuterium NMR. *J. Phys. Chem. B* **2017**, *121*, 110-117.

CHAPTER III

DISRUPTIONS IN THE CRYSTALLINITY OF POLY(LAURYL METHACRYLATE) DUE TO ADSORPTION ON SILICA

Note: This chapter was published in *J. Polym. Sci., Part B: Polym. Phys.* **2018**, 56, 89 – 96. DOI: 10.1002/polb.24525 and reprinted with permission from John Wiley and Sons and Copyright clearance center.

Abstract

The effects of adsorption of poly(lauryl methacrylate) (PLMA), a side-chain crystalline polymer, on silica were investigated. Fourier transform infrared spectroscopy and differential scanning calorimetry (DSC) measurements were made on both bulk and adsorbed PLMA. The reversible heat flow rates were observed as a function of temperature and the degree of crystallinity of the samples determined based on the broad melting transitions of the side chains in the surface samples. It was found that adsorption caused a disruption of the side-chain crystallinity primarily in the tightly-bound layer of the polymer, but did not significantly affect its glass transition temperature. A change in the packing of the hydrophobic side chains, as a result of adsorption, was also observed

for the tightly adsorbed polymer. These results indicated that PLMA side chains in proximity to the silica surface have different properties from those in bulk PLMA.

Introduction

Polymer nanocomposites have been subjected to extensive investigations due to their wide range of applications and properties, which depend on both components and their interfaces.[1] Studies of the interfacial properties and dynamics can be extended to side chain crystalline polymers that are heterogeneous due to the presence of crystalline nano-domains.[2,3] The interrelation between side chain crystallization and chain dynamics has been studied in a number of systems.[2-6] Of particular interest are poly(n-alkyl methacrylates) that are seen to be ideal models for the investigation of surface dynamics and interfacial phenomena.[7] It has been shown that the dynamics of the amorphous regions of these semi-crystalline polymers differ from the dynamics of purely amorphous polymers. The longer alkyl side chains of the polymers form nano-domains due to the incompatibility of the main- and side-chains.[2] For this class of polymers, increased side chain length results in increased melting peak intensity (which corresponds to an increase in enthalpy of melting, ΔH_m) and melting temperature.[2]

Poly(lauryl methacrylate) (PLMA), which has 12 carbon atoms per side chain, is the shortest in the poly(n-alkyl methacrylate) series to show the effect of side chain crystallization.[2] It has been suggested that PLMA contains a rigid amorphous region due to the confinement of the chains as a result of the presence of the nano-domains.[2] However, studies have shown that the adsorption of shorter-chain methacrylate polymers onto silica instead results in a tightly bound layer which has a higher glass transition

temperature than bulk polymer.[8-10] The interest in PLMA is due to its high mobility[11] (T_g is around -65 °C) and hydrophobicity,[12] which allow its use as a viscosity modifier of motor oils.[13] Nanocomposites with low T_g polymers such as PLMA have also been used in pressure sensitive adhesives,[12] and thermally reversible light scattering films.[14] It is known that the physical and mechanical properties of this polymer are affected by its crystallinity,[15] thus understanding the thermal behavior of PLMA under polymer chain confinement is of importance.

Different techniques have been used in the determination of the degree of crystallinity of polymers. These include x-ray diffraction (XRD),[16-18] differential scanning calorimetry (DSC),[14,16-18] NMR,[16,17] and FTIR.[19] DSC is an invaluable technique used to study, among other things, glass transitions, melting behavior, polymer morphology and degrees of crystallinity.[20] Unfortunately, DSC has some shortcomings including uncertainties in the pre- and post-melting baselines.[21] Despite these shortcomings, this technique is still widely used to determine crystallinity. The sensitivity of FTIR to the conformation of molecules is also often employed to determine polymer structure and order. The shifting of the ester carbonyl stretching frequency, for example, shows the adsorption of the polymer via hydrogen bonding.[22] FTIR and its variants are often used because they are simple, rapid, and non-destructive. Information about the presence, and nature of specific intermolecular interactions and conformational changes can also be determined with vibrational spectroscopy.[23]

In this study, we examine the effect of confinement of PLMA on Cab-O-Sil silica in terms of the glass transition temperature and crystallinity using DSC and FTIR. The aim is to understand how the presence of side chains affects the behavior of PLMA on

silica and also to investigate how the side chain crystallinity and glass transition are affected upon adsorption.

Experimental

Materials. PLMA was purchased as a 28.8% solution in toluene from Scientific Polymer Products, Inc. (Ontario, NY) and used as received. The molecular mass and polydispersity index (PDI) of PLMA was determined using gel permeation chromatography (GPC) equipped with a DAWN EOS light scattering instrument and an Optilab interferometer refractive index detector (Wyatt Technologies, Santa Barbara, CA). The Mark-Houwink and refractive index (dn/dc) (0.079 mL/g) constants (for PLMA in THF) were obtained from literature.[24,25] The polymer was found to have an M_n value of 213000 g/mol and a polydispersity index (PDI) of 2.62. Cab-O-Sil M-5P fumed silica, with a specific surface area of 200 m^2/g was obtained from Cabot Corp. (Tuscola, IL) and used as the substrate.

Preparation of adsorbed samples. PLMA solutions of varying concentration were prepared in toluene. These solutions were added separately to about 0.3 g of silica that had been wetted with toluene and sonicated. The mixtures were shaken on a mechanical shaker for 48 h; subsequently, dry air was bubbled through overnight to evaporate the solvent. The resulting powder was then put under vacuum for 2 days to ensure complete removal of the solvent. Thermogravimetric analysis was used to determine the amount of polymer adsorbed on the silica and also to test for the absence of solvent. The adsorbed amount of polymer was calculated based on the difference in the mass of the sample before and after the polymer was burned off.

Glass transition and melting measurements. Differential scanning calorimetry (DSC) measurements were made on the samples using a TA Instruments DSC Q2000 (New Castle, DE) with TA Universal Analysis software. Because these samples had a low temperature transition, a TA Refrigerated Cooling System 90 cooling system was used for the Q2000. Sample pans were referenced against empty pans and a nitrogen gas flow rate of 25 mL/min was used to purge the cell. The samples were initially held at -85 °C for 2 min and then heated to 50 °C at a rate of 10 K/min. The samples were then cooled back to -85 °C at the same heating rate. A second heating was performed in a similar manner to the first heating and the resulting heat flow curves were used to obtain the melting enthalpies and glass transition temperatures of the bulk and adsorbed samples.

Attenuated total reflectance FTIR measurements. Attenuated total reflectance (ATR) FTIR spectra were recorded using a Nicolet iS50 FTIR spectrometer (Thermo Scientific, Waltham, MA) in the range of 4000-500 cm^{-1} and a resolution of 4 cm^{-1}. Omnic software 9.0, Thermo Fisher Scientific Inc. (Waltham, MA) and Origin Pro 9.1 software, Origin Lab Corporation (Northhampton, MA) were used to fit the experimental curves.

Results

The effects of adsorption of PLMA on the silica surface were investigated using Fourier transform infrared spectroscopy with attenuated total reflectance (ATR). The full FTIR spectrum is shown in the **Supporting Information**. There were two main regions of interest. The first was the 1800 – 1600 cm^{-1} region (C=O stretching) which shows a

shift in frequency due to the hydrogen bonding of the carbonyl groups of PLMA to the surface silanol groups of silica. The second was the 900 – 700 cm^{-1} region (C_β-H out-of-plane bending and $(CH_2)_n$ in-phase rocking)[26] which was due to the crystalline portion of PLMA consisting of alkyl side chains.

Examination of the 3950 – 3150 cm^{-1} portion of the FTIR spectra, shown in Figure 1a, showed that the small sharp peak at 3750 cm^{-1} present in the silica spectrum was not observed in the absorbed sample spectra. This indicated that effectively all of the free silanol groups on the silica surface were hydrogen bonded upon the adsorption of PLMA. There was also a broad hydrogen bonded silanol peak centered at around 3450 cm^{-1} in all the spectra, showing the hydrogen bonded silanol groups in all the samples. A further indication of the adsorption of PLMA onto silica was seen in the carbonyl resonance that ranged 1760-1660 cm^{-1} as shown in Figure 1b. A single resonance was observed for the bulk polymer, while the absorbed samples showed an overlap of two resonances. The resonance at the higher frequency (~1730 cm^{-1}) was associated with the free carbonyl groups and the resonance at the lower frequency (~1705 cm^{-1}) was associated with the carbonyl groups bound to the silica surface.[22,24]

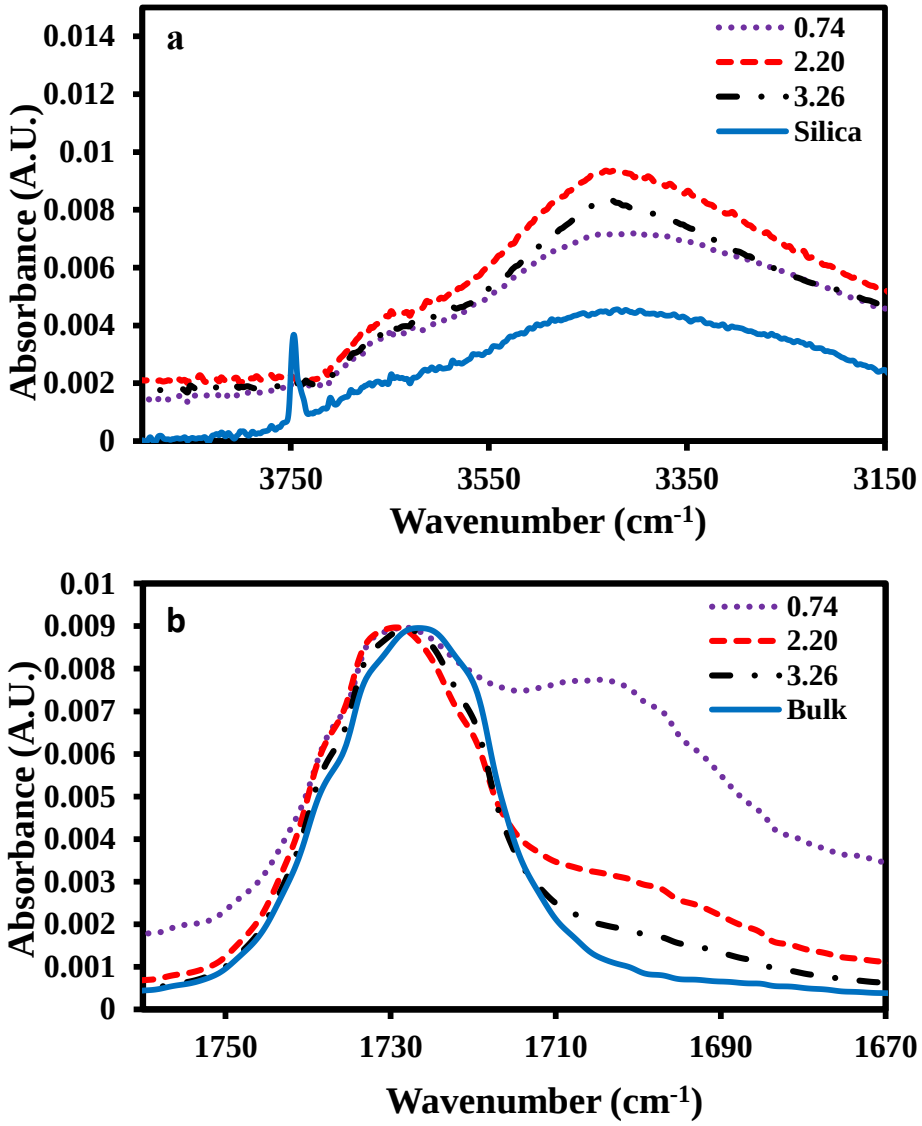

Figure 1. (a) FTIR spectra of Cab-O-Sil M5P silica and PLMA-silica in the silanol region. The values in the legend represent the adsorbed amount of PLMA (mg polymer/m^2 silica). The isolated silanol groups were covered upon adsorption. The plots were offset vertically for clarity. (b) FTIR spectra of bulk and adsorbed PLMA samples in the 1760-1660 cm^{-1} region showing the free (1730 cm^{-1}) and H-bonded (1705 cm^{-1}) carbonyl resonances. The spectra were scaled so that the intensities of the free carbonyl resonances were roughly equal.

The spectra of the carbonyl peaks for each adsorbed sample were fitted based on contributions from free and bound carbonyls. An example of the fitting is shown in Figure 2. From the fittings, the intensities of each resonance were determined. From these, the bound fraction of carbonyl groups, *p*, was calculated from eq (1) or

$$p = \frac{(A_b/X)}{[A_b/X + A_f]} \quad (1)$$

where X is molar extinction coefficient ratio of bound to free carbonyls, A_f is the intensity of the free carbonyl band, and A_b is that of the bound carbonyl band.[24,27] This estimation requires knowledge of the adsorption coefficients of the bound and free carbonyl or their ratio denoted as X in the equation above.[27] The value of X for PLMA was determined to be 11.9 ± 2.0 using FTIR-ATR (see **Supporting Information**) and had been previously estimated as X = 11.1 ± 2.9 using transmission mode FTIR.[24] The bound carbonyl fractions calculated in this way are shown in Table 1. The fraction of bound carbonyl groups to free carbonyl groups decreased with increasing adsorbed amounts of PLMA. These changes in intensity were due to the smaller *fractions* of bound carbonyls at larger adsorbed amounts.[24]

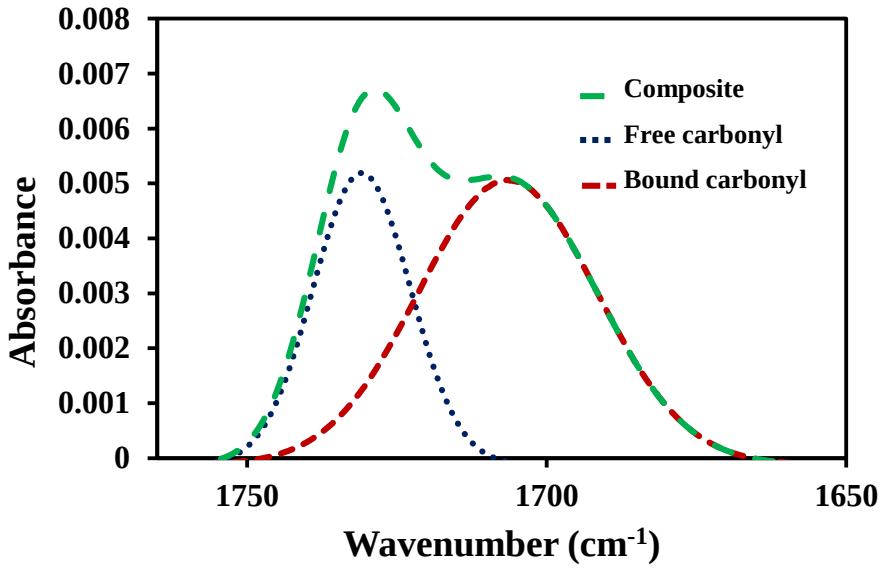

Figure 2. Fitting of the FTIR-ATR carbonyl peak with free and bound components for the 0.74 mg/m^2 adsorbed amount sample. The bound carbonyl was centered at 1705 cm^{-1} and the free carbonyl at 1730 cm-^{1}.

Table 1. Bound fractions of adsorbed PLMA on silica.

Adsorbed amount (mg/m^2)	Bound carbonyl fraction
0.74	0.140
2.20	0.032
3.26	0.010

The FTIR spectra showed intense resonances due to the Si-O-Si stretching frequency in the 1100-800 cm^{-1} region[28] which partially obscured the peaks which were in the 900-700 cm^{-1} spectral area of interest. Thus, a spectrum of Cab-O-Sil M5-P was subtracted from the composite peaks, which were then analyzed in that region. The resulting spectra are shown in Figure 3 for the 770-700 cm^{-1} range.

The bulk polymer and the 2.2 and 3.3 mg/m^2 adsorbed amounts had a resonance centered at around 720 cm^{-1}, corresponding to hexagonal packing, shown in Figure 3a.[29] The smallest adsorbed amount sample was found to have a peak at 720 cm^{-1} and also had shoulders at 713 and 730 cm^{-1} which corresponded to a triclinic and orthorhombic arrangement, respectively.[17] Figure 3b shows the 780 to 700 cm^{-1} range for only the 0.74 mg/m^2 adsorbed amount. Two shoulders are clearly seen at the aforementioned frequencies indicating the presence of orthorhombic and triclinic packing. This indicates that adsorption onto the surface of silica affects the alkyl chain packing of a thin layer of PLMA. The alkyl chain packing of thicker layers did not appear to be affected by adsorption. The observation of the CH_2 stretching frequencies of bulk and adsorbed CTAB supported the finding that the surface affects the packing of the alkyl chains. The frequencies for the symmetric and asymmetric stretching of the CH_2 groups (at 2855 and 2923 cm^{-1} respectively) decreased with increasing adsorbed amounts as shown in Table 2.

Table 2. CH_2 stretching frequencies of bulk and adsorbed PLMA

	Symmetric stretching frequency (cm^{-1})	Asymmetric stretch frequency (cm^{-1})
0.74 mg/m^2	2855.6	2926.0
2.20 mg/m^2	2854.1	2924.0
3.56 mg/m^2	2853.2	2923.1
Bulk PLMA	2852.7	2922.6

.

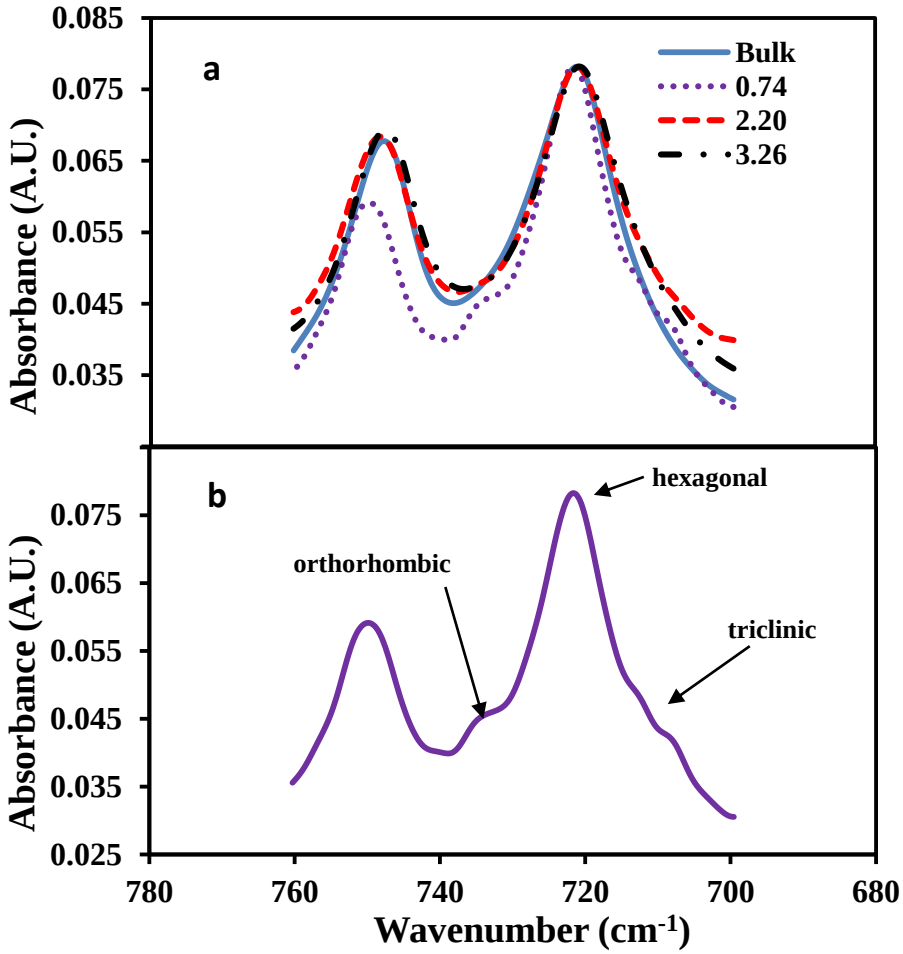

Figure 3. (a) FTIR spectra of PLMA in bulk and different adsorbed amounts on silica (in mg/m^2) with the neighboring silica peaks subtracted in the 770-700 cm^{-1} range. The 0.74 mg/m^2 sample showed a different type of alkyl packing from the other adsorbed amount samples. (b) FTIR spectrum of only 0.74 mg/m^2 bound amount in the 770-700 cm^{-1} range. In addition to hexagonal packing, there was evidence of triclinic and orthorhombic alkyl arrangements.

The behavior of the adsorbed PLMA was also studied by differential scanning calorimetry (DSC). The DSC thermograms of the bulk and adsorbed samples are shown in Figure 4. The heat flow curves of the bulk PLMA showed a melting peak at -34 °C and

a glass transition temperature at -64 °C. These temperatures were in agreement with those found in the literature.[30] The bulk polymer showed the largest amount of crystallinity which was reduced as the amount of adsorbed PLMA decreased. The heat of melting (ΔH_m) was calculated from the area under the endothermic peak of the curves in Figure 4a. There was no distinguishable peak in the melting region for the 0.74 mg/m^2 sample. The heat of melting *per gram of polymer* was calculated and is shown together with the melting and glass transition temperatures in Table 3.

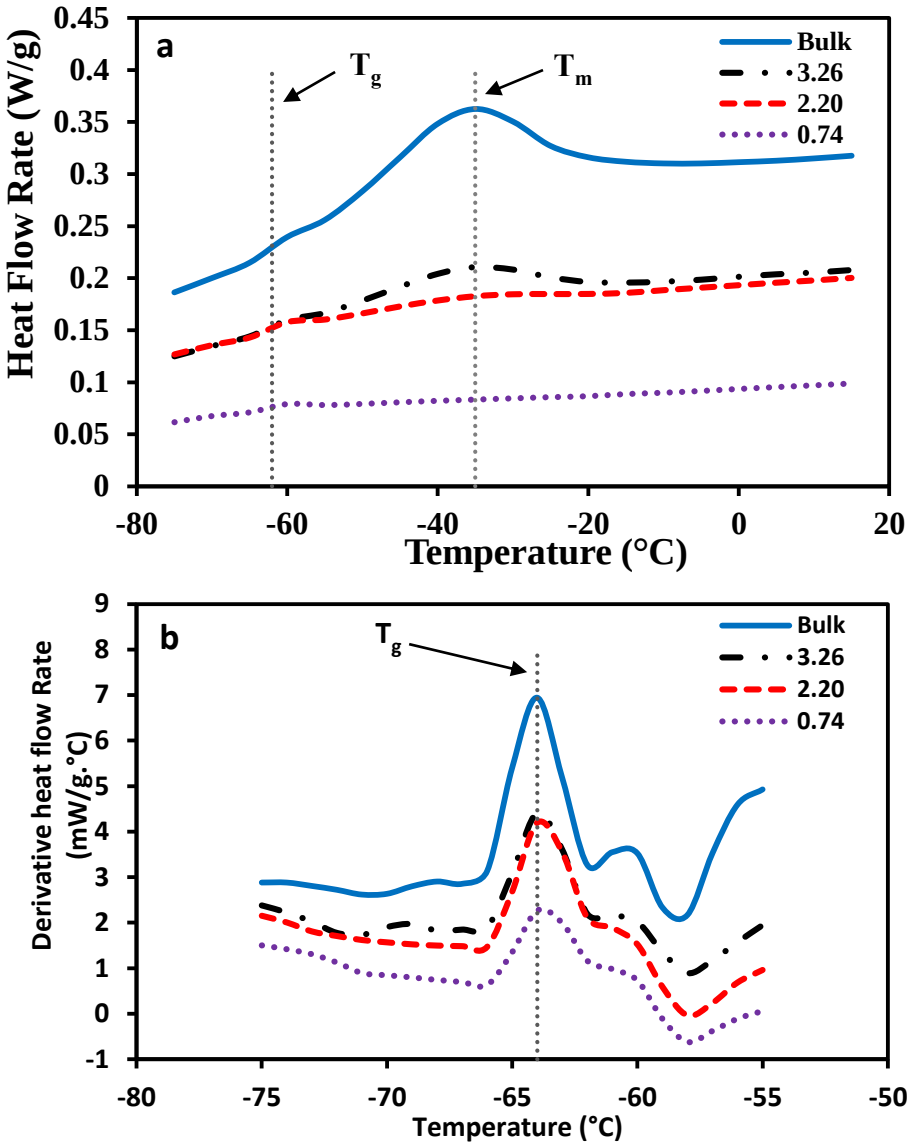

Figure 4. (a) DSC thermograms of bulk and adsorbed PLMA samples (mg/m^2). (b) Derivative heat flow rate curves of the bulk polymer and adsorbed polymer samples in the glass transition region. The amount of crystallinity decreased with decreased adsorbed amounts, however, the glass transition temperature was not affected by adsorbed amount.

Table 3. Calorimetric results for adsorbed samples of PLMA

Adsorbed amount (mg/m^2)	ΔH_m (J/g sample)	ΔH_m (J/g polymer)	T_g (°C)	T_m (°C)	ΔT* (°C)
0.74	0	0	-63.9	-	-
2.2	1.39	3.2	-63.9	-35.6	7.3
3.3	4.38	6.7	-64.0	-36.1	7.3
Bulk	11.4	11.4	-64.0	-35.3	6.1

*$T_{melting}$ - $T_{freezing}$

The enthalpy of melting was found to be 11.4 J/g for bulk PLMA. This value was larger than that found in the literature (9 J/g of PLMA).[2] As the amount of polymer adsorbed on the surface increased, the crystallinity of the polymer side chains increased as indicated by an increase in the enthalpy of melting of the polymer as shown in Table 3. For PLMA, adsorption caused a disruption of the side-chain crystallinity, but did not significantly affect the glass transition or melting temperature of the polymer. In Figure 4b, the derivative mode was used to highlight the glass transition behavior since, compared to the melting transition, the glass transition was weak. Super-cooling was also observed in the samples in which there was crystallinity (see **Supporting Information**). The amount of super-cooling (ΔT) increased slightly upon adsorption and is shown in Table 3. No crystallinity was observed for the 0.74 mg/m^2 sample.

The degree of crystallinity, D_{cal}, for the bulk polymer and adsorbed samples were estimated based on the enthalpies of melting of the samples using equation (2).

$$D_{cal} = \frac{\Delta H_m}{\Delta H_{CH_2}} \quad (2)$$

where ΔH_{CH_2} is the heat of fusion of CH_2 groups. The degree of crystallinity estimations were based on a heat of fusion of n-alkanes in hexagonal packing with 3.4 kJ/mole per CH_2 unit.[31] The results of these calculations are shown in Table 4. As previously mentioned, there was no observable ΔH for the 0.74 mg/m^2 sample. The calculation of the fraction of crystalline chains indicates that there is the equivalent of roughly one carbon atom per alkyl group involved in crystallization. This is in agreement with literature.[2] The degree of crystallinity also showed a decrease with decreasing adsorbed amount. It should be noted that the estimated degree of crystallinity is a minimum estimate. However, given that the melting points for the crystals are unchanged with adsorption, the crystals might be fairly similar, making the crystallinity estimate reasonably accurate. In general, the main chain of the polymer prevents the side chains from packing as closely as alkane chains do. This has been shown with other comb-like polymers.[17,32]

Table 4. Thermal properties of bulk PLMA and PLMA composites

Adsorbed amount (mg/m^2)	ΔH_m (J/g polymer)	ΔH_m (kJ/mol)	D_{cal} (mol%)[a]
Bulk	11.4	2.90	7.1
3.26	4.38	1.12	2.7
2.20	1.39	0.36	0.9
0.74	~ 0	~ 0	~ 0

[a] based on 40.8 kJ/mol for 12 CH_2 groups.

Discussion

Studies have demonstrated that when acrylate or methacrylate polymers are adsorbed on silica, interactions between the carbonyl groups on the polymer and the silanol groups on the silica result in the decreased mobility and increased T_g of the polymer.[8,24,33,34] Hydrogen bonding was observed in Figure 1 from the shift in the

carbonyl resonance frequency as well as the disappearance of the isolated silanol `peak. The effect of main chain mobility and structure on side chain crystallinity has also been extensively studied.[17,32,35-40] It has been reported that chain stiffness retards the attainment of crystallinity.[40] The retardation of crystallization was evident in the smallest adsorbed amount sample (0.74 mg/m^2) which showed effectively no crystallinity. This sample had the largest fraction of bound carbonyl groups directly on the surface, suggesting that it was in a configuration with less chain mobility[22] and confinement in accord with the shape of the silica surface. Crystallinity requires the cooperative movement of the main chain and side chain units.[40] When adsorbed, the polymer backbone of PLMA appears to be constrained as a result of hydrogen bonds between the carbonyl groups and the silica surface resulting in a reduction in the amount of crystallinity. A similar reduction in crystallinity occurred with adsorbed poly(vinyl acetate-stat-ethylene) on silica.[9] The larger adsorbed amount samples (2.20 mg/m^2 and 3.26 mg/m^2) had much smaller fractions of bound carbonyls and as a result, the decrease in crystallinity was not as much as in the smallest adsorbed amount sample.

Previously, it has been shown that the fraction of bound carbonyls decreased with increased side chain length.[24] PLMA was the exception to this trend and showed the largest fraction of bound carbonyls. Its low T_g was suggested as the reason for this deviation. The flexibility, indicated by a low T_g, would allow the polymer to adopt configurations that allow more surface contact.[24] This effect has been observed in another study which shows that, due to the ability of PLMA to reorient as a result free rotation about each monomeric unit and side group, certain proteins can be adsorbed on it without losing their native conformations.[7] The bound fraction values obtained in Table 1 and the

X value used to obtain them were comparable (based on the margins of error) with those obtained from the previous study.[24] It is useful to note that the value of *X* for the system is the same for transmission and ATR experiments. The values obtained showed that a larger fraction of adsorbed carbonyl groups correlated with a decrease in crystallinity. Also, at smaller adsorbed amounts (larger bound fractions), the polymer is likely to be more spread out on the silica surface[22] and thus some of the crystalline domains may be disrupted as a result. This effect was not as pronounced for the larger adsorbed amount samples. These samples exhibited smaller amounts of crystallinity than the bulk sample, but still had some crystallinity as there were more segments away from the surface. Similar effects with adsorbed amounts and crystallinity for adsorbed cetyltrimethylammonium bromide (CTAB) have also been observed.[41,42] CTAB samples on silica showed a decrease in the enthalpy of melting with decreasing adsorbed amounts and the supercooling of the alkyl chains (16 °C for bulk) increased with decreasing amounts.

Information about the packing of the polymer alkyl side chains could be obtained from the 770 cm^{-1} to 700 cm^{-1} region shown in Figure 3. The 720 cm^{-1} resonance corresponds to the rocking vibration of 4 or more CH_2 groups and shows hexagonal packing.[29,43] A doublet at 719 cm^{-1} and 730 cm^{-1} is indicative of orthorhombic packing and a single band at 713 cm^{-1} corresponds to triclinic packing.[44] Figure 3a showed that for bulk PLMA and the 2.20 mg/m^2 and 3.26 mg/m^2 adsorbed amounts, there was hexagonal packing as shown by the presence of only one peak in that area.[29,43] Figure 3b showed that the 0.74 mg/m^2 adsorbed amount sample contained, in addition to hexagonal packing, orthorhombic and triclinic packing. The observation of these conformations only

for the smallest adsorbed amount suggests that the surface had a direct effect on the aggregation of the alkyl side chains. This change in conformation may have been a result of the smallest adsorbed samples having the highest bound fraction and thus being more intimately associated with the surface. As the adsorbed amount increased, there was no noticeable change in the structure of the alkyl aggregates; only the smallest adsorbed amount showed a change in structure. This indicated that at larger adsorbed amounts, the surface did not have as significant of an impact on the side chain conformations. The symmetric and asymmetric CH_2 stretching vibrations also showed that the surface had an impact on the alkyl side chain configurations. Both stretching frequencies decreased slightly with increased adsorbed amounts, as shown in Table 2, indicating an increase in gauche conformations within the alkyl chains.[42,45]

The 0.74 mg/m^2 sample, which had the smallest adsorbed amount of PLMA behaved differently from the bulk and larger adsorbed amount samples. At this composition, there was no crystallinity and the conformations of the alkyl chains at the surface were obviously different. Deviation from bulk behavior at small adsorbed amounts has also been observed for other polymers such as PMMA and PVAc which show increased glass transition and decomposition temperatures that correspond to a layer of polymer that is tightly-bound to the silica surface.[8,34] Although there was no apparent change in T_g for PLMA upon adsorption, the adsorbed sample that consisted of only tightly-bound PLMA could still be distinguished at around 0.74 mg/m^2. The tightly-bound amount of PLMA is close to that of PMMA and PVAc which have tightly bound amounts of 1.21 mg/m^2 and 0.78 mg/m^2 respectively.[34] The effect of the surface on the

properties of polymer segments decreased with increasing distance from the surface. The length scales for adsorbed PMMA, PVAc and PLMA were all approximately the same.

Upon adsorption onto silica, PLMA did not show any significant change in glass transition temperature. This lack of change is in contrast to other alkyl methacrylate polymers, which on adsorption showed increases in glass transition temperatures. These increases could be up to 50 °C as in the case of poly(methyl methacrylate).[8] The interaction between the polymer and the surface determines the effect on the glass transition; a strong attractive interaction results in an increase in the T_g.[10] There was an attractive interaction between PLMA and silica that was observed from the shift of the carbonyl peak and the disappearance of the isolated silanol peak in the FTIR spectra shown in Figure 1. However, there was no significant decrease or increase in the T_g when the polymer was adsorbed onto silica, suggesting that the adsorbed polymer, despite its H-bonding to the surface, had a mobility similar to the bulk polymer. The surface changed the conformation of the polymer backbone to allow adsorption and decrease crystallinity, but it did not affect the inherent mobility of the adsorbed polymers. One possible reason for this lack of increased glass transition might be that the flexibility of the side chains allowed fast exchange of the carbonyl groups on the surface. As such, the constraints on the surface could be minimal.

Information about the dynamics of adsorbed polymer systems can be obtained by looking at the heat capacity difference (ΔC_p) at the glass transition.[8,46] Typically, polymer that is tightly bound to the silica surface is more confined to the surface and thus has a lower ΔC_p as a result of restricted motion.[46] As previously mentioned, no distinct transition was observed for bound PLMA segments in the DSC despite evidence of

bound carbonyl groups to the surface. For more information, ΔC_p was calculated for both the bulk and adsorbed samples to determine any differences in dynamics. These values are shown in Table 5. Bulk PLMA had the smallest ΔC_p value indicating that the bulk sample has a smaller change in mobility through the glass transition. The behavior of PLMA and its silica composites deviates from what has typically been observed in other methacrylate polymer composite systems. One possible reason for this deviation is the presence of side chains in PLMA which become less ordered at smaller adsorbed amounts. The 3.56 mg/m^2 which is the most bulk-like has a slightly larger ΔC_p value than the bulk polymer, while the 0.74 mg/m^2 and 2.20 mg/m^2 samples had ΔC_p values much larger than that of the bulk polymer.

Table 5. ΔC_p for bulk and adsorbed samples

	Cp (J/g C)
0.74 mg/m2	0.295
2.20 mg/m2	1.407
3.56 mg/m2	0.070
Bulk PLMA	0.064

The glass transition temperature is a complex property that is affected by a number of factors.[47,48] Although the FTIR spectra of PLMA samples show interactions between the carbonyl groups and the surface silanol groups, the DSC results are harder to interpret due to the complexity of this side-chain crystalline system. One factor that could account for the differences observed between PMMA and PLMA systems is fragility. PMMA is considered a fragile polymer while PLMA is considered to be a "strong" polymer.[4] Fragile polymers are those which show steep variations close to the T_g (show non-Arrhenius temperature dependence) and whereas strong polymers show Arrhenius

dependence.[48] It has been suggested that for strong polymers such as PLMA, changes in structure within the glass transition temperature are small, but are a lot more evident in fragile polymers such as PMMA.[47] This was observed from the differences in behavior of the two methacrylate polymers upon adsorption. Due to the complexity of this system, we have yet to observe the dynamics of PLMA polymer segments that are directly bound to the surface.

This system differed from other side chain crystalline systems observed. One such system, a cationic polypeptide, poly(L-lysine)/clay nanocomposite system showed a decrease in side-chain crystallinity which was attributed to a decrease in the dimensions of the crystallites.[18] The reason for this decrease in crystallinity was hypothesized to be due to the clay particles acting as nuclei for crystallization, increasing the number of crystals, and thus decreasing the size of those crystals. In the case of adsorbed PLMA, the melting point remained constant indicating that the dimensions of the aggregates remained unchanged but the number of aggregates decreased. The adsorption of poly(ethylene-stat-vinyl acetate), on silica was also studied.[9] The effect of adsorption on the crystallinity of the ethylene units was observed. Like PLMA, this statistical copolymer had an attractive interaction with silica due to the presence of vinyl acetate units. Unlike PLMA, however, this system showed a decrease in the melting temperature with a decreasing adsorbed amount suggesting again a decrease in the size of the ethylene unit aggregates.

Conclusions

The effect of confinement on the side chain crystallinity of PLMA was studied using DSC and ATR-FTIR. A decrease in the amount of crystallinity of the PLMA side chains was found, but there was no significant change observed in the melting and glass transition temperatures. The polymer showed attractive interactions with silica, but unlike other methacrylate polymers, did not show an increased T_g. The smallest adsorbed amount sample showed the largest proportion of bound carbonyl groups, which likely caused a more extended backbone structure on the surface of silica resulting in a significant decrease in crystallinity. The smallest adsorbed amount sample was also found to show, in addition to hexagonal packing, orthorhombic and triclinic packing of the alkyl chains. The increased supercooling also suggested that the formation of crystals was hampered by adsorption. The surface affected the polymer units closest to the surface (tightly-bound) at around the same length scale for other polymers such as PMMA and PVAc, but the interesting and different properties of long chain polymethacrylates may be useful in different applications.

Acknowledgements. The financial support of the National Science Foundation (US) under Grant 1005606 and Oklahoma State University are acknowledged.

References

(1) Novak, B. M. Hybrid Nanocomposite Materials—between inorganic glasses and organic polymers. *Adv. Mater.* **1993**, *5*, 422-433.

(2) Hempel, E.; Huth, H.; Beiner, M. Interrelation between side chain crystallization and dynamic glass transitions in higher poly(n-alkyl methacrylates). *Thermochim. Acta* **2003**, *403*, 105-114.

(3) Beiner, M.; Schröter, K.; Hempel, E.; Reissig, S.; Donth, E. Multiple glass transition and nanophase separation in poly(n-alkyl methacrylate) homopolymers. *Macromolecules* **1999**, *32*, 6278-6282.

(4) Floudas, G.; Placke, P.; Stepanek, P.; Brown, W.; Fytas, G.; Ngai, K. L. Dynamics of the "strong" polymer of n-lauryl methacrylate below and above the glass transition. *Macromolecules* **1995**, *28*, 6799-6807.

(5) O'Leary, K. A.; Paul, D. R. Physical properties of poly(n-alkyl acrylate) copolymers. Part 2. Crystalline/non-crystalline combinations. *Polymer* **2006**, *47*, 1245-1258.

(6) Gao, H.; Harmon, J. P. An empirical correlation between glass transition temperatures and structural parameters for polymers with linear and branched alkyl substituents. *J. Appl. Polym. Sci.* **1997**, *64*, 507-517.

(7) Fromell, K.; Yang, Y.; Ekdahl, K. N.; Nilsson, B.; Berglin, M.; Elwing, H. Absence of conformational change in complement factor 3 and factor XII adsorbed to acrylate polymers is related to a high degree of polymer backbone flexibility. *Biointerphases* **2017**, *12*, 02D417.

(8) Blum, F. D.; Young, E. N.; Smith, G.; Sitton, O. C. Thermal analysis of adsorbed poly(methyl methacrylate) on silica. *Langmuir* **2006**, *22*, 4741-4744.

(9) Maddumaarachchi, M.; Blum, F. D. Thermal analysis and FT-IR studies of adsorbed poly(ethylene-stat-vinyl acetate) on silica. *J. Polym. Sci., Part B: Polym. Phys.* **2014**, *52*, 727-736.

(10) Porter, C. E.; Blum, F. D. Thermal characterization of PMMA thin films using modulated differential scanning calorimetry. *Macromolecules* **2000**, *33*, 7016-7020.

(11) Mathis, C. H.; Divandari, M.; Simic, R.; Naik, V. V.; Benetti, E. M.; Isa, L.; Spencer, N. D. ATR-IR investigation of solvent interactions with surface-bound polymers. *Langmuir* **2016**, *32*, 7588-7595.

(12) Krajnc, U. Š. a. M.: *Acrylic-clay nanocomposites by suspension and emulsion polymerization*; Royal Society of Chemistry: Cambridge, 2010.

(13) Ma, Y.; Zheng, X.; Shi, F.; Li, Y.; Sun, S. Synthesis of poly(dodecyl methacrylate)s and their drag-reducing properties. *J. Appl. Polym. Sci.* **2003**, *88*, 1622-1626.

(14) Puig, J.; Williams, R. J. J.; Hoppe, C. E. Poly(dodecyl methacrylate) as solvent of paraffins for phase change materials and thermally reversible light scattering films. *ACS Appl. Mater. Interfaces* **2013**, *5*, 9180-9185.

(15) He, Y.; Inoue, Y. Novel FTIR method for determining the crystallinity of poly(ε-caprolactone). *Polym. Int.* **2000**, *49*, 623-626.

(16) Neugebauer, D.; Theis, M.; Pakula, T.; Wegner, G.; Matyjaszewski, K. Densely heterografted brush macromolecules with crystallizable grafts. synthesis and bulk properties. *Macromolecules* **2005**, *39*, 584-593.

(17) Shi, H.; Zhao, Y.; Jiang, S.; Xin, J. H.; Rottstegge, J.; Xu, D.; Wang, D. Order–disorder transition in eicosylated polyethyleneimine comblike polymers. *Polymer* **2007**, *48*, 2762-2767.

(18) Krikorian, V.; Kurian, M.; Galvin, M. E.; Nowak, A. P.; Deming, T. J.; Pochan, D. J. Polypeptide-based nanocomposite: Structure and properties of poly(L-lysine)/Na+-montmorillonite. *J. Polym. Sci., Part B: Polym. Phys.* **2002**, *40*, 2579-2586.

(19) Hagemann, H.; Snyder, R. G.; Peacock, A. J.; Mandelkern, L. Quantitative infrared methods for the measurement of crystallinity and its temperature dependence: polyethylene. *Macromolecules* **1989**, *22*, 3600-3606.

(20) Reading, M.; Luget, A.; Wilson, R. Modulated differential scanning calorimetry. *Thermochim. Acta* **1994**, *238*, 295-307.

(21) Khanna, Y. P. Estimation of polymer crystallinity by dynamic mechanical techniques. *J. Appl. Polym. Sci.* **1989**, *37*, 2719-2726.

(22) Fontana, B. J.; Thomas, J. R. The configuration of adsorbed alkyl methacrylate polymers by infrared and sedimentation studies. *J. Phys. Chem.* **1961**, *65*, 480-487.

(23) Coleman, M. M.; Moskala, E. J. FTIR studies of polymer blends containing the poly(hydroxy ether of bisphenol A) and poly(ε-caprolactone). *Polymer* **1983**, *24*, 251-257.

(24) Krisanangkura, P.; Packard, A. M.; Burgher, J.; Blum, F. D. Bound fractions of methacrylate polymers adsorbed on silica using FTIR. *J. Polym. Sci., Part B: Polym. Phys.* **2010**, *48*, 1911-1918.

(25) Brandrup, J.; Immergut, E. H.: *Polymer Handbook*; John Wiley & Sons: New York, 1989.

(26) Guo, Y.; Jin, Y.; Su, Z. Spectroscopic study of side-chain melting and crystallization of regioregular poly(3-dodecylthiophene). *Polym. Chem.* **2012**, *3*, 861-864.

(27) Kulkeratiyut, S.; Kulkeratiyut, S.; Blum, F. D. Bound carbonyls in PMMA adsorbed on silica using transmission FTIR. *J. Polym. Sci., Part B: Polym. Phys.* **2006**, *44*, 2071-2078.

(28) Mansur, H. S.; Oréfice, R. L.; Mansur, A. A. P. Characterization of poly(vinyl alcohol)/poly(ethylene glycol) hydrogels and PVA-derived hybrids by small-angle X-ray scattering and FTIR spectroscopy. *Polymer* **2004**, *45*, 7193-7202.

(29) Jian, Y.; He, Y.; Wang, J.; Yang, W.; Nie, J. Rapid solid-state photopolymerization of octadecyl acrylate: low shrinkage and insensitivity to oxygen. *Polym. Int.* **2013**, *62*, 1692-1697.

(30) Murai, Y.; Yoshikawa, M. Polymeric pseudo-liquid membranes from poly(dodecyl methacrylate): KCl transport and optical resolution. *Polym J* **2013**, *45*, 1058-1063.

(31) Höhne, G. W. H. Another approach to the Gibbs–Thomson equation and the melting point of polymers and oligomers. *Polymer* **2002**, *43*, 4689-4698.

(32) Shi, H.; Zhao, Y.; Zhang, X.; Zhou, Y.; Xu, Y.; Zhou, S.; Wang, D.; Han, C. C.; Xu, D. Packing mode and conformational transition of alkyl side chains in N-alkylated poly(p-benzamide) comb-like polymer. *Polymer* **2004**, *45*, 6299-6307.

(33) Kabomo, M. T.; Blum, F. D.; Kulkeratiyut, S.; Kulkeratiyut, S.; Krisanangkura, P. Effects of molecular mass and surface treatment on adsorbed poly(methyl methacrylate) on silica. *J. Polym. Sci., Part B: Polym. Phys.* **2008**, *46*, 649-658.

(34) Mortazavian, H.; Fennell, C. J.; Blum, F. D. Structure of the interfacial region in adsorbed poly(vinyl acetate) on silica. *Macromolecules* **2016**, *49*, 298-307.

(35) Morillo, M.; Martínez de Ilarduya, A.; Muñoz-Guerra, S. Copoly(γ,dl-glutamate)s containing short and long linear alkyl side chains. *Polymer* **2003**, *44*, 7557-7564.

(36) Shibasaki, Y.; Saitoh, H.; Chiba, K. DSC and X-ray studies on side-chain crystallization of comb-like polymers. *J. Therm. Anal.* **1997**, *49*, 115-121.

(37) Kunisada, H.; Yuki, Y.; Kondo, S.; Igarashi, H. Synthesis and polymerization of isopropenyltriazines containing two alkyl groups and side-chain crystallization of the resulting polymers. *Polymer* **1991**, *32*, 2283-2288.

(38) Jordan, E. F.; Artymyshyn, B.; Speca, A.; Wrigley, A. N. Side-chain crystallinity. II. Heats of fusion and melting transitions on selected copolymers incorporating n-octadecyl acrylate or vinyl stearate. *J. Polym. Sci., Part A: Polym. Chem.* **1971**, *9*, 3349-3365.

(39) Jordan, E. F. Side-chain crystallinity. III. Influence of side-chain crystallinity on the glass transition temperatures of selected copolymers incorporating n-octadecyl acrylate or vinyl stearate. *J. Polym. Sci., Part A: Polym. Chem.* **1971**, *9*, 3367-3378.

(40) Jordan, E. F.; Riser, G. R.; Artymyshyn, B.; Pensabene, J. W.; Wrigley, A. N. Side-chain crystallinity. IV. Mechanical properties and transition temperatures of

copolymers of methyl methacrylate with higher n-alkyl acrylates and N-n-alkylacrylamides. *J. Polym. Sci., Part B: Polym. Phys.* **1972**, *10*, 1657-1679.

(41) Zhang, T.; Xu, G.; Li, Z.-F.; Regev, O.; Maddumaarachchi, M.; Blum, F. D. PS/CTAB/silica composites from room temperature polymerization of high internal phase emulsion gels. *J. Coll. Interf. Sci.* **2015**, *451*, 161-169.

(42) Zhang, T.; Xu, G.; Puckette, J.; Blum, F. D. Effect of silica on the structure of cetyltrimethylammonium bromide. *J. Phys. Chem. C* **2012**, *116*, 11626-11634.

(43) Platé, N. A.; Shibaev, V. P.; Petrukhin, B. S.; Zubov, Y. A.; Kargin, V. A. Structure of crystalline polymers with unbranched long side chains. *J. Polym. Sci., Part A: Polym. Chem.* **1971**, *9*, 2291-2298.

(44) Shi, H.; Zhao, Y.; Jiang, S.; Rottstegge, J.; Xin, J. H.; Wang, D.; Xu, D. Effect of main-chain rigidity on the phase transitional behavior of comblike polymers. *Macromolecules* **2007**, *40*, 3198-3203.

(45) Li, Y.; Ishida, H. Concentration-dependent conformation of alkyl tail in the nanoconfined space: Hexadecylamine in the silicate galleries. *Langmuir* **2003**, *19*, 2479-2484.

(46) Khatiwada, B. K.; Hetayothin, B.; Blum, F. D. Thermal properties of PMMA on silica using temperature-modulated differential scanning calorimetry. *Macromol. Symp.* **2013**, *327*, 20-28.

(47) Hu, Y.-F.; Zhang, X.-M.; Song, M. An approach for prediction of dynamic fragility of polymeric glasses. *Macromolecules* **2010**, *43*, 7391-7393.

(48) Sokolov, A. P.; Novikov, V. N.; Ding, Y. Why many polymers are so fragile. *J. Phys. Conden. Matter* **2007**, *19*, 205116.

CHAPTER IV

DYNAMICS OF METHYL METHACRYLATE SEGMENTS IN POLY(STYRENE-CO-METHYL METHACRYLATE) IN BULK AND ON SILICA

Abstract

The effect of adsorption and copolymer composition on the segmental dynamics of bulk and adsorbed samples of poly(methyl methacrylate) and poly(styrene-co-methyl methacrylate) copolymers on silica was studied using solid-state deuterium NMR spectroscopy. The experimental ^{2}H-NMR spectra were simulated based on a soccer ball model (truncated icosahedron) in which small angle jumps between one site and its three nearest neighbors occur with equal probability. The solid-state ^{2}H-NMR spectra bulk and adsorbed homo- and copolymers had significant differences, which indicated that as a result of adsorption, certain polymer segments had more restricted segmental motion. In addition, it appeared that the copolymers had larger fractions of bound MMA units than the homopolymer, PMMA, suggesting that MMA units are more readily found on the silica surface.

Introduction

Knowledge of the chemistry and physics of polymer-surface interactions is necessary for understanding composite systems. Polymer composites, in which polymers are mixed with a filler material such as fibers, sheets, or particles, have numerous applications of which the interactions of the polymers with the filler material surfaces are an integral part.[1] These interactions, due to adsorption, often result in changes in the physical and mechanical properties of the bulk polymers.[2] Therefore, the analysis of adsorbed polymers for understanding their behavior in a wide number of applications is important.

Homopolymers, block copolymer, and random copolymers have interfacial interactions that are of interest and have been studied extensively. Their properties can depend on a number of factors which include the interactions of comonomers, sequence distribution, and blockiness.[3] There are two possibilities in random copolymer adsorption; the first is one in which the comonomers interact with the surface in a similar manner and the second is one in which one comonomer interacts more with the surface than the other.[4] An example in which the second possibility is seen is in copolymers of styrene and methyl methacrylate (MMA) or (PS-r-MMA) in which the MMA groups interact more strongly with the silica surface due to the hydrogen bonding of these MMA groups to the silica surface silanols hydrogen bonding.[5]

A few studies have been made specifically on PS-r-MMA and other similar polymers that have led to significant conclusions. One such study, carried out by Kawaguchi and coworkers[6], showed that composition affected the adsorption of

polymers. In this study, it was determined that for styrene-methyl methacrylate copolymers, copolymers with higher styrene content were adsorbed preferentially on silica regardless of their size. They also found, in a similar study, that the adsorption behavior of these copolymers were mainly governed by the interaction between the surface and the monomer units, and thus, the surface coverage of these polymers decreases with increasing styrene content.[7] In addition to these experimental studies, molecular simulation has also become an increasingly important tool used to study these systems.[8-10] Using molecular simulations, the distributions of structurally random block copolymer molecules were determined and compared in the bulk thus providing a microscopic picture that can be difficult to obtain experimentally.

Studying the polymer-surface interface is challenging due to the thickness of the interphase. Fortunately, a wide variety of characterization techniques are available for the study of adsorbed polymers. These techniques included temperature modulated differential scanning calorimetry (TMDSC),[11-13] FTIR spectroscopy,[4,7,14-21] and nuclear magnetic resonance (NMR) which has been particularly useful for the analysis of the structures and dynamics of surface adsorbed polymers.[11-13] Solid state ^{2}H-NMR spectroscopy in particular can be used as an effective probe of the dynamics of polymers through the glass transition region because the solid state ^{2}H-NMR line shape is affected by the amplitude and frequency of molecular motion.

In this paper, we used solid state ^{2}H-NMR to investigate the behavior and microstructure of poly(styrene-co-methyl methacrylate) copolymers on silica. Specifically, the adsorption and dynamics of MMA-d_3 on silica at very small adsorbed amounts were probed as a function of polymer composition. The findings were compared

to those obtained from a previous study of bulk and adsorbed copolymers to facilitate a better understanding of these polymer-silica systems.[22]

Experimental

Materials. The polymers and adsorbed polymer samples studied were synthesized as reported in a previous study.[22] The synthesis and preparation of these polymers and adsorbed polymer samples are described briefly below.

Polymer synthesis. Deuterated methyl methacrylate (MMA-d_3) was synthesized first.[22,23] PMMA-d_3 and PS-*r*-PMMA-d_3 copolymers with different compositions (10%, 26%, 50 %, and 71% MMA-d_3) were synthesized via free radical polymerization using AIBN as the initiator at 60 °C. The polymers were precipitated from methanol. The copolymer compositions were determined using ^{1}H-NMR in $CDCl_3$ and gel permeation chromatography (in THF at 25 °C) was used to determine the molecular mass distributions of the polymers. The dn/dc values[24] and Mark-Houwink parameters[25] used were obtained from the literature.

Table 1. The copolymer compositions, weight average molecular masses (M_w) and polydispersity indices (PD) of the synthesized polymers.

Polymer	mol % of MMA-d_3	Molar mass (M_w) (kDa)	PD
PMMA-d_3	100	171	1.8
PS-*r*-PMMA-d_3 71% MMA-d_3	71	88	2.3
PS-*r*-PMMA-d_3 50 % MMA-d_3	50	91	1.9
PS-*r*-PMMA-d_3 26% MMA-d_3	26	87	2.2
PS-*r*-PMMA-d_3 10% MMA-d_3	10	94	1.9

Preparation of adsorbed samples. Adsorbed samples of PMMA-d_3 and PS-*r*-PMMA-d_3 copolymers were prepared by combining solutions of the homo- or copolymers in toluene with Cab-O-Sil M-5P fumed silica in test tubes. These test tubes were then shaken for 48 h. Following the shaking, the samples were dried by using a Pasteur pipette to pass air into them and then under vacuum at 60 °C for 48 h. The amount of polymer adsorbed in each sample was determined by thermogravimetric analysis (TGA) using a TA Instruments 2950 Thermogravimetric Analyzer (TA Instruments, New Castle, DE, USA) with a heating rate of 20 °C/min.

Characterization. The ^{2}H-NMR spectra of adsorbed samples of homo- and copolymers (~1 mg) were obtained using a Tecmag Discovery 400 WB spectrometer equipped with a Doty 8 mm ^{2}H wideline probe (DSI-1432) and a Doty Scientific temperature controller (Doty Scientific Inc., Columbia, SC, USA). A quadrupole-echo pulse sequence (delay-90-τ-90-τ-acquisition) with ^{2}H frequency of 61.48 MHz, a 90°

pulse width of 3.5 μs, and an echo time of 31 μs was used. The relaxation time between scans was 8 s. The number of scans collected for the bulk and adsorbed polymer samples was between 256 for bulk polymers and 16384 for composites with the smallest adsorbed amounts and the smallest MMA content. The spectra thus obtained were compared to results obtained from a previous study.[22]

^{2}H-NMR spectra simulation. The experimental ^{2}H-NMR spectra of the small adsorbed amount homo and copolymer samples were simulated using the EXPRESS program.[26] Prior to perfoming the simulations, symmetrization of the experimental spectra were done. A soccer ball model (truncated icosahedron), which was developed by Metin et al.,[12,27] was used to simulate the NMR line shapes. A 90° pulse width of 3.5 μs, a pulse spacing of 31 μs, and a reduced quadrupolar coupling constant of 50 kHz, to account for the fast methyl rotation, were used in the simulations. The EXPRESS program was used to obtain a series of simulated line shapes with different jump rates. MATLAB (The Mathworks, Inc., Natick, MA) was then used to fit the experimental line shapes with the simulated line shapes by minimizing the sum of the squares of the residuals of experimental and sum of the simulated spectra.[28] The weight fractions of each simulated spectrum used to generate the fits were also obtained by MATLAB.[28] These simulated results were again compared to the results from a previous study.[22]

Results

The solid state ^{2}H-NMR quadrupole echo spectra of bulk PMMA-d_3 and copolymers of PS-*r*-PMMA-d_3 with different compositions as a function of temperature are shown in Figure 1.[22] At low temperatures all the spectra shown in Figure 1 showed

powder patterns with splittings of about 37 kHz at the horns (points with the highest intensity). Increasing the temperature resulted in a change in the line shapes of the powder patters and the appearance of a middle peak. An ultimate collapse of the powder pattern to a single peak was observed upon further increasing the temperature. These effects were seen at all polymer compositions.

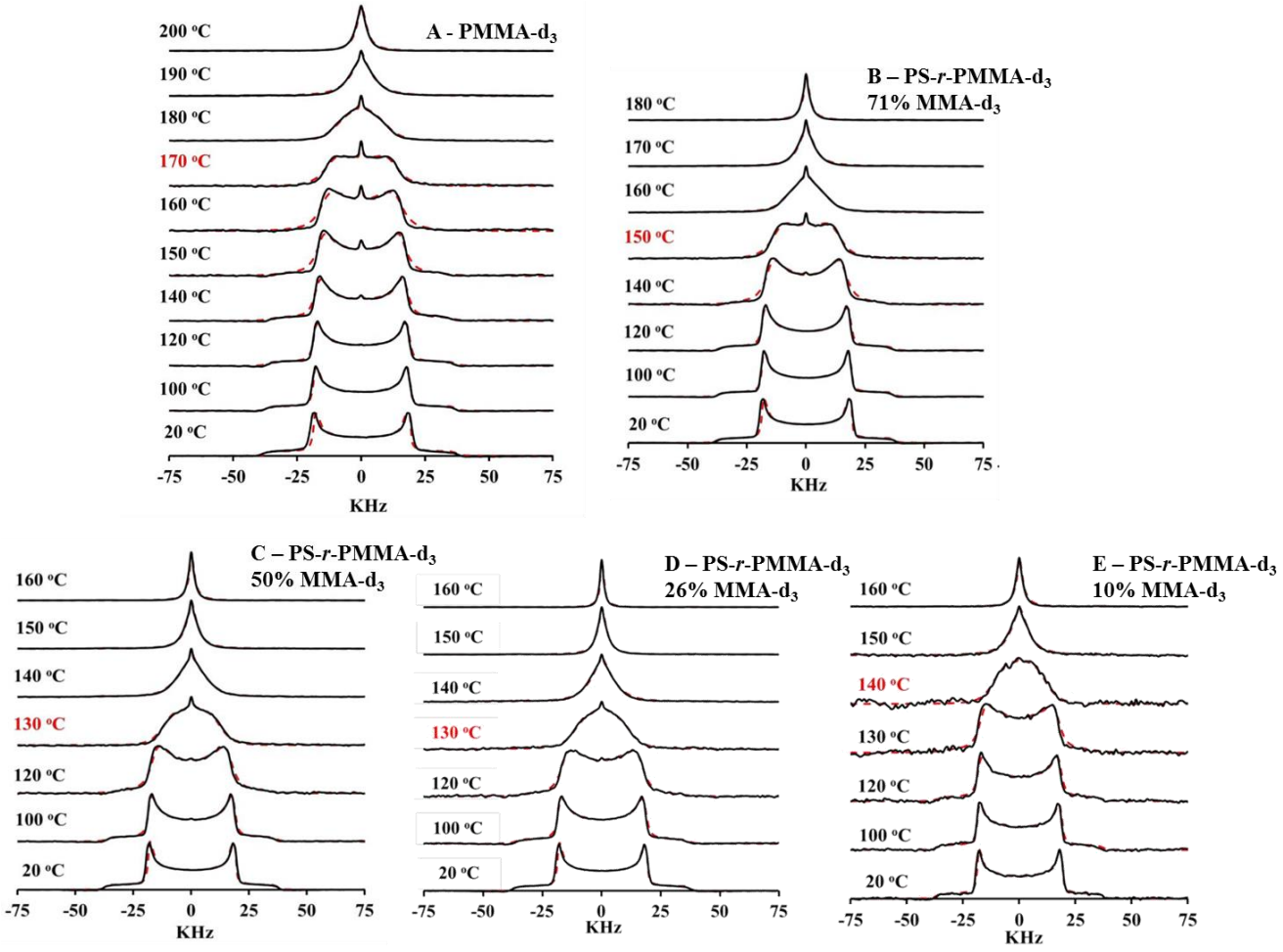

Figure 1. Experimental (solid) and simulated (dashed) ^{2}H-NMR quadrupole echo spectra for bulk A) PMMA-d_3, B) PS-*r*-PMMA-d_3 71% MMA-d_3, C) PS-*r*-PMMA-d_3 50% MMA-d_3, D) PS-*r*-PMMA-d_3 26% MMA-d_3, and E) PS-*r*-PMMA-d_3 10% MMA-d_3 as a function of temperature. Reproduced with permission.[22]

A series of jump rates (k), characterized as slow, intermediate or fast, from 1 Hz to $1x10^9$ Hz, were used to fit the experimental line shapes. The $k \leq 1 \times 10^6$ Hz region, where no significant intensity was lost during the quadrupole echo, was labeled as the slow region. The intermediate region is where 1×10^4 Hz $\leq k \leq 1 \times 10^6$ Hz and shows a significant intensity loss in the spectrum during the quadrupole echo. The fast region is for $k > 1 \times 10^6$ Hz where a small amount of intensity loss from the echo can be observed. Figure 2 shows the distribution of jump rates used to fit the experimental spectra of the bulk homo- and copolymers. The mass fractions of simulated spectra at different jump rates used in the fitting are shown as the height of the columns in the Figure 2. Figure 2 shows that for each bulk homo- and copolymer, the most intense contributions of jump rates for the fits moved from slow to intermediate region as the temperature increased.

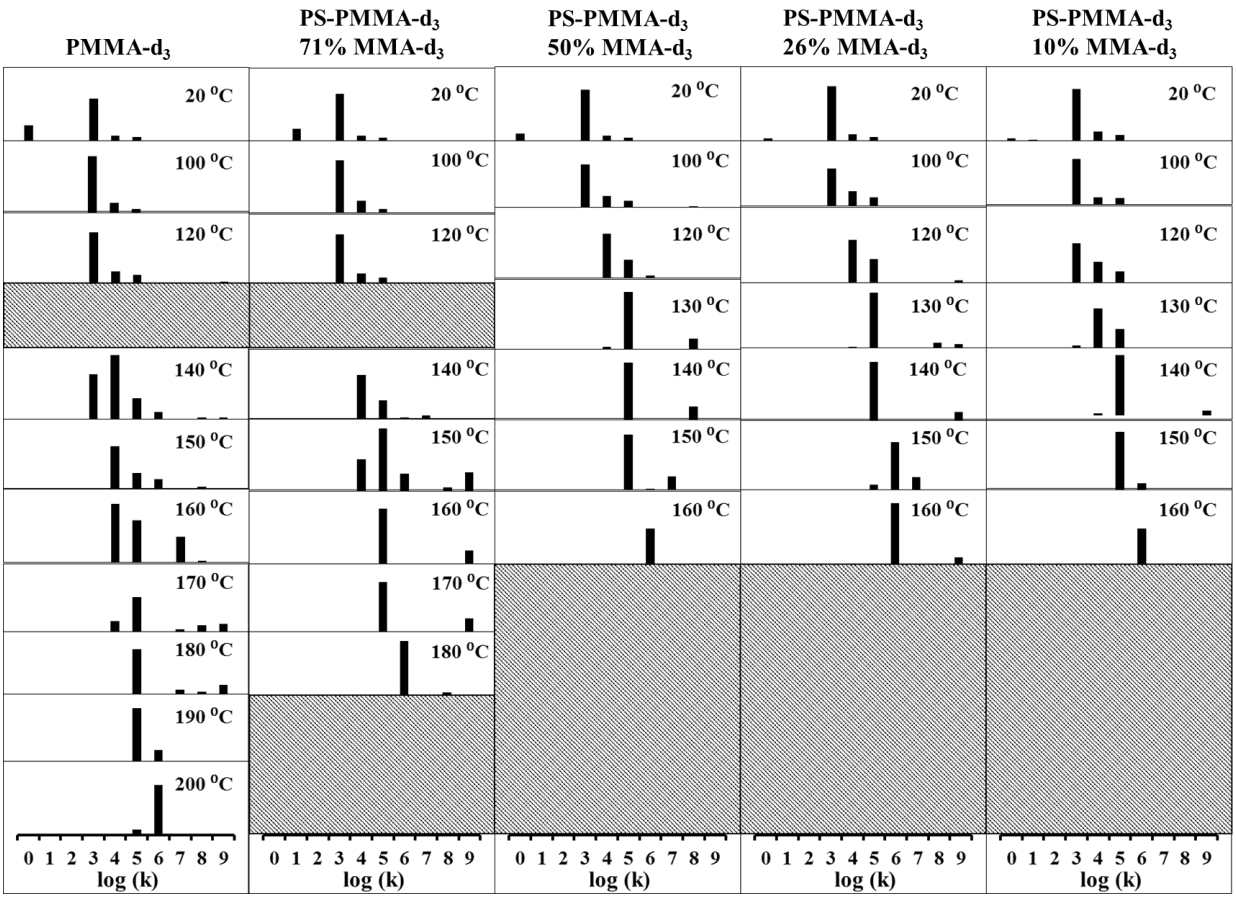

Figure 2. Distributions of jump rates used to fit the experimental spectra of bulk homo- and copolymers. Reproduced with permission.[22]

The experimental and simulated spectra of bulk and adsorbed PMMA-d_3 and copolymers of PS-*r*-PMMA-d_3 as a function of temperature are shown in Figures 3 – 7. In these figures, the spectra obtained from this study (~ 1mg/m^2) are compared to the spectra obtained from a previous study (bulk and 2mg/m^2).[22]

As can be seen from Figure 3, the bulk and adsorbed PMMA-d_3 samples had similar ^{2}H-NMR spectral line shapes up to around 120 °C. At temperatures above 150 °C,

the ^{2}H-NMR spectrum of bulk PMMA-d_3 showed a narrow central resonance which was not seen for the adsorbed samples. For the bulk polymer, as the temperature increased, the splitting of the powder pattern narrowed and eventually collapsed at higher temperatures into a single peak. At 200 °C, where the bulk polymer showed a single, relatively narrow resonance, the adsorbed sample spectra were still quite broad. This was particularly clear in the case of the smallest adsorbed amount. The narrowing of the powder pattern could be attributed to the increase in mobility of the polymer. The adsorbed samples, particularly the 1.02 mg/m^2 samples, showed significantly less mobility.

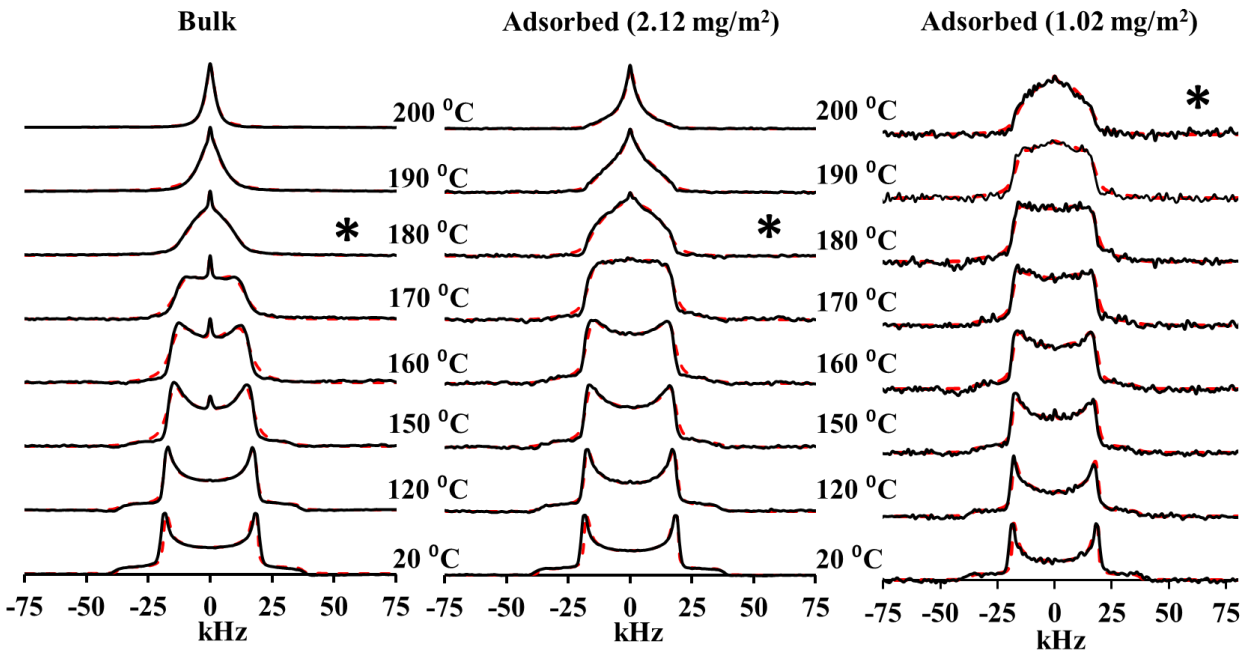

Figure 3. ^{2}H-NMR quadrupole echo spectra for bulk and adsorbed (2.12 mg/m^2 and 1.02 mg/m^2) PMMA-d_3 samples as a function of temperature. The spectra marked with the (*) are at the NMR glass transition. The spectra for the bulk and adsorbed 2.12 mg/m^2 sample were included in the figure with permission.[22]

^{2}H-NMR quadrupole echo spectra of bulk and adsorbed (1.79 mg/m^2 and 1.00 mg/m^2) PS-r-PMMA-d$_3$ 71% MMA-d$_3$ samples are shown in Figure 4 as a function of temperature. As was the case in Figure 3, the bulk and adsorbed spectra were similar until 120 °C. From 140 °C and higher, differences between bulk and adsorbed spectra could be seen. For the bulk polymer, the powder patter disappeared at 150 °C and no broader components could be seen at temperatures higher than 170 °C. However, in the spectra of the adsorbed samples, significant amounts of broad component were observed for the 1.79 mg/m^2 adsorbed at 180 °C and at 200 °C for the 1.00 mg/m^2 sample.

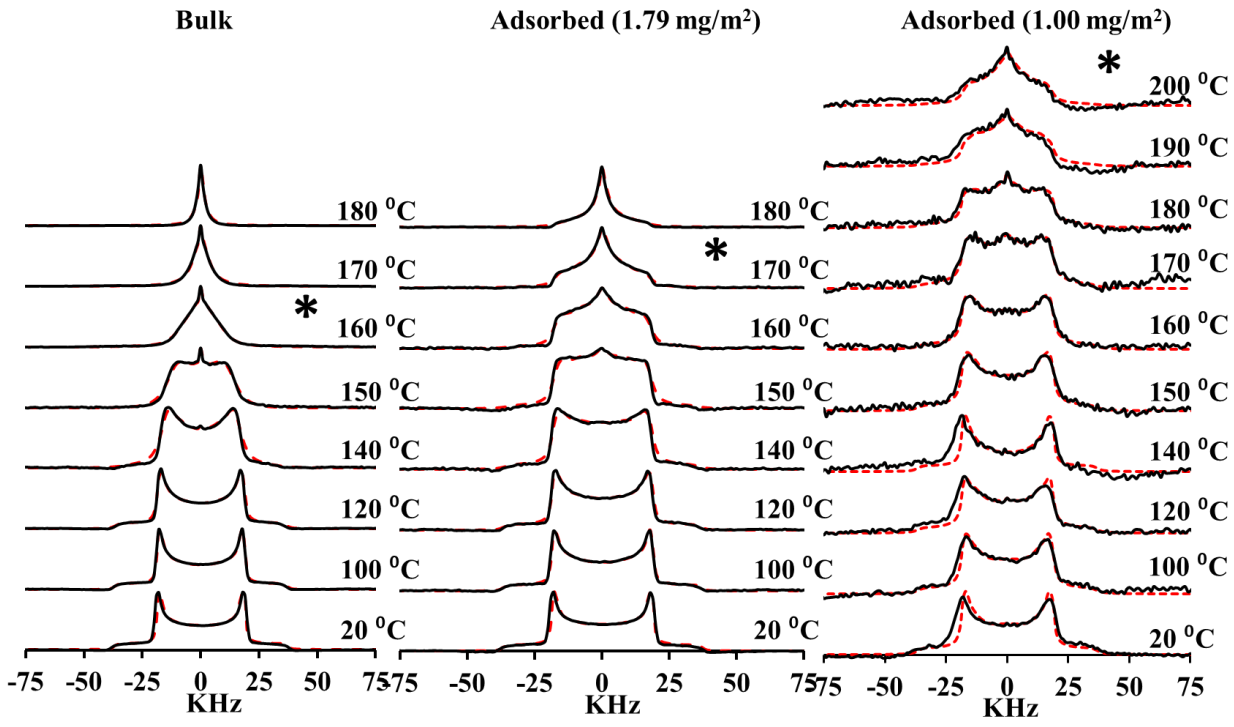

Figure 4. ^{2}H-NMR quadrupole echo spectra for bulk and adsorbed (1.79 mg/m^2 and 1.00 mg/m^2) PS-*r*-PMMA-d$_3$ 71% MMA-d$_3$ samples as a function of temperature. The spectra

marked with the (*) are at the NMR glass transition. The spectra for the bulk and adsorbed 1.79 mg/m^2 sample were included in the figure with permission.[22]

^{2}H-NMR spectra for bulk and adsorbed (1.89 mg/m^2 and 0.95 mg/m^2) PS-*r*-PMMA-d_3 50% MMA-d_3 samples are shown in Figure 5 as a function of temperature. Again, the spectra of bulk and adsorbed PS-*r*-PMMA-d_3 50% MMA-d_3 samples were similar at temperatures below 120 °C. For the bulk polymer, the powder pattern disappeared at around 130 °C and completely collapsed at 160 °C. In the case of the 1.89 mg/m^2 adsorbed sample, a significant amount of the residual powder pattern remained even at 160 °C. For the 0.95 mg/m^2 sample at this temperature, there was no complete powder pattern collapse.

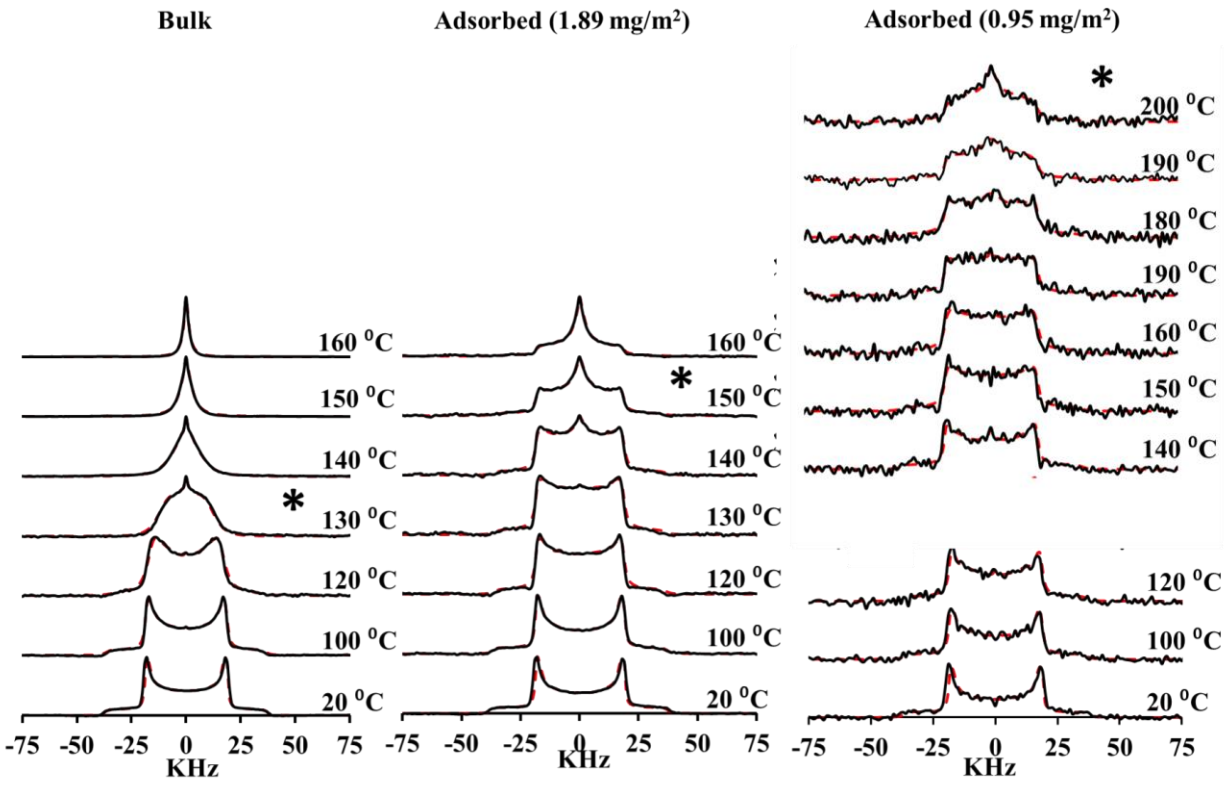

Figure 5. ^{2}H-NMR quadrupole echo spectra for bulk and adsorbed (1.89 mg/m^2 and 0.95

mg/m^2) PS-*r*-PMMA-d_3 51% MMA-d_3 samples as a function of temperature. The spectra marked with the (*) are at the NMR glass transition. The spectra for the bulk and adsorbed 1.89 mg/m^2 sample were included in the figure with permission.[22]

^{2}H-NMR quadrupole echo spectra for bulk and adsorbed (2 mg/m^2 and 0.98 mg/m^2) PS-*r*-PMMA-d_3 26% MMA-d_3 samples are shown in Figure 6 as a function of temperature. The spectra of bulk and adsorbed samples of PS-*r*-PMMA-d_3 26% MMA-d_3 were similar at temperatures below 120 °C. At around 150 °C the powder pattern of the bulk polymer completely collapsed, but a significant amount of the residual powder pattern can still be seen for the 2 mg/m^2 adsorbed. The spectra of the 0.98 mg/m^2 sample at that temperature showed a powder pattern indicating almost complete immobility. Even at 200 °C, a residual powder pattern remained.

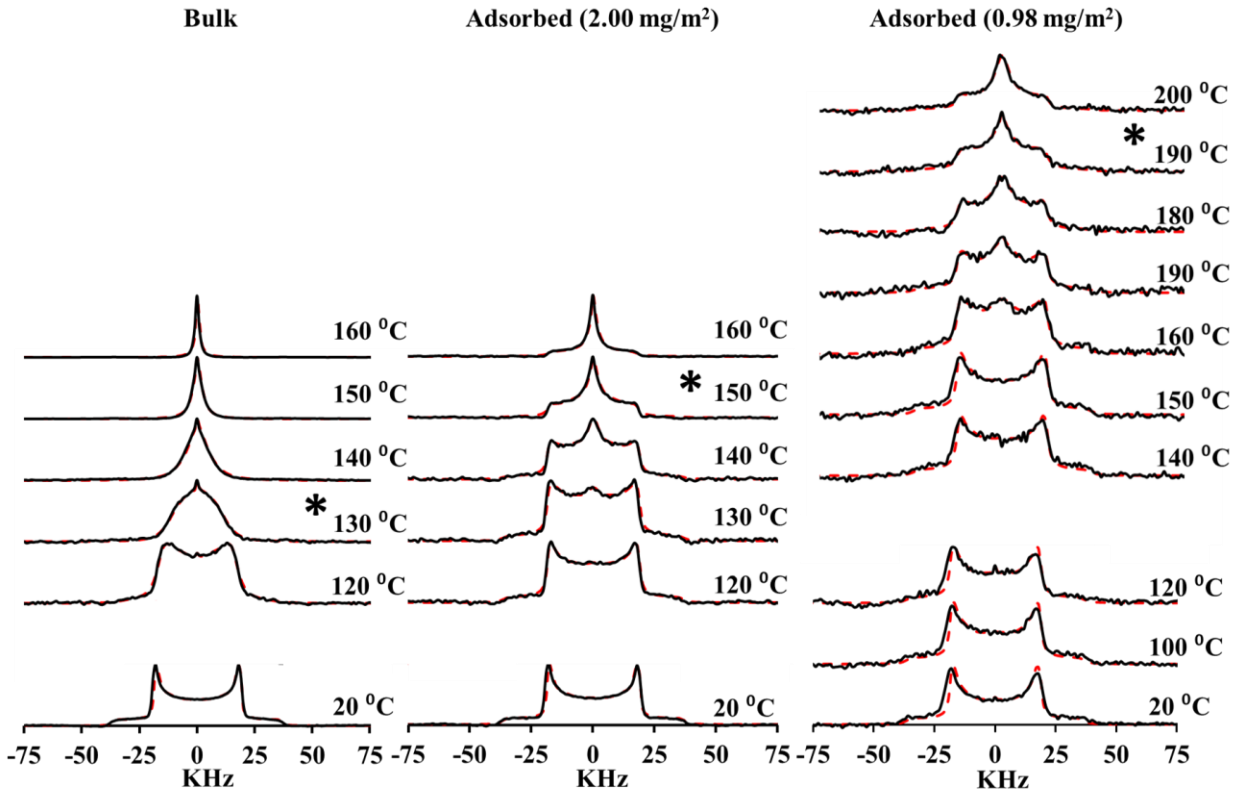

Figure 6. ^{2}H-NMR quadrupole echo spectra for bulk and adsorbed (2 mg/m^2 and 0.98 mg/m^2) PS-r-PMMA-d$_3$ 26% MMA-d$_3$ samples as a function of temperature. The spectra marked with the (*) are at the NMR glass transition. The spectra for the bulk and adsorbed 2 mg/m^2 sample were included in the figure with permission.[22]

^{2}H-NMR quadrupole echo spectra for bulk and adsorbed (2.24 mg/m^2 and 0.96 mg/m^2) PS-*r*-PMMA-d$_3$ 10% MMA-d$_3$ samples are shown in Figure 7 as a function of temperature. For the bulk polymer, the powder pattern disappeared at around 140 °C and completely collapsed at around 160 °C. The spectra of the 2.24 mg/m^2 adsorbed polymer also collapsed into a single peak with a very small residual powder pattern at 160 °C

showing slightly less mobility than the bulk polymer. The difference between these samples and the 0.96 mg/m^2 sample is quite striking. Even at 200 °C this adsorbed sample did not collapse and remained a powder pattern demonstrating the immobility of the MMA-d_3 units in the polymer.

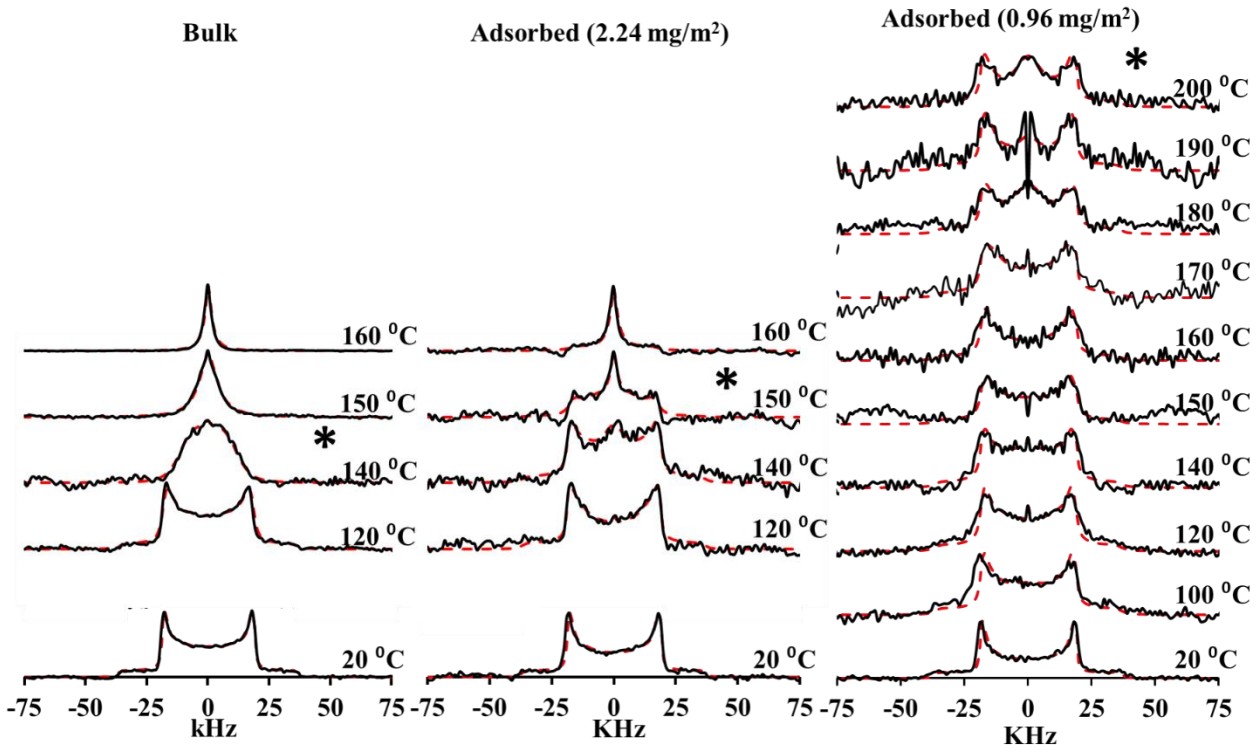

Figure 7. ^{2}H-NMR quadrupole echo spectra for bulk and adsorbed (2.24 mg/m^2 and 0.96 mg/m^2) PS-*r*-PMMA-d_3 10% MMA-d_3 samples as a function of temperature. . The spectra marked with the (*) are at the NMR glass transition. The spectra for the bulk and adsorbed 2.24 mg/m^2 sample were included in the figure with permission.[22]

The distributions of jump rates used to fit the experimental spectra of the adsorbed polymers as a function of temperature are shown in Figures 8 and 9. According

to these figures, at each sample composition, the most intense contributions of jump rates for the fits moved from the slow to the intermediate region with increasing temperature. A comparison of Figure 8 and Figure 2 showed that fits of adsorbed polymers contained a broader distribution of jump rates than the bulk polymers. Further, even at higher temperatures, significant amounts of slow and intermediate components were required for the fits of the adsorbed polymers. This was not the case for the bulk polymers.

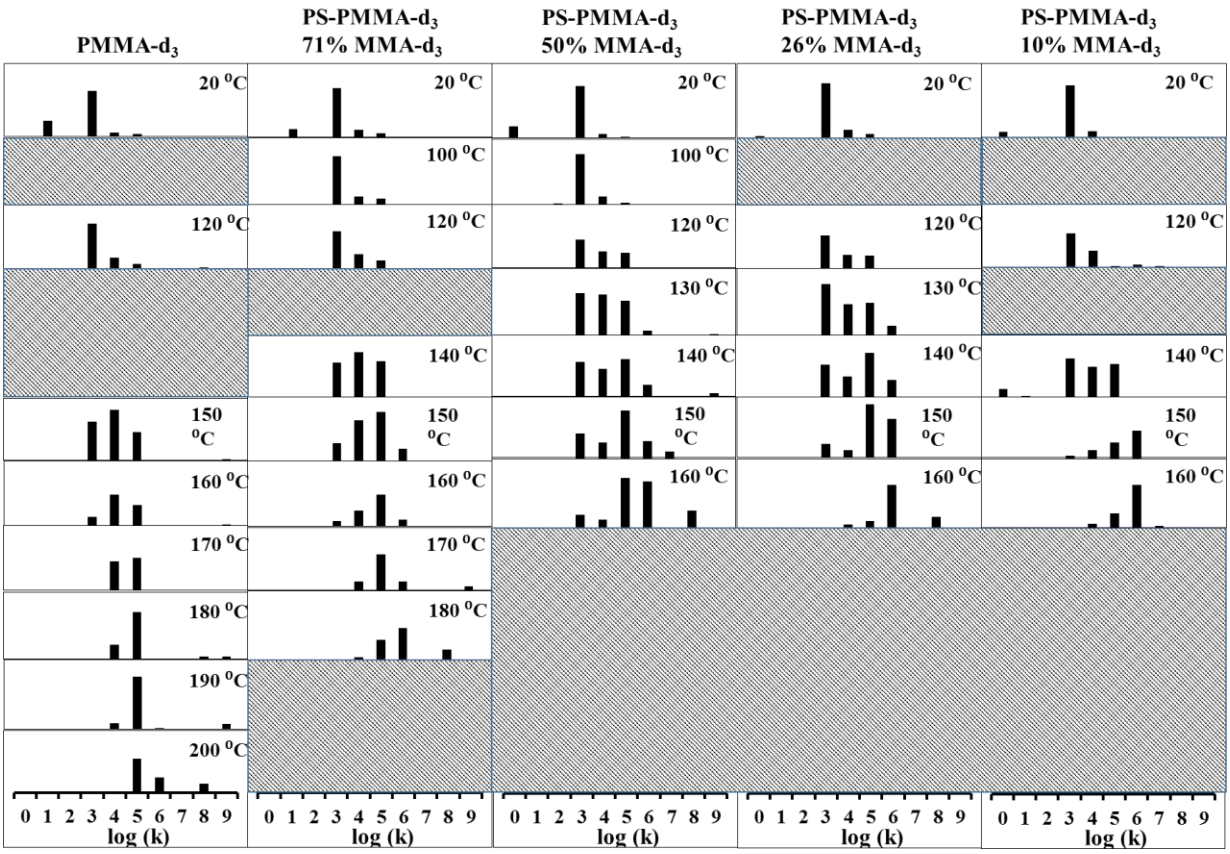

Figure 8. Distributions of jump rates used to fit the experimental spectra of adsorbed (~ 2 mg/m^2) homo- and copolymers. Reproduced with permission.[22]

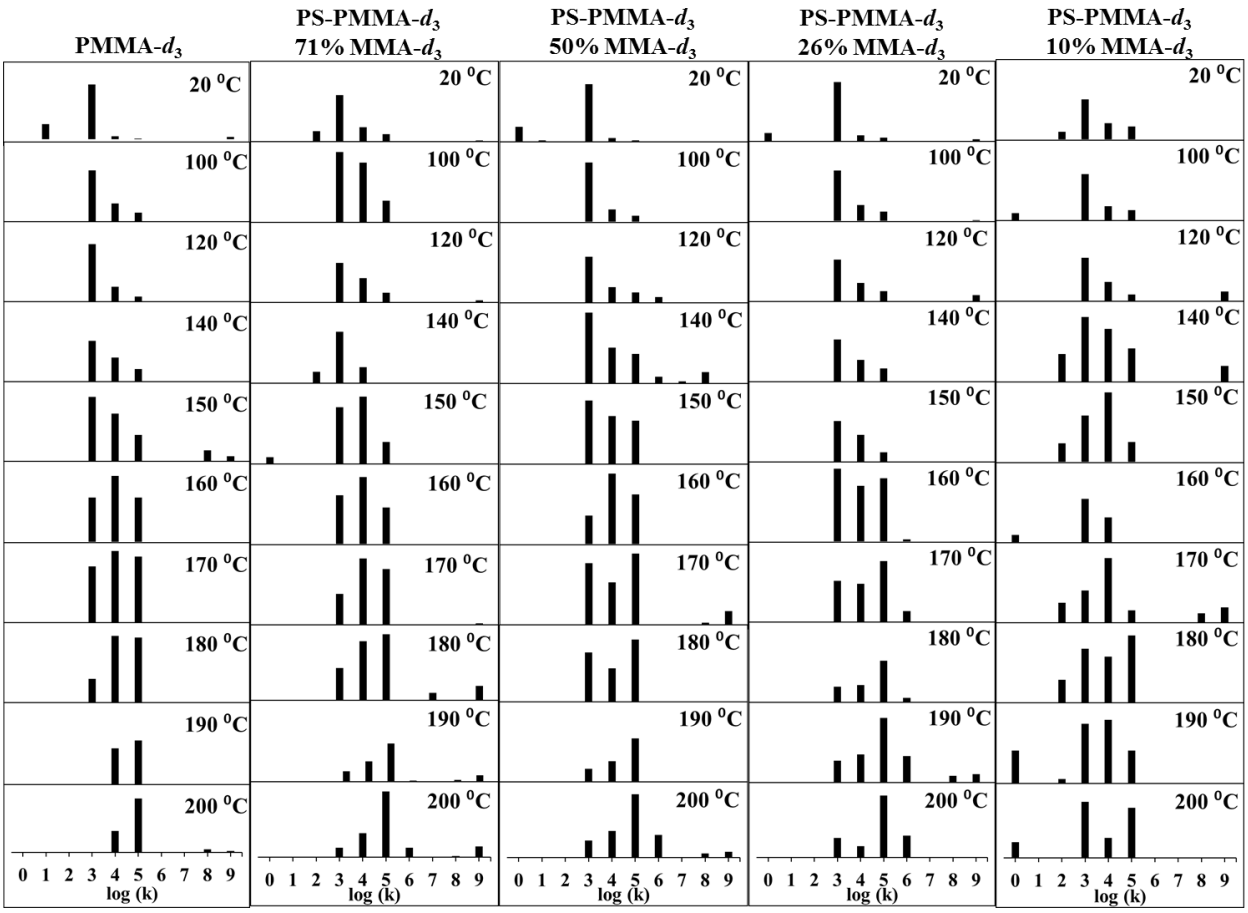

Figure 9. Distributions of jump rates used to fit the experimental spectra of adsorbed (~ 1 mg/m^2) homo- and copolymers.

The comparison of the NMR line shapes of different polymer compositions at different adsorbed amounts for a single temperature is shown in Figure 10. At each polymer composition, adsorption results in a higher fraction of MMA-d_3 segments with reduced mobility. This effect is not clearly seen in the PMMA-d_3 homopolymer, but can be observed at higher temperatures. The greatest reduction in mobility occured in the 1 mg/m^2 adsorbed amount samples. Figure 10 also allowed the comparison between different polymer compositions at 160 °C. This temperature was chosen for comparison because it showed variation in the spectra at different compositions. In the bulk polymer,

the mobility of the copolymers increased with the decreases in the amount of MMA-d_3 in the polymer. When the polymers are adsorbed at roughly 2 mg/m^2, the same trend is observed with a decrease in mobility and an increase in the amount of MMA-d_3 in the adsorbed polymer samples. However, this behavior was different from that seen in the copolymers when adsorbed at 1 mg/m^2. The 1 mg/m^2 samples showed significantly restricted motion relative to the bulk and the 2 mg/m^2 samples. As the amount of MMA-d_3 decreased, the mobility of the MMA-d_3 units increased except for the 10% MMA-d_3 sample which showed the most restricted motion.

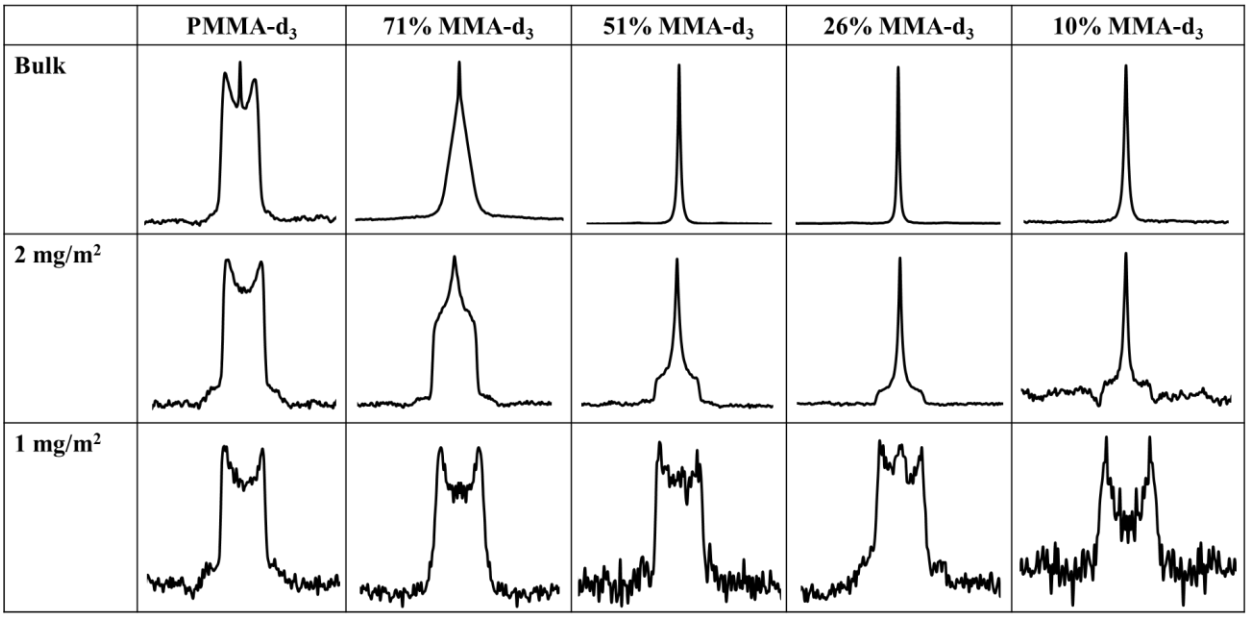

Figure 10. ^{2}H-NMR quadrupole echo spectra of bulk and adsorbed (~2 mg/m^2 and ~1 mg/m^2) of PMMA-d_3 and PS-*r*-PMMA-d_3 copolymers as a function of the polymer composition and adsorbed amount at 160 °C. The spectra for the bulk and 2 mg/m^2 used in this figure have been reproduced with permission.[22]

The polymer dynamics of PS-r-MMA can be evaluated using the average values of the jump rates, $\langle k \rangle$, used to fit experimental line shape. As a result of a broad distribution of jump rates required to fit the experimental spectra, the log of the average jump rates, $\langle k \rangle$ is dominated by the large k values. Therefore, the average of the logarithm of the jump rate, $\langle \log k \rangle$ was more appropriate for use in polymer dynamics comparisons than the $\log \langle k \rangle$. The $\langle \log k \rangle$ values of bulk and adsorbed homo- and copolymers as a function of temperature at different polymer compositions are shown in Figure 11. Figure 11 shows that adsorption results in restricted mobility as can be seen from the general decrease in $\langle \log k \rangle$ upon adsorption. As the temperature increased, the deviation between the $\langle \log k \rangle$ values for bulk and adsorbed polymers increased at all polymer compositions. The sample with 10% MMA-d_3 showed that the $\langle \log k \rangle$ did not increase with temperature as was seen for other polymer compositions.

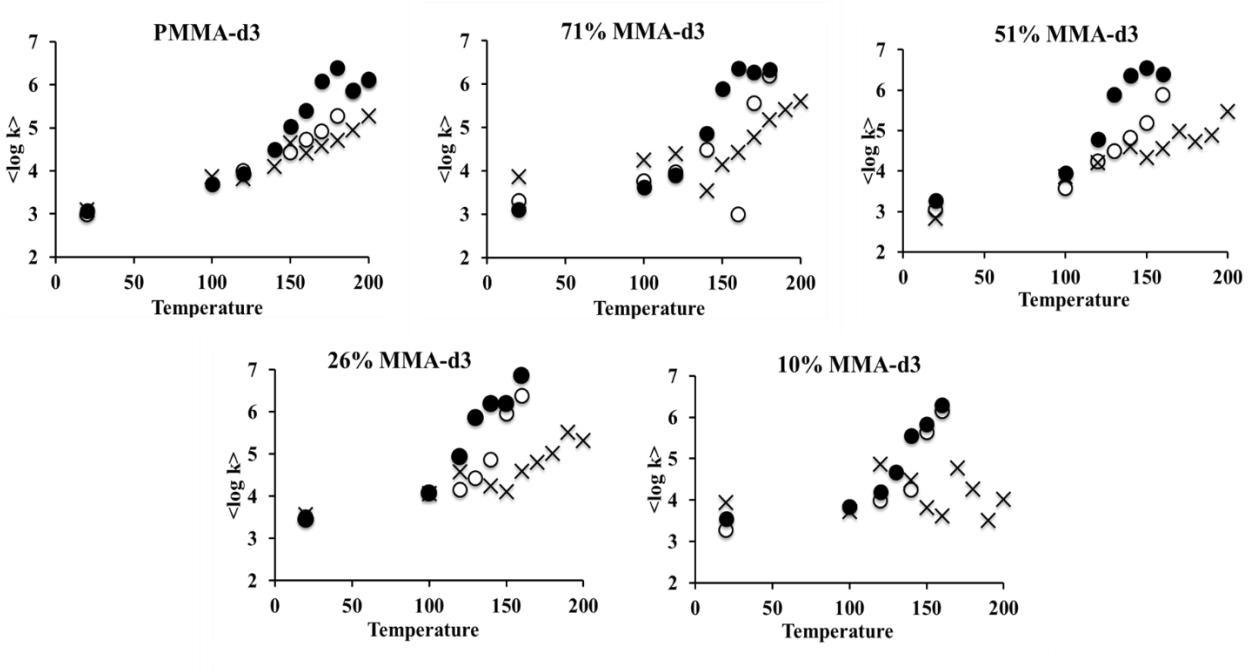

Figure 11. <log *k*> of the bulk (●)and adsorbed, 2 mg/m^2 (○)and 1 mg/m^2 (×), homo- and copolymers as a function of temperature for different polymer compositions.

Discussion

The dynamics of polymer segments on surfaces depend on the type of interaction between the polymer segment and the surface as well as the proximity of the polymer segments to the surface. Interactions of the polymer segments with surfaces can be either attractive or repulsive. In the case of PMMA on silica, adsorption is due to hydrogen bonding between the surface silanols of silica and the carbonyl groups of MMA; [14,15,29-31] this attractive interaction results in an increased T_g.[32,33] Not all polymer segments stick to the surface and the behavior of polymer segments at the surface can be visualized as trains (directly attached to the surface), loops (connecting two trains with no direct

surface contact) and tails.[3] The polymer segments in trains have restricted mobility resulting in a higher T_g than the bulk polymer; polymer segments in loops and tails have fewer restrictions and have T_gs that are similar to or slightly higher than those of the bulk polymer.[33] In the case of polystyrene (PS) on silica, the interactions between PS segments and the surface are weaker than those of PMMA which are preferentially attached to the surface.[34] Therefore, most of the PS segments adsorbed on silica surface more or less have bulk-like properties.[5] Due to the difference in the strengths of the interactions of PMMA and PS on silica one can expect that there would be more MMA segments in the trains than styrene for random copolymers of styrene and MMA.

The line shapes of ^{2}H-NMR spectra depend on the motions of polymer segments and can be used as an effective probe of the temperature dependence of a system. Figure 1 shows that the line shapes of the powder patterns of both homo- and copolymers change as temperature increases. This shows that as the temperature changes, the motions of the polymer segments change. Powder patterns with quadrupolar splittings of about 40 kHz at the horns were seen at low temperatures and indicated a glassy state. The C-D bond in static methyl groups has a quadrupolar coupling constant of about 170 kHz[35-37] which results in a static quadrupolar splitting of about 128 kHz. When the methyl groups undergo fast, continuous rotation around their symmetric axis, the quadrupolar splitting is reduced to 40 kHz. At higher temperatures, a middle peak associated with fast moving polymer segments appears. The initial appearance of this narrow middle peak could initially be attributed to more mobile chain ends.[12,13] Increasing the temperature further eventually led to the narrowing and collapse of the powder patter to a single, narrower resonance indicating that the polymer was now in a rubbery state. It is worth noting that

this process occurred at different temperatures for the bulk and adsorbed polymers due to their different glass transition temperatures.

The ^{2}H-NMR spectra of bulk and adsorbed homo- and copolymers of PMMA are shown in Figures 3 – 7. In these spectra, the appearance of a middle resonance was observed as the temperature increased. This central resonance could be associated with polymer segments in loops and tails which are loosely bound to silica. At higher temperatures, residual powder patterns were due to polymer segments which were tightly-bound to silica in trains and had the most restricted mobility. It should be noted in Figure 1, which showed the ^{2}H-NMR spectra of the bulk homo- and copolymers, all of the polymer segments showed similar behavior and could be referred to as "spatially homogeneous" with respect to the uniform narrowing of powder patterns with increased temperature. In other words, all the polymer segments in different parts of the sample behaved similarly. In contrast, the adsorbed samples of homo- and copolymers showed the presence of components with different dynamics and could be referred to as "spatially heterogeneous".[12,13,27]

The distribution of jump rates used in the fitting of experimental line shapes can be used as an effective indicator of the motional heterogeneity in these systems. As shown in Figure 2, for bulk homo- and copolymers, at low and intermediate temperatures, there was a broad distribution of jump rates indicating a distribution of segmental motions. At higher temperatures, the breadth of the distribution of jump rates significantly reduced indicating more isotropic motion beyond the T_g of the polymers. The main difference in the distribution of jump rates of the homo and copolymers was the temperature at which the distribution of jump rates was narrowed; this difference was due

to the inherent differences in the T_gs of the bulk homo- and copolymers due to their different compositions.

The distribution of jump rates used to fit the experimental line shapes can be used to evaluate the motional heterogeneity of the polymer segments adsorbed on the silica surface. Figures 2, 8 and 9 show comparisons of jump rates for bulk and adsorbed samples. These figures show that the fits of adsorbed polymers comprise of a broader distribution of jump rates than the bulk polymers. The higher degree heterogeneity of adsorbed polymer segments was demonstrated by the larger amounts of slow and intermediate components needed to fit adsorbed polymers even at high temperatures. This was not the case for bulk polymers. Figure 11 showed that at higher temperatures, adsorbed samples had smaller <*log k*> values than the bulk samples. The 1 mg/m^2 samples had, on average, the smallest <*log k*> values confirming the restricted mobility of the polymer segments due to the adsorption. The restriction in mobility was strongest in the 1 mg/m^2 adsorbed sample of the PS-*r*-PMMA-d_3 10% MMA-d_3 as shown by the fact that its <*log k*> values did not increase consistently with temperature like other polymer compositions.

Information obtained from ^{2}H-NMR studies gives a detailed view of the adsorbed polymer structure. The ^{2}H-NMR spectra of all the samples were obtained at the same temperature of 160 °C and compared according to polymer composition and adsorbed amount in Figure 10. A study done by Nasreddine and coworkers showed that for polyethylene-co-acrylic acid adsorbed on zirconia at low coverage, the acrylic acid group binds to the surface and the polyethylene segments loop out into the solvent environment.[38] When dried, the conformation of the polymer depended on the constraints

created by the bound acrylic acid groups. This provides an interesting system to compare ours to. Figure 10 shows that the smallest coverage samples, the 1 mg/m^2 samples, have the most restriction in motion indicating that the methyl methacrylate segments are directly bound to the surface with the styrene segments looping out into the solvent. This was most evident for the copolymer composition with 10 % MMA-d_3. For copolymers adsorbed at higher adsorbed amounts, the polymer chains are in more extended configurations and in some cases, not directly attached to the surface.[38] As a result, such polymer chains would be more bulk-like in terms of mobility and morphology. Figure 10 showed that the samples with larger adsorbed amounts showed bulk-like behavior in addition to some restricted segmental motion.

The solid state ^{2}H-NMR spectra of adsorbed homo- and copolymers show that the fraction of MMA-d_3 segments with restricted mobility increased with decreasing MMA content. This effect was particularly striking for the copolymer with the lowest MMA content at the lowest adsorbed amount. Solid state ^{2}H-NMR was able to reflect the preferential binding of MMA segments over styrene.

Conclusions

The dynamics of PMMA-d_3 and its styrene copolymers were studied in bulk and at different adsorbed amounts using solid state ^{2}H-NMR. It was found that the MMA segments closest to the silica surface have restricted mobilities as a result of adsorption. It was also clear that the adsorbed polymer samples had motional gradients which resulted in heterogeneous behavior. Simulations of the NMR lineshapes also provided some insight. The $\langle \log k \rangle$ decreased with decreasing adsorbed amount indicating restricted

mobility. This was especially evident in the 1 mg/m^2 adsorbed sample of PS-*r*-PMMA-d_3 10% MMA-d_3 which had the least MMA-d_3 and did not show a significant increase in mobility with temperature.

Acknowledgements. The financial support of the National Science Foundation (US) is acknowledged as is Mr. Damith C. Perera for his assistance with NMR simulations using MATLAB. Some of the data used in this chapter was used with the permission of Dr. Madhubhashini Madduma Arachchilage. In particular the ^{2}H-NMR spectra for bulk and adsorbed (~ 2mg/m^2) homo and copolymer samples.

References

(1) Hetayothin, B.; Cabaniss, R. A.; Blum, F. D. Does plasticizer penetrate tightly bound polymer in adsorbed poly(vinyl acetate) on silica? *Macromolecules* **2017**, *50*, 2092-2102.

(2) Zou, H.; Wu, S.; Shen, J. Polymer/silica nanocomposites: preparation, characterization, properties, and applications. *Chem. Rev.* **2008**, *108*, 3893-3957.

(3) Fleer, G.; Stuart, M. C.; Scheutjens, J.; Cosgrove, T.; Vincent, B.: *Polymers at interfaces*; Chapman & Hall: London, 1993.

(4) Kawaguchi, M.; Funayama, A.; Yamauchi, S.-I.; Takahashi, A.; Kato, T. Adsorption of ethylene-vinyl acetate copolymer on silica surfaces II. *J. Colloid Interface Sci.* **1988**, *121*, 130-135.

(5) Zhang, B.; Blum, F. D. Modulated differential scanning calorimetry of ultrathin adsorbed PS-r-PMMA copolymers on silica. *Macromolecules* **2003**, *36*, 8522-8527.

(6) Kawaguchi, M.; Itoh, K.; Yamagiwa, S.; Takahashi, A. Random copolymer adsorption. II. Competitive and displacement adsorption. *Macromolecules* **1989**, *22*, 2204-2207.

(7) Yamagiwa, S.; Kawaguchi, M.; Kato, T.; Takahashi, A. Random copolymer adsorption. I. Infrared study at a silica surface. *Macromolecules* **1989**, *22*, 2199-2203.

(8) Lishchuk, S. V.; Ettelaie, R.; Annable, T. On the structural polydispersity of random copolymers adsorbed at interfaces: comparison of surface and bulk distributions. *Mol. Phys.* **2017**, *115*, 1343-1351.

(9) Sun, L.; Peng, C.; Liu, H.; Hu, Y.; Jiang, J. Analogy in the adsorption of random copolymers and homopolymers at solid-liquid interface: A Monte Carlo simulation study. *J. Chem. Phys.* **2007**, *126*, 094905.

(10) Kłos, J. S.; Romeis, D.; Sommer, J. U. Adsorption of random copolymers from a melt onto a solid surface: Monte Carlo studies. *J. Chem. Phys.* **2010**, *132*, 024907.

(11) Blum, F. D.; Xu, G.; Liang, M.; Wade, C. G. Dynamics of poly(vinyl acetate) in bulk and on silica. *Macromolecules* **1996**, *29*, 8740-8745.

(12) Metin, B.; Blum, F. D. Molecular mass and dynamics of poly(methyl acrylate) in the glass-transition region. *J. Chem. Phys.* **2006**, *124*, 054908.

(13) Lin, W.-Y.; Blum, F. D. Segmental dynamics of bulk and silica-adsorbed poly (methyl acrylate)-d 3 by deuterium NMR: the effect of molecular weight. *Macromolecules* **1998**, *31*, 4135-4142.

(14) Kulkeratiyut, S.; Kulkeratiyut, S.; Blum, F. D. Bound carbonyls in PMMA adsorbed on silica using transmission FTIR. *J. Polym. Sci., Part B: Polym. Phys.* **2006**, *44*, 2071-2078.

(15) Krisanangkura, P.; Packard, A. M.; Burgher, J.; Blum, F. D. Bound fractions of methacrylate polymers adsorbed on silica using FTIR. *J. Polym. Sci., Part B: Polym. Phys.* **2010**, *48*, 1911-1918.

(16) Korn, M.; Killmann, E. Infrared and micro-calorimetric studies of the adsorption of polymers with ester groups, in the main or side-chain, at the silica-carbon tetrachloride interface. *J. Colloid Interface Sci.* **1980**, *76*, 19-31.

(17) Landry, C. J.; Coltrain, B. K.; Landry, M. R.; Fitzgerald, J. J.; Long, V. K. Poly(vinyl acetate)/silica-filled materials: material properties of in situ vs fumed silica particles. *Macromolecules* **1993**, *26*, 3702-3712.

(18) Kawaguchi, M.; Inoue, A.; Takahashi, A. Adsorption of ethylene-vinyl acetate copolymer on silica surface. *Polym. J.* **1983**, *15*, 537-542.

(19) Botham, R.; Thies, C. The adsorption behavior of polymer mixtures. *J. Polym. Sci., Part C: Polym. Symp.* **1970**, *30*, 369-380.

(20) Hara, K.; Mizuhara, K.; Imoto, T. Adsorption of polymers at the solution-solid interfaces. *Kolloid. Z. Z. Polym.* **1970**, *238*, 438-441.

(21) Maddumaarachchi, M.; Blum, F. D. Thermal analysis and FT-IR studies of adsorbed poly(ethylene-stat-vinyl acetate) on silica. *J. Polym. Sci., Part B: Polym. Phys.* **2014**, *52*, 727-736.

(22) Arachchilage, M. M. Structure and dynamics of polymers and surfactants in bulk and on silica. PhD Thesis, Oklahoma State University, Stillwater, OK, 2015.

(23) Jenkins, A. D.; Rayner, M. G. The effect of polymerization temperature on the structure of radical copolymers. *Eur. Polym. J.* **1972**, *8*, 221-236.

(24) Zhang, B. Thermal behavior of thin-polymer films on silica. Missouri University of Science and Technology, 2003.

(25) Goldwasser, J.; Rudin, A. Analysis of block and statistical copolymers by gel permeation chromatography: Estimation of Mark-Houwink constants. *J. Liq. Chromatogr.* **1983**, *6*, 2433-2463.

(26) Vold, R. L.; Hoatson, G. L. Effects of jump dynamics on solid state nuclear magnetic resonance line shapes and spin relaxation times. *J. Magn. Reson.* **2009**, *198*, 57-72.

(27) Metin, B.; Blum, F. D. Segmental dynamics in poly (methyl acrylate) on silica: Molecular-mass effects. *J. Chem. Phys.* **2006**, *125*, 054707.

(28) Hetayothin, B. Effect of structure and plasticizer on the glass transition of adsorbed polymer. Missouri University of Science and Technology, 2010.

(29) Berquier, J.-M.; Arribart, H. Attenuated total reflection Fourier transform infrared spectroscopy study of poly (methyl methacrylate) adsorption on a silica thin film: polymer/surface interactions. *Langmuir* **1998**, *14*, 3716-3719.

(30) Fontana, B. J.; Thomas, J. R. The configuration of adsorbed alkyl methacrylate polymers by infrared and sedimentation studies. *J. Phys. Chem.* **1961**, *65*, 480-487.

(31) Soga, I.; Granick, S. Segmental orientations of trains versus loops and tails: the adsorbed polymethylmethacrylate system when the surface coverage is incomplete. *Colloids Surf., A* **2000**, *170*, 113-117.

(32) Blum, F. D.; Young, E. N.; Smith, G.; Sitton, O. C. Thermal analysis of adsorbed poly(methyl methacrylate) on silica. *Langmuir* **2006**, *22*, 4741-4744.

(33) Porter, C. E.; Blum, F. D. Thermal characterization of PMMA thin films using modulated differential scanning calorimetry. *Macromolecules* **2000**, *33*, 7016-7020.

(34) Van der Beek, G.; Stuart, M. C.; Fleer, G.; Hofman, J. Segmental adsorption energies for polymers on silica and alumina. *Macromolecules* **1991**, *24*, 6600-6611.

(35) Jelinski, L. W.; Sullivan, C.; Torchia, D. 2H NMR study of molecular motion in collagen fibrils. *Nature* **1980**, *284*, 531-534.

(36) Beshah, K.; Olejniczak, E. T.; Griffin, R. G. Deuterium NMR study of methyl group dynamics in L-alanine. *J. Chem. Phys.* **1987**, *86*, 4730-4736.

(37) Hiyama, Y.; Roy, S.; Guo, K.; Butler, L. G.; Torchia, D. A. Unusual asymmetry of methyl deuterium EFG in thymine: a solid state deuterium NMR and ab initio MO study. *J. Am. Chem. Soc.* **1987**, *109*, 2525-2526.

(38) Nasreddine, V.; Halla, J.; Reven, L. Conformation of adsorbed random copolymers: A solid-state NMR and FTIR-PAS study. *Macromolecules* **2001**, *34*, 7403-7410.

CHAPTER V

THE GLASS TRANSITION OF "LOOSELY BOUND" PMMA ADSORBED ON SILICA IS MOLECULAR MASS DEPENDENT

Abstract

Poly(methyl methacrylate) polymers with different molecular masses were adsorbed on silica and studied using FTIR and temperature modulated DSC. The adsorption of PMMA on silica resulted in glass transition temperature increases for all molecular masses observed. The glass transition of the polymer on the surface of silica increased with decreasing molecular mass. FTIR specifically confirmed the hydrogen bonding of the carbonyl groups to the silica surface silanols and the molecular mass dependence of the bound fraction. Lower molecular mass polymers had larger bound fractions indicating that they are more extended on the surface than higher molecular mass polymers. TMDSC also shed light on the effect of molecular mass on adsorption. Smaller adsorbed amounts showed larger increases in glass transitions and their 'loosely bound' fractions were seen to be more restricted on the surface than that of higher molecular mass polymers.

Introduction

Polymer nanocomposites are a class of materials that continue to attract a lot of attention because of their properties and importance in a large number of applications.[1] Many studies have shown that the polymers present at the interface of these materials generally have different properties than bulk polymers. This is especially true of polymer nanocomposites with relatively small amounts of polymer.[2] The change in polymer properties is usually the result of the presence of interfacial interactions, such as hydrogen bonding, between the polymer and the surface of the filler.[3] Quite a few studies have shown that polymers that have attractive interactions with a solid substrate have restricted mobility due to the presence of interactions. This reduction in mobility is confined to a few nanometers (tightly bound) from the surface[4] and has been shown by many techniques.[4-7] In some cases, the tightly bound layer is seen to be somewhat immobilized[6,8-10] and in others, a second, broader glass transition was observed.[11-18]

There are different factors that affect the adsorption of polymers onto surfaces. Polymer adsorption is determined first by, the attraction of monomers to the surface due to attractive interactions between the surface and the monomers and second, entropic repulsion between the monomers that are confined to the surface.[19] Studies have shown that molecular mass also has an impact on polymer adsorption. It has been found that larger polymer chains in randomly adsorbed polymers will displace smaller chains are not easily displaced or desorbed.[20]

In addition to impacting adsorption, the molecular mass also has an effect on other polymer properties such as glass transition temperature, and viscosity. The reason

for this effect on different properties is the increased chain end concentration; this is especially important at very low molecular masses. The dependence of glass transition is shown in the Fox-Flory equation which is shown in equation (1) below.

$$T_g = T_{g,\infty} - \frac{K}{M_n} \quad (1)$$

where $T_{g,\infty}$ is the T_g in the limit of infinite M_n and K is an empirical parameter for a particular polymer species.

Previous studies have shown that polymers adsorbed at interfaces have a looped structure with a fraction of their segments directly attached to the surface.[21] It is thus possible to have different local structures on the surface. On one hand, it is possible to have relatively flat polymer layers and on the other hand, there could be layers which are highly extended away from the surface.[22] The fraction of bound polymer segments can be determined by a number of spectroscopic techniques. These include reflectometry, ellipsometry, small angle neutron scattering, and nuclear magnetic resonance and electron spin resonance.[23] Using these techniques, the concentrations of free and bound segments can be determined and the bound fraction of the polymer can be calculated. These measurements can give significant insight into the polymer surface structure.[22,24] The bound fraction is related to the configuration of the polymer chain on the surface. The larger the fraction of attached segments per chain, the flatter the chain configuration is expected to be. Combining these techniques with other techniques such as DSC, can give an idea of the behavior of polymers at the interphase and how the configuration affects the properties of polymers adsorbed on surfaces.

One of the techniques particularly suited for the study of polymer behavior on the surface due to hydrogen bonding is FTIR spectroscopy which has been used in quite a few studies.[25-30] For example, a study by Fontana and Thomas used FTIR to estimate the amount of bound polymer segments of alkyl methacrylate polymers based on the spectral shift of the carbonyl vibration associated with the formation of hydrogen bonds with surface silanol groups on silica.[31] Thermal analysis is also a very useful method of analysis. It has the advantage of sensitivity to longer-range interactions making it sensitive to the behavior of segments that are not directly bound whose behavior might be affected by nearby bound segments which are directly bound.[2,32]

This study used FTIR and DSC to first observe the effect of molecular mass on the configuration or structure of PMMA polymer chains adsorbed on silica and second to see the effect of molecular mass on the glass transitions of the adsorbed polymers.

Experimental

Materials. Bromooctane from Eastman Chemical Co. (Kingsport, TN, USA), ethanol from Aaper Alcohol and Chemical Co. (Shelbyville, KY, USA), thiourea from Sigma Aldrich (St. Louis, MO, USA), sodium hydroxide from EMD Chemical Inc. (Gibbstown, NJ, USA), sulfuric acid from EM Science (Gibbstown, NJ, USA), and magnesium sulfate from Fisher Scientific (Fair Lawn, NJ, USA) were used as received. Cab-O-Sil M5 and EH5 fumed silica (surface area of 200 m^2/g and 380 m^2/g) were obtained from Cabot Corp. (Tuscola, IL, USA) and dried at 150 ^{0}C for at least 24 hours prior to use. Methyl methacrylate from Acros Organics (NJ, USA) was passed through a

basic alumina column and 2,2-azobisisobutyronitrile from Aldrich Chemical Company, Inc. (Milwaukee, WI, USA) was recrystallized from methanol.

Synthesis of chain transfer agent. Octanethiol was synthesized for use as a chain transfer agent to control the resulting molecular masses of the poly(methyl methacrylate) polymers synthesized. Bromooctane (14.5 mL), ethanol (40 mL) and thiourea (6.25 g) were combined in a 100 mL round-bottomed flask and refluxed for 3 h. A solution of sodium hydroxide (8.3 M) in deionized water was added to the refluxing mixture. Refluxing continued for another 3. Following this, the reaction mixture was cooled and washed with a solution of sulfuric acid (2.0 M). The organic layer obtained was dried with magnesium sulfate and the resulting oil was distilled to give the desired product.

PMMA synthesis. Poly(methyl methacrylate) samples with different molecular masses were synthesized. Methyl methacrylate (MMA), azoisobutyrylnitrile (AIBN), toluene and octanethiol (OT) were mixed in different ratios to give the molecular masses shown in Table 1. The mixtures were degassed by purging with dry nitrogen gas for 30 min and subsequently heated for 30 min. The resulting mixture was dissolved in THF and then precipitated from methanol.

Characterization of PMMA. The PMMA samples prepared were characterized using ^{1}H- NMR and gel permeation chromatography (GPC) to determine the tacticities and molecular masses of the synthesized polymers, respectively. The tacticities are determined via the alpha-methyl peaks which are between 0.8 – 1.3 ppm. The peak areas of the different peaks corresponding to the three triad tacticities (isotactic, heterotactic,

syndiotactic) were obtained and are listed in Table 1. The polymers were somewhat atactic with a tendency to be locally syndiotactic.

Table 1. Molecular masses and tacticities of synthesized PMMA polymers from GPC and ^{1}H-NMR

			Diad tacticity data		
Polymer	Molecular mass (kg/mol)	Polymerization conditions [MMA]:[AIBN]:[OT]	***mm***	***mr***	***rr***
P1	4.99	49 : 1 : 16	0.129	0.321	0.549
P2	20.4	49 : 1 : 0.32	0.0640	0.352	0.584
P3	38.8	49 : 1 : 0	0.0818	0.345	0.574
P4	181	998 : 1 : 0	0.0595	0.353	0.588

Preparation of adsorbed PMMA samples. The two types of Cab-O-Sil fumed silica used were M5 and EH-5. For each adsorbed sample composition, roughly 0.3 g of silica was wetted with toluene and the appropriate amount of polymer was dissolved in 10 mL of toluene. These polymer solutions were subsequently added to the wetted silica samples and mixed and shaken for at least 3 d. Following this, the toluene was bubbled off using air. The resulting solid samples were allowed to dry in a vacuum desiccator for 2 d at 60 °C.

Characterization of adsorbed PMMA. The characterization of the prepared adsorbed silica samples was done with a number of techniques. A Q50 TGA from TA Instrument (New Castle, DE) was used to determine the adsorbed amounts of each prepared sample. A TA Instruments Q2000 DSC (New Castle, DE) was also used to measure the thermal transitions undergone by the adsorbed samples. For this analysis, a

heating rate of 3 °C/min with a modulation of ±1 °C every 60 sec was used. These measurements were made from -50 to 200 °C. A Nicolet iS50 FTIR spectrometer was used to obtain ATR-FTIR spectra which were used to determine the fraction of bound carbonyls in each sample.

Results

FTIR spectra show the presence of hydrogen bonding between the carbonyl groups in PMMA and silanol groups on the silica surface. Figure 1 shows the FTIR spectra of adsorbed polymer samples (4990 g/mol) in the 1550 to 1800 cm^{-1} range. These spectra show that in addition to a resonance at ~1730 cm^{-1} corresponding to free carbonyl groups, there is a peak at a lower frequency (~1711 cm^{-1}) shoulder corresponding to carbonyl groups that are hydrogen bonded to the surface.

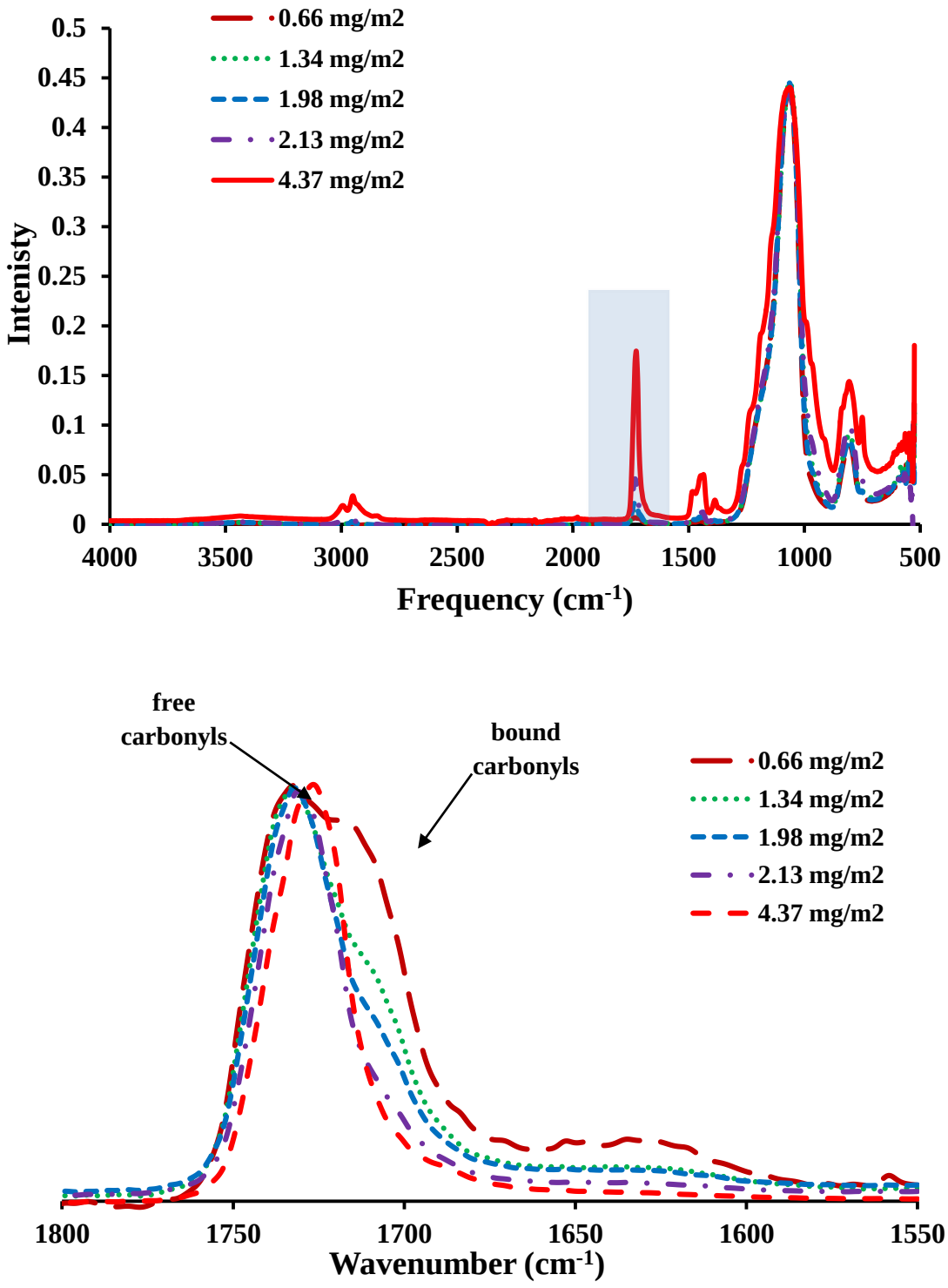

Figure 1. (a) FTIR spectra of PMMA (4990 g/mol) adsorbed samples. The intensities of the spectra have been scaled so that the maximum in the resonance for the Si-O-Si

stretches are approximately equal (b) FTIR spectra of PMMA (4990 g/mol) adsorbed samples in the 1550 to 1800 cm^{-1} region. The intensities of the spectra have been scaled so that the maximum in the resonance for the free carbonyls are approximately equal.

As can be seen from Figure 1, the intensities of the resonances corresponding to bound carbonyl groups decrease as the adsorbed amounts increased. These intensity variations show that samples with smaller adsorbed amounts have larger fractions of bound carbonyls. The FTIR of PMMA as function of molecular mass were observed in Figure 2. FTIR spectra were taken for two types of silica substrates, Cab-O-sil EH-5 and M5.

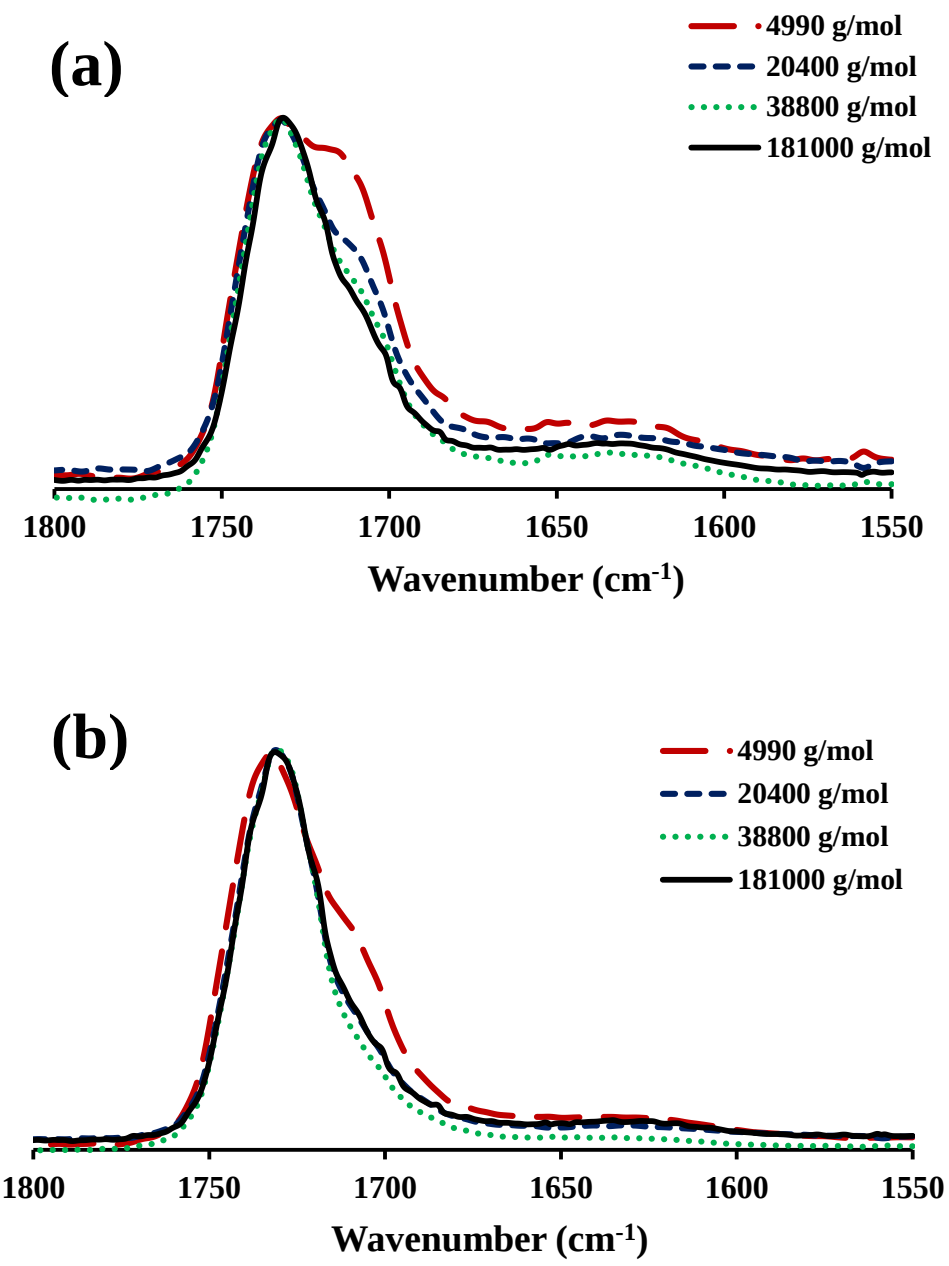

Figure 2. FTIR spectra of adsorbed PMMA on silica (Cab-O-Sil M5) as a function of molecular mass at different adsorbed amounts (a) 0.5 mg/m^2 and (b) 1.5 mg/m^2

From the FTIR spectra obtained, the bound carbonyl fraction was estimated for the bulk polymers and their composites using a method developed by Kulkeriyat et al.[33,34]

The values obtained were plotted against molecular mass above at 0.5 mg/m^2 and 1.5 mg/m^2.

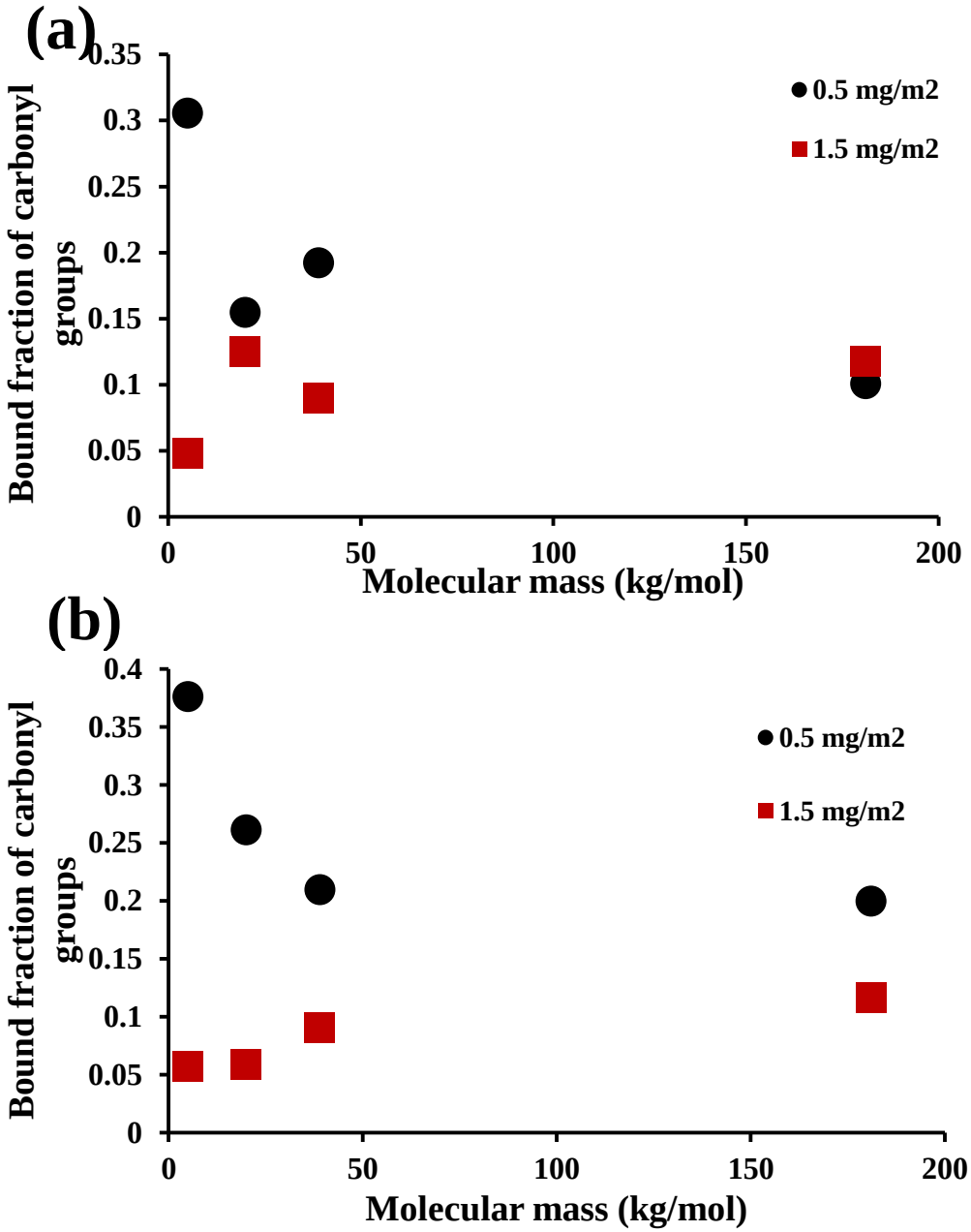

Figure 3. Bound fraction of carbonyl groups as a function of molecular mass for (a) M5 silica (200 m^2/g) and (b) EH-5 silica (380 m^2/g) at 0.5 and 1.5 mg/m^2.

The main result of the FTIR studies is that the lower molecular mass polymers appear to be more extended on the surface than higher molecular mass polymers at low surface coverage. This effect is observed in Figure 3. It also shows that as the molecular mass increases, this effect becomes less significant. To obtain more information about the effect of the silica surface on polymer chains, temperature modulated DSC thermograms were collected for the different molecular mass polymers. These thermograms are shown in Figures 4 – 7.

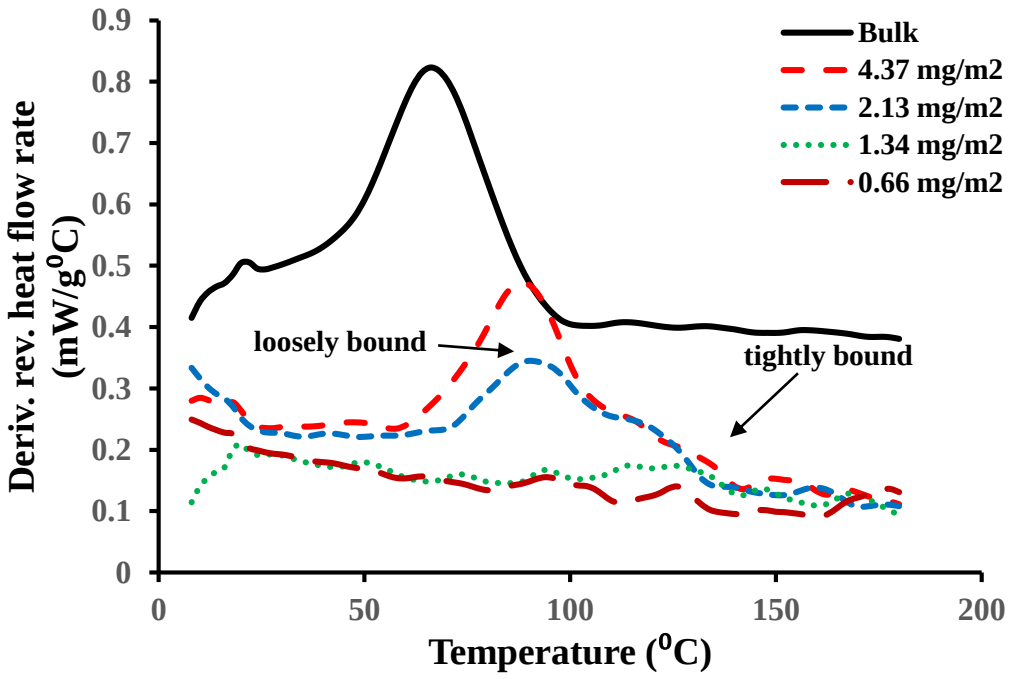

Figure 4. Derivative heat flow rate curves of the bulk polymer (4990 g/mol) and adsorbed polymer samples (on 200 m^2/g silica) in the glass transition region. The curve for the bulk polymer has been scaled and offset for clarity.

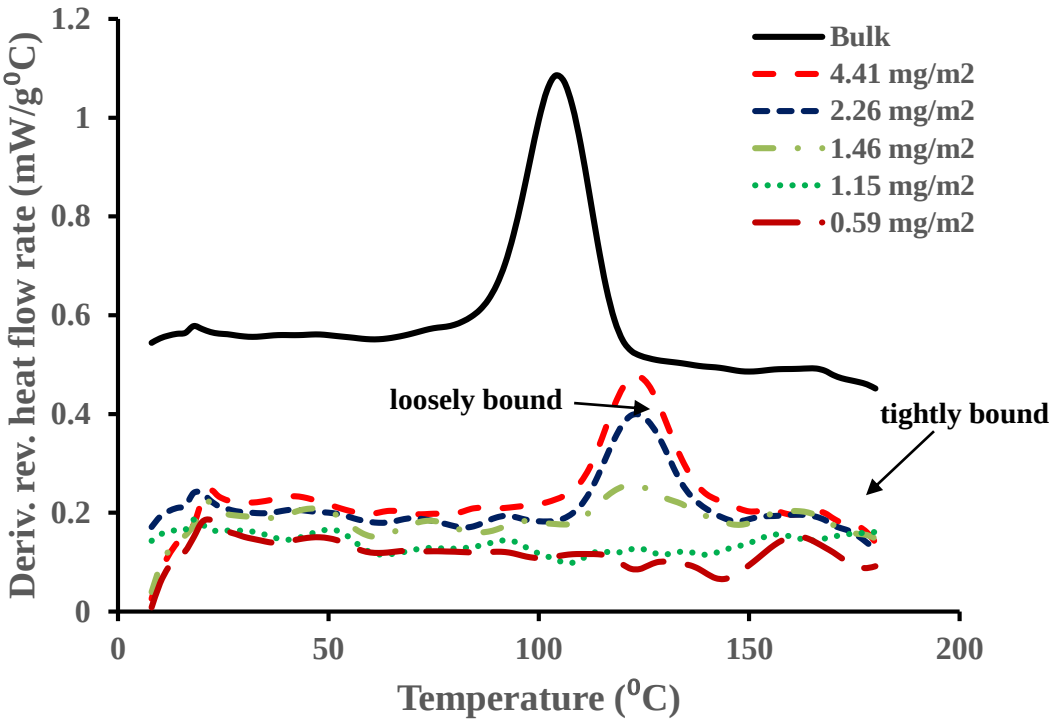

Figure 5. Derivative heat flow rate curves of the bulk polymer (20400 g/mol) and adsorbed polymer samples (on 200 m^2/g silica) in the glass transition region. The curve for the bulk polymer has been scaled and offset for clarity.

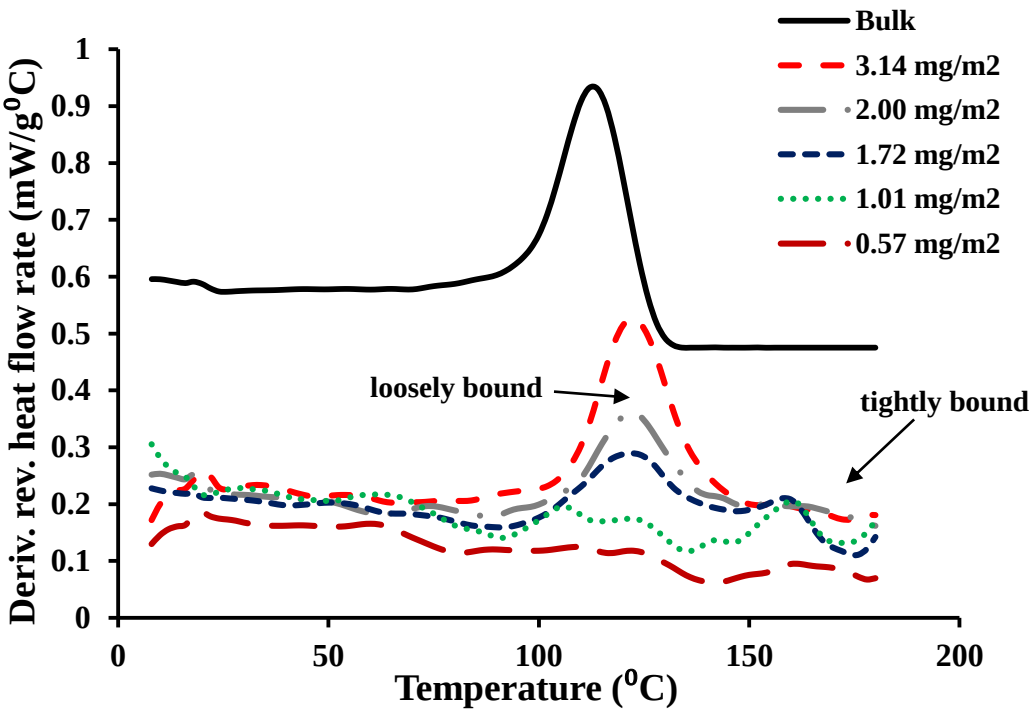

Figure 6. Derivative heat flow rate curves of the bulk polymer (38800 g/mol) and adsorbed polymer samples (on 200 m^2/g silica) in the glass transition region. The curve for the bulk polymer has been scaled and offset for clarity.

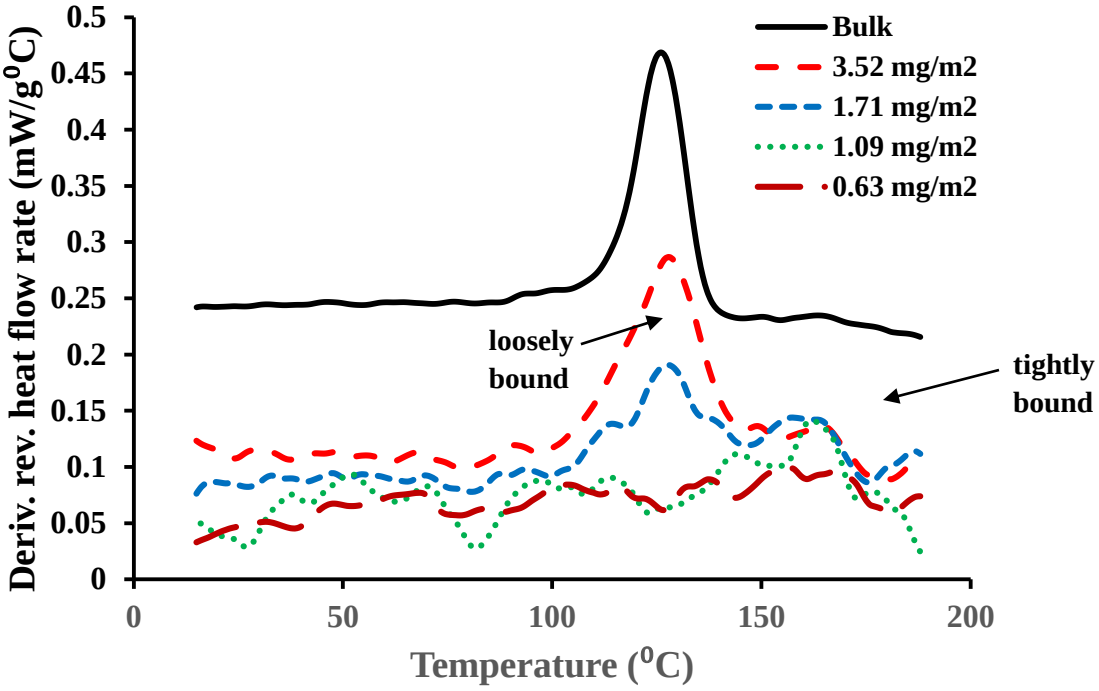

Figure 7. Derivative heat flow rate curves of the bulk polymer (181000 g/mol) and adsorbed polymer samples (on 200 m^2/g silica) in the glass transition region. The curve for the bulk polymer has been scaled and offset for clarity.

From Figures 4 – 7, it is clear that adsorption onto silica resulted in an increase in glass transition with the presence of both tightly- and loosely-bound PMMA observed for all molecular masses and similar types of behavior for both types of silica. At an adsorbed amount of about 1 mg/m^2, only tightly bound polymer was observed. As the adsorbed amount increased, the appearance of polymer with a lower glass transition designated "loosely bound" polymer was observed. The intensity of this region increased with increasing adsorbed amount. The temperatures at which the tightly bound polymer was observed was the same for all but the lowest molecular mass polymer which showed

tightly bound polymer T_g at around 160 °C and loosely bound polymer at around 125 °C regardless of the bulk T_g.

Discussion

The FTIR spectra shown in Figure 1 show evidence of hydrogen bonding between the PMMA carbonyl groups and the surface silanol groups of silica in the adsorbed polymer samples.[29,35] The presence of a shoulder in the carbonyl stretching region corresponding to bound carbonyl groups was apparent.[34] The intensity of this bound carbonyl resonance was found to increase with decreasing adsorbed amount as has been observed for this and other adsorbed polymer-silica systems in other studies.[34] In this particular study, the molecular masses of the polymers, and the surface area (particle size) of the silica substrate used were varied. The results shown indicated that the surface area had no impact on the adsorption of the polymers and their properties as far as reported by the FTIR. The molecular masses of the polymers were found to affect the behavior of adsorbed PMMA on silica and this will be discussed in more detail.

The intensities of the resonances corresponding to free and bound carbonyl groups were obtained from the FTIR spectra of the adsorbed polymer samples, some of which are shown in Figure 1, and used to determine the bound fraction of carbonyl groups (*p*) for each of the samples using a model previously developed by Kulkeratiyut.[33,34] This model allows the estimation of *p* while taking into account the difference between the absorptivity ratios of the bound and free carbonyl groups. The *p* values of different adsorbed samples consisting of polymers with different molecular

masses were compared at two adsorbed amounts 0.5 mg/m^2 (below the tightly bound amount) and 1.5 mg/m^2 (above the tightly bound amount) and this is shown in Figure 3. At a small adsorbed amount (0.5 mg/m^2), the smallest molecular mass polymer sample had a higher *p* value than the larger molecular mass samples. As the molecular mass increased, the molecular mass dependence of *p* decreased. This suggested that low molecular mass polymers, when adsorbed at smaller adsorbed amounts or before the surface is fully covered, are more extended on the surface as indicated by the *p* value. Higher molecular mass polymers were not as extended on the surface.

TMDSC was used to observe the effects of adsorption on the thermal properties of the PMMA as a function of molecular mass. Quite a few studies have been made on PMMA adsorption on silica and a few of those have focused on the effect of molecular mass on this process.[2,36] It has been found that upon adsorption of polymers, such as PMMA on silica, the layer that is closest to the silica surface, called the "tightly-bound layer", exhibits an increased glass transition, in some cases as much as 50 K.[37] TMDSC measurements of the adsorbed PMMA samples are shown in Figure 4. There are a few things of interest to note. Firstly, for all molecular masses, except for the lowest molecular mass sample, there was the presence of a broad glass transition corresponding to a tightly bound layer of polymer at the surface. It is interesting to note that this region was seen at roughly the same temperature for the molecular masses. This indicates that at this 'tightly bound' level, the PMMA polymer segments are immobilized to the same extent regardless of molecular mass. Secondly, there was a thermal transition corresponding to 'loosely bound' polymer i.e. polymer that is not directly bound to the silica surface. The thermal behavior of this layer of polymer was found to vary with

molecular mass. It was found that the lowest molecular mass polymer had the biggest difference in temperature between the bulk temperature and that of the 'loosely bound' polymer whereas the highest molecular mass polymer had the smallest. This implies that the lower molecular mass polymers are more affected by the surface than the higher molecular mass polymers.

One way to rationalize the greater effect of the surface on low molecular mass PMMA, is to first of all recall what was observed from Figure 3. FTIR studies showed that low molecular mass polymers were more extended on the surface. This suggests that these polymers on the surface would consist mostly of trains and tails with fewer loops whereas higher molecular mass polymers would have more and larger loops.[32,38] A study on poly(2-vinylpyridine) (P2VP) adsorbed on silica carried out by Voylov et. al. showed that adsorption of this polymer showed a molecular mass dependence with longer polymer chains less densely packed on the surface than shorter polymer chains.[39] Low molecular mass polymers would consist of many trains and tails with few or short loops whereas higher molecular mass polymers have larger loops. The polymer segments in these larger loops would be farther away from the surface. As a result, other polymer chain segments not directly bound to the surface ("loosely bound") would not interact with the surface as strongly.

One of the factors that affects the properties of polymers is stereoregularity or tacticity.[40] One of the most striking instances of this is the case of poly(methyl methacrylate) in which the glass transition temperatures of the syndiotactic and isotactic versions of the polymers differ by up to 80 °C.[41] The influence of tacticity of the properties of polymers is not limited to the bulk polymer. The tacticity of a polymer has

been shown to affect the adsorption of the polymer onto surfaces such as silica. For instance, it is known that isotactic PMMA adsorbs preferentially to silica over syndiotactic PMMA.[42] As a result, for this study, it was fitting that the tacticities of the polymers studied did not play a significant role in adsorption. The tacticities of the polymers synthesized were determined using ^{1}H-NMR and are shown in Table 1. The triad tacticity analysis performed showed that the polymers all had similar tacticities and thus tacticity did not play a significant role in adsorption.

There have been quite a few studies conducted on the molecular mass dependence of polymer adsorption and a couple are of particular interest in the context of this study. One such study by Blum et. al. used solid state deuterium NMR to study the dynamics of a low and high molecular mass PMMA in bulk and adsorbed states.[36] This study showed that while in bulk, the lower molecular mass polymers were more mobile, but when adsorbed, the lower molecular mass sample showed less mobility. This was also seen in a study by Metin and Blum.[43] These NMR observations are consistent with our findings using FTIR and DSC that the silica surface has a stronger effect on the 'loosely bound' polymer segments of low molecular mass PMMA. Another study centered on molecular mass by Kabomo et. al.[2] which used TMDSC and showed that the surface had a stronger immobilizing effect on the smallest adsorbed amount sample. It should be noted that this study dealt with small adsorbed amounts (< 2mg/m^2).[2]

It is interesting to note the different experimental techniques that have been used to determine the structure and behavior of polymers adsorbed on surfaces. To mention a few, TMDSC, NMR, EPR, FTIR, x-ray photoelectron spectroscopy (XPS) and sum frequency generation spectroscopy (SGF) have been used to this end.[2,30,31,34,36,39,43,44]

While the ways in which they work are different, with TMDSC measuring longer range motions of polymers and FTIR looking directly at the functional groups directly bound to the surface or affected by adsorption,[45] the results of studies using these varied techniques all point to the same conclusions. Firstly, lower molecular mass polymers on the surface have flatter configurations and secondly, the 'loosely bound' layer of higher molecular mass polymers are not as strongly affected by the surface due to the screening of the surface functional groups by large loops in higher molecular mass polymers. This is illustrated in Figure 8 below.

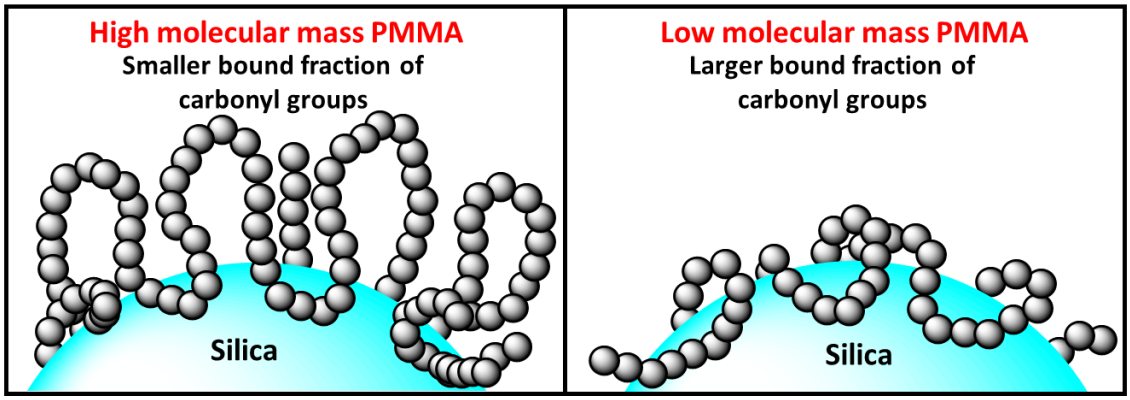

Figure 8. Schematic illustration of high molecular mass and low molecular mass PMMA adsorbed on silica.

Conclusions

The effect of molecular mass on the adsorption of PMMA on silica was studied using both FTIR and TMDSC. FTIR showed the adsorption of PMMA via the hydrogen bonding of the carbonyl groups to the surface silanol groups of silica. From the FTIR measurements made, the bound fractions of the adsorbed polymer samples were determined and found to have some dependence on both adsorbed amount and molecular

mass. Adsorbed samples consisting of lower molecular mass polymers were found to have larger bound fractions than samples consisting of higher molecular mass polymers suggesting that lower molecular mass polymers were more extended on the silica surface than higher molecular mass polymers. TMDSC was used to study the dependence of the thermal behavior of adsorbed PMMA on molecular mass. From these TMDSC measurements, the adsorbed polymer samples were all found to have two regions of thermal activity. The first region, broad and at around 150 °C, was attributed to tightly bound polymer segments and was found to be around the same temperature for all molecular masses. The second region which was due to loosely bound polymer was found to vary with molecular mass and was attributed to polymer that was not directly bound to the surface. Two different types of silica with different surface areas were used in these studies. It was found that the surface area had no effect on the behavior of the polymers in the adsorbed polymers samples.

Acknowledgements. The financial support of the National Science Foundation (US) under Grant 1005606 and Oklahoma State University are acknowledged.

References

(1) Nunnery, G.; Hershkovits, E.; Tannenbaum, A.; Tannenbaum, R. Adsorption of poly(methyl methacrylate) on concave Al(2)O(3) surfaces in nanoporous membranes. *Langmuir* **2009**, *25*, 9157-9163.

(2) Kabomo, M. T.; Blum, F. D.; Kulkeratiyut, S.; Kulkeratiyut, S.; Krisanangkura, P. Effects of molecular mass and surface treatment on adsorbed poly(methyl methacrylate) on silica. *J. Polym. Sci., Part B: Polym. Phys.* **2008**, *46*, 649-658.

(3) Alcoutlabi, M.; McKenna, G. B. Effects of confinement on material behaviour at the nanometre size scale. *J. Phys.: Condens. Matter* **2005**, *17*, R461-R524.

(4) Arrighi, V.; McEwen, I. J.; Qian, H.; Prieto, M. B. S. The glass transition and interfacial layer in styrene-butadiene rubber containing silica nanofiller. *Polymer* **2003**, *44*, 6259-6266.

(5) Kirst, K. U.; Kremer, F.; Litvinov, V. M. broad-band dielectric-spectroscopy on the molecular-dynamics of bulk and adsorbed poly(dimethylsiloxane). *Macromolecules* **1993**, *26*, 975-980.

(6) Miwa, Y.; Drews, A. R.; Schlick, S. Detection of the direct effect of clay on polymer dynamics: The case of spin-labeled poly(methyl acrylate)/clay nanocomposites studied by ESR, XRD, and DSC. *Macromolecules* **2006**, *39*, 3304-3311.

(7) Mammeri, F.; Rozes, L.; Le Bourhis, E.; Sanchez, C. Elaboration and mechanical characterization of nanocomposites thin films - Part II. Correlation between structure and mechanical properties of SiO2-PMMA hybrid materials. *J. Europ. Ceram. Soc.* **2006**, *26*, 267-272.

(8) Lee, D. C.; Jang, L. W. Preparation and characterization of PMMA-clay hybrid composite by emulsion polymerization. *J. Appl. Polym. Sci.* **1996**, *61*, 1117-1122.

(9) Vieweg, S.; Unger, R.; Hempel, E.; Donth, E. Kinetic structure of glass transition in polymer interfaces between filler and SBR matrix. *J. Non-Crystal. Solids* **1998**, *235*, 470-475.

(10) Sargsyan, A.; Tonoyan, A.; Davtyan, S.; Schick, C. The amount of immobilized polymer in PMMA SiO(2) nanocomposites determined from calorimetric data. *Eur. Polym. J.* **2007**, *43*, 3113-3127.

(11) Tsagaropoulos, G.; Eisenberg, A. dynamic-mechanical study of the factors affecting the 2 glass-transition behavior of filled polymers - similarities and differences with random ionomers. *Macromolecules* **1995**, *28*, 6067-6077.

(12) Blum, F. D.; Xu, G.; Liang, M.; Wade, C. G. Dynamics of poly(vinyl acetate) in bulk and on silica. *Macromolecules* **1996**, *29*, 8740-8745.

(13) Lin, W.-Y.; Blum, F. D. Segmental dynamics of bulk and adsorbed poly(methyl acrylate)-d3 by deuterium NMR: effect of adsorbed amount. *Macromolecules* **1997**, *30*, 5331-5338.

(14) Fryer, D. S.; Peters, R. D.; Kim, E. J.; Tomaszewski, J. E.; de Pablo, J. J.; Nealey, P. F.; White, C. C.; Wu, W. L. Dependence of the glass transition temperature of polymer films on interfacial energy and thickness. *Macromolecules* **2001**, *34*, 5627-5634.

(15) Hartmann, L.; Gorbatschow, W.; Hauwede, J.; Kremer, F. Molecular dynamics in thin films of isotactic poly(methyl methacrylate). *Eur. Phys. J. E* **2002**, *8*, 145-154.

(16) Blum, F. D.; Young, E. N.; Smith, G.; Sitton, O. C. Thermal analysis of adsorbed poly(methyl methacrylate) on silica. *Langmuir* **2006**, *22*, 4741-4744.

(17) Mortazavian, H.; Fennell, C. J.; Blum, F. D. Structure of the interfacial region in adsorbed poly(vinyl acetate) on silica. *Macromolecules* **2016**, *49*, 298-307.

(18) Mortazavian, H.; Fennell, C. J.; Blum, F. D. Surface bonding is stronger for poly(methyl methacrylate) than for poly(vinyl acetate). *Macromolecules* **2016**, *49*, 4211-4219.

(19) Hershkovits, E.; Tannenbaum, A.; Tannenbaum, r. Polymer adsorption on curved surfaces: a geometric approach. *J.Phys. Chem. C* **2007**, *111*, 12369-12375.

(20) Kawaguchi, M.; Itoh, K.; Yamagiwa, S.; Takahashi, A. Random copolymer adsorption. II. Competitive and displacement adsorption. *Macromolecules* **1989**, *22*, 2204-2207.

(21) Silberberg, A. Adsorption of flexible macromolecules. Iv. Effect of solvent–solute interactions, solute concentration, and molecular weight. *J. Chem. Phys.* **1968**, *48*, 2835-2851.

(22) Thies, C. The adsorption of polystyrene-poly(methyl methacrylate) mixtures at a solid-liquid interface1. *J. Phys. Chem.* **1966**, *70*, 3783-3790.

(23) Sakai, H.; Imamura, Y. Molecular-weight dependence of the polymer adsorption at solid-liquid interfaces as studied by ESR spectroscopy. *Bull. Chem. Soc. Jpn* **1987**, *60*, 1261-1267.

(24) Yamagiwa, S.; Kawaguchi, M.; Kato, T.; Takahashi, A. Random copolymer adsorption. I. Infrared study at a silica surface. *Macromolecules* **1989**, *22*, 2199-2203.

(25) Van der Beek, G. P.; Stuart, M. A. C.; Fleer, G. J. Polymer desorption by monomeric and polymeric displacers, as studied by attenuated total reflection FT-IR spectroscopy. *Macromolecules* **1991**, *24*, 3553-3561.

(26) Kobayashi, K.; Araki, K.; Imamura, Y. Adsorption of Poly(methyl methacrylate) on Silica Surfaces Having Various Silanol Densities. *Bull. Chem. Soc. Jpn* **1989**, *62*, 3421-3425.

(27) Kawaguchi, M.; Yamagiwa, S.; Takahashi, A.; Kato, T. Adsorption of polystyrene and poly(methyl methacrylate) onto a silica surface studied by the infrared technique. Comparison with theory. *J. Chem. Soc., Faraday Trans.* **1990**, *86*, 1383-1387.

(28) Botham, R.; Thies, C. The adsorption behavior of polymer mixtures. *J. Polym. Sci., Part C: Polym. Symp.* **1970**, *30*, 369-380.

(29) Korn, M.; Killmann, E. Infrared and micro-calorimetric studies of the adsorption of polymers with ester groups, in the main or side-chain, at the silica-carbon tetrachloride interface. *J. Colloid Interface Sci.* **1980**, *76*, 19-31.

(30) Cohen Stuart, M. A.; Fleer, G. J.; Bijsterbosch, B. H. Adsorption of poly(vinyl pyrrolidone) on silica. II. The fraction of bound segments, measured by a variety of techniques. *J. Colloid Interface Sci.* **1982**, *90*, 321-334.

(31) Fontana, B. J.; Thomas, J. R. The configuration of adsorbed alkyl methacrylate polymers by infrared and sedimentation studies. *J. Phys. Chem.* **1961**, *65*, 480-487.

(32) Fleer, G.; Stuart, M. C.; Scheutjens, J.; Cosgrove, T.; Vincent, B.: *Polymers at interfaces*; Chapman & Hall: London, 1993.

(33) Kulkeratiyut, S.; Kulkeratiyut, S.; Blum, F. D. Bound carbonyls in PMMA adsorbed on silica using transmission FTIR. *J. Polym. Sci., Part B: Polym. Phys.* **2006**, *44*, 2071-2078.

(34) Krisanangkura, P.; Packard, A. M.; Burgher, J.; Blum, F. D. Bound fractions of methacrylate polymers adsorbed on silica using FTIR. *J. Polym. Sci., Part B: Polym. Phys.* **2010**, *48*, 1911-1918.

(35) Berquier, J.-M.; Arribart, H. Attenuated total reflection Fourier transform infrared spectroscopy study of poly (methyl methacrylate) adsorption on a silica thin film: polymer/surface interactions. *Langmuir* **1998**, *14*, 3716-3719.

(36) Blum, F. D.; Lin, W.-Y.; Porter, C. E. Dynamics of adsorbed poly(methyl acrylate) and poly(methyl methacrylate) on silica. *Colloid and Polymer Science* **2003**, *281*, 197-202.

(37) Khatiwada, B. K.; Hetayothin, B.; Blum, F. D. Thermal properties of PMMA on silica using temperature-modulated differential scanning calorimetry. *Macromol. Symp.* **2013**, *327*, 20-28.

(38) Fleer, G. J. Polymers at interfaces and in colloidal dispersions. *Advances in Colloid and Interface Science* **2010**, *159*, 99-116.

(39) Voylov, D. N.; Holt, A. P.; Doughty, B.; Bocharova, V.; Meyer, H. M.; Cheng, S.; Martin, H.; Dadmun, M.; Kisliuk, A.; Sokolov, A. P. Unraveling the Molecular Weight Dependence of Interfacial Interactions in Poly(2-vinylpyridine)/Silica Nanocomposites. *ACS Macro Lett.* **2017**, *6*, 68-72.

(40) Karasz, F.; MacKnight, W. The influence of stereoregularity on the glass transition temperatures of vinyl polymers. *Macromolecules* **1968**, *1*, 537-540.

(41) Goode, W.; Owens, F.; Fellmann, R.; Snyder, W.; Moore, J. Crystalline acrylic polymers. I. Stereospecific anionic polymerization of methyl methacrylate. *J. Polym. Sci., Part A: Polym. Chem.* **1960**, *46*, 317-331.

(42) Carriere, P.; Grohens, Y.; Spevacek, J.; Schultz, J. Stereospecificity in the Adsorption of Tactic PMMA on Silica. *Langmuir* **2000**, *16*, 5051-5053.

(43) Metin, B.; Blum, F. D. Segmental dynamics in poly (methyl acrylate) on silica: Molecular-mass effects. *J. Chem. Phys.* **2006**, *125*, 054707.

(44) Robb, I. D.; Smith, R. Adsorption of polymers at the solid-liquid interface: a comparison of the e.p.r. and i.r. techniques. *Polymer* **1977**, *18*, 500-504.

(45) Berquier, J.-M.; Arribart, H. Attenuated Total Reflection Fourier Transform Infrared Spectroscopy Study of Poly(methyl methacrylate) Adsorption on a Silica Thin Film: Polymer/Surface Interactions. *Langmuir* **1998**, *14*, 3716-3719.

CHAPTER VI

ADSORPTION OF POLY(VINYL PYRROLIDONE) ON SILICA

Abstract

Thermogravimetric analysis, differential scanning calorimetry and infrared spectroscopy were used to study the thermal behavior of poly(vinylpyrrolidone) adsorbed on silica. These characterization techniques showed that when adsorbed, PVP showed lower mobility than in the bulk polymer due to attractive hydrogen bonding between the polymer segments and the silica surface. Firstly, TGA measurements showed a decrease in the decomposition temperature of PVP when it was adsorbed on silica due to an increase in chain stiffness. Secondly, ATR-FTIR showed the presence of hydrogen bonding between the amide carbonyl groups and the silica surface silanol groups. Finally, the reduced mobility of the PVP chains on the surface was observed using TMDSC. Derivative reversing heat flow curves showed that adsorption resulted in an increase in glass transition of polymer segments on the silica surface. The presence of a tightly- and loosely-bound layer were observed using this technique.

Introduction

Polymers at interfaces behave differently than those in bulk.[1] In many instances, the reason for these changes in behavior is the presence of interfacial interactions between the polymer and surface.[2] Numerous studies done on polymers with attractive interactions with surfaces have shown that on surfaces, their mobilities are restricted. The restriction of polymer chains is known to have the most impact on the tightly bound layer of the polymer[3] which has been shown by many techniques.[3-6] Varying results have been observed from studies of this tightly bound layer. In some instances, this tightly bound layer was seen to be essentially immobilized[5,7-9] and in others, a second, broader glass transition was observed.[10-17]

The different methods used to probe polymer dynamics include ellipsometry[18] which has been used to observe a decrease in glass transition of polystyrene upon adsorption on silicon,[19] x-ray reflectivity,[20] back scattering,[21] adhesion,[22] solvent diffusion,[23] fluorescence,[24] infrared spectroscopy,[25-32] NMR.[11,12,33] and thermal analysis[9,15,34,35] including differential scanning calorimetry, thermogravimetric analysis and dynamic thermal analysis. Thermal analysis has the advantage of sensitivity to longer-range interactions making it responsive to the behavior of segments that are not directly bound whose behavior might be affected by nearby bound segments which are directly bound.[1,36] On the other hand, infrared spectroscopy gives information about specific intermolecular interactions and conformational changes for example hydrogen bonding can be detected from the shifting of the ester carbonyl stretching frequency.[32,37]

Our polymer of interest, poly(vinylpyrrolidone), because it is a water soluble polymer that is also soluble in a wide range of organic solvents.[38] It has been used in applications using biocompatible coatings such as in contact lenses and in blood plasma. Studies conducted on PVP have shown that it adsorbs onto silica via hydrogen bonding between the PVP carbonyl groups and silica surface silanols.[38] Studies by Cohen Stuart and coworkers have shown that PVP can have an adsorption plateau of up to 1 mg/m^2 and that the bound fraction of PVP carbonyl groups on silica is approximately 30%.[39,40] It is well know that polymers such as PVP have large numbers of internal degrees of freedom. The degrees of freedom are affected upon adsorption.[40] The aim of this paper was to determine what impact adsorption has on the properties of PVP using TMDSC and FTIR.

Experimental

Materials. Cab-O-Sil M-5 fumed silica from Cabot Corp. (Tuscola, IL) (specific surface area 200 m^2/g) was used as the substrate. Poly(vinylpyrrolidone), with a molecular mass of 40000 g/mol was obtained from Polysciences, Inc. (Warrington, PA) and chloroform (reagent grade) from Pharmco-aaper (Brookefield, CT). All the reagents listed above were used as received.

Preparation of adsorbed polymer samples. PVP solutions with varying concentrations were first prepared by dissolving different masses of PVP (30 mg to 600 mg) in 10 mL of chloroform. Silica (0.3 g) was weighed into tubes, wetted with 5 mL of chloroform, and subsequently sonicated for 20 minutes. The resulting gels and PVP solutions were combined and mixed on a mechanical shaker for 48 hours; after which the chloroform was removed. This was done by transferring the polymer, silica and

chloroform as a mixture to an aluminum pan and stirring it until the chloroform evaporated. The resulting powders were then dried under vacuum for an additional 3 days to ensure the complete removal of solvent. It was essential that the prepared samples were kept free of moisture. For this reason, prior to characterization they were heated in a vacuum oven for 50 to 100 °C for at least 2 days and subsequently kept in a dessicator.

Characterization of adsorbed samples. The adsorbed samples were characterized using a number of techniques. Thermogravimetric analysis which was used to determine the amounts of polymer adsorbed. For this, a TA Instruments (New Castle, DE) Q2950 Thermogravimetric analyzer was used. The samples were heated from 20 to 800 °C at a heating rate of 20 °C/min using air as the purge gas at a flow rate of 50 mL/min. The adsorbed amounts were then calculated based on the mass of the residual material which consisted of only silica using the following equation.

$$AA\left(\frac{mg}{m^2}\right) = \frac{\Delta m \times 1000}{R \times SA} \qquad (1)$$

where *AA* is the adsorbed polymer amount in milligrams per m^2, Δm is the mass loss due to the polymer, *R* is the mass of the inorganic residue and *SA* is the specific surface area of the substrate.

Attenuated total reflectance (ATR) FTIR measurements of the adsorbed samples were carried out using a Nicolet iS50 FTIR spectrometer (Thermo Scientific, Waltham, MA) in the range of 4000-500 cm^{-1} and a resolution of 4 cm^{-1}. Origin Pro 9.1 software, Origin Lab Corporation (Northhampton, MA) was used to fit the experimental spectra.

The reversing heat flow curves for PVP, silica and the adsorbed samples were obtained using a TA Instruments (New Castle, DE) Q2000 DSC. The samples were weighed into T Zero pans and subsequently hermitically sealed to minimize the absorption of water by the sample. The samples were heated from 50 to 250 °C at a rate of 3 K/min. The samples were then cooled at the same rate and subsequently reheated at the same rate. The heat flow curves were obtained from the second heating and subsequently used to determine the thermal transitions of this polymer. Prior to the all the measurements, a baseline calibration was done by heating the empty cell, as well as heat capacity and temperature calibrations using sapphire and indium, respectively. To ensure good thermal contact, the adsorbed polymers, many of which were light and fluffy, were compressed into pellets using an IR pellet press before measurements were made. The pressure applied to make the pellets was around 10000 psi.

Results

Thermogravimetric analysis was done on the adsorbed samples and some of the resulting thermograms are shown in Figure 1. The thermograms shown indicate that the decomposition of PVP is a two-step process. In the first process, a major decomposition step was seen at around 410 °C and accounted for roughly 85 % of the overall mass loss. This step was followed by a second step that started around 525 °C and accounted for roughly 14 %. Adsorption of PVP on silica resulted in a decrease in the decomposition temperature with an onset decomposition temperature of 270 °C. Despite the adsorption, PVP decomposition remained a multi-step process. It should be noted that for these

samples, little mass loss was found at temperatures lower than 250 °C, where the loss of water would be anticipated.

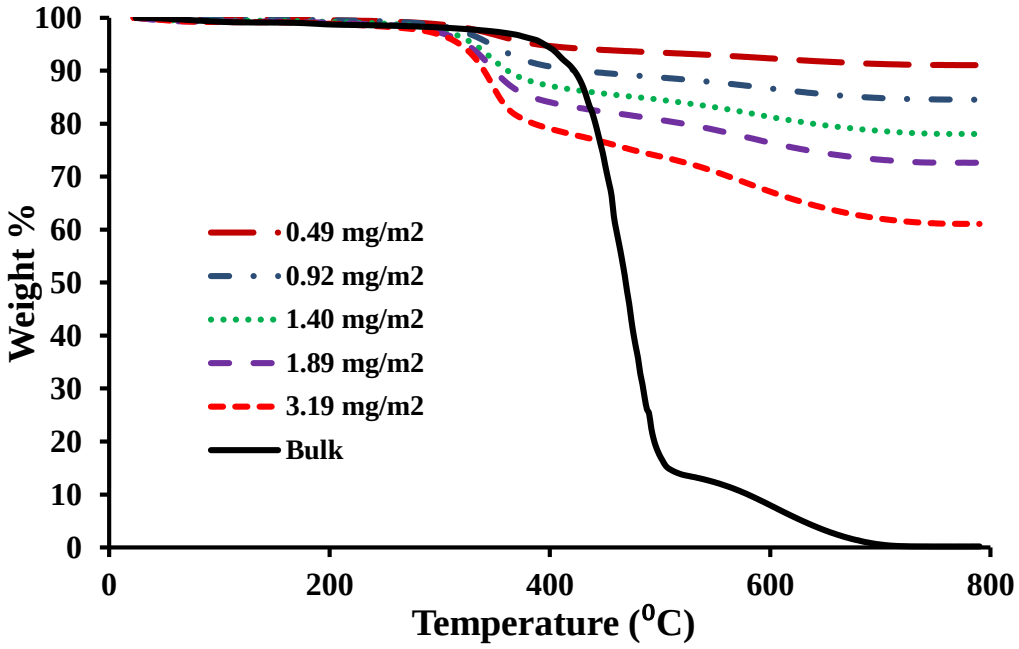

Figure 1. Decomposition profiles of bulk and adsorbed PVP obtained via thermogravimetric analysis.

ATR-FTIR spectra of the adsorbed samples were collected and analyzed in the carbonyl region (1800 to 1550 cm^{-1}) and the isolated silanol region (4000 to 3400 cm^{-1}). Analysis in these regions has been useful in previous cases to determine how the polymer interacts with the surface. In previous instances, a shift in the carbonyl peak and the appearance of a shoulder indicated the presence of hydrogen bonding between the carbonyl groups of poly(n-alkyl methacrylates).[30,32,36] Figure 2 shows the FTIR spectra of PVP in the carbonyl and isolated silanol regions. There is a sharp peak corresponding to isolated silanol groups for the silica sample. The intensity of this peak was greatly decreased in the sample for the smallest adsorbed amount and disappeared completely for

other adsorbed samples. In the carbonyl peak region, the presence of a shift in the carbonyl peak and the appearance of a shoulder is clear. The intensity of this shoulder is seen to increase as the adsorbed amount decreases, as is clear from Figure 2 below.

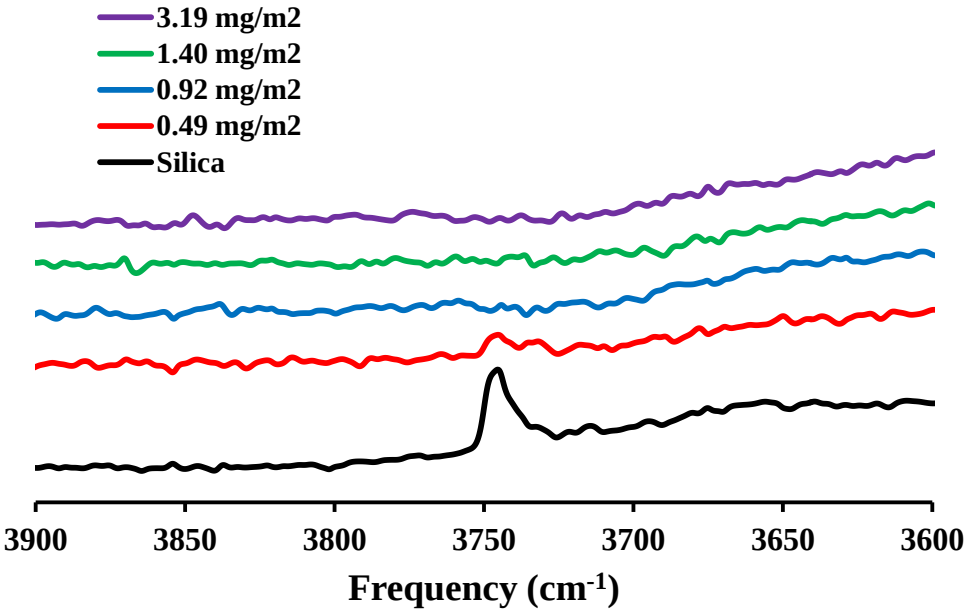

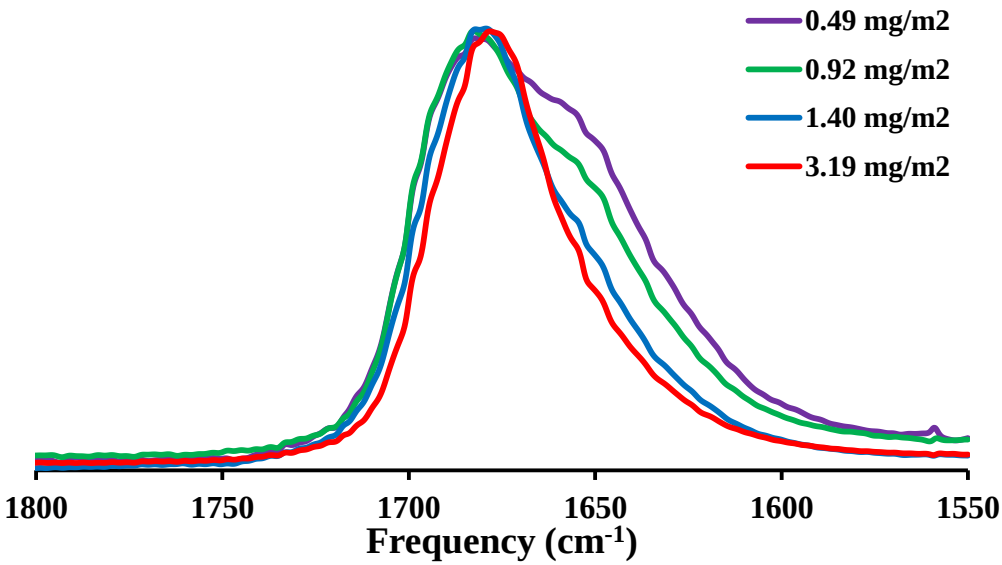

Figure 2. FTIR spectra of adsorbed PVP samples in the (a) isolated silanol group region (4000 to 3400 cm^{-1}) and the (b) carbonyl group region (1800 to 1550 cm^{-1}). These spectra were scaled and vertically offset for clarity. The curves are in the same order as shown in the legend.

The resonances in the carbonyl region were resolved into two peaks corresponding to a bound- and a free-carbonyl peak using Origin software. An example of the deconvolution of the spectra into two components is shown in Figure 3(a). The total adsorbed amount was plotted against the ratio of the areas of the free and bound peaks based on a model developed by Kulkeratiyut et. al. shown in equation 2.[41] The resulting graph is shown in Figure 3 below.

$$M_t = M_b + \left({A_f}/{A_b}\right) X M_b \qquad (2)$$

where M_t is the total adsorbed amount of polymer, M_b is the mass of bound carbonyl groups, and X is the ratio of the adsorption coefficients of bound and free carbonyl groups.

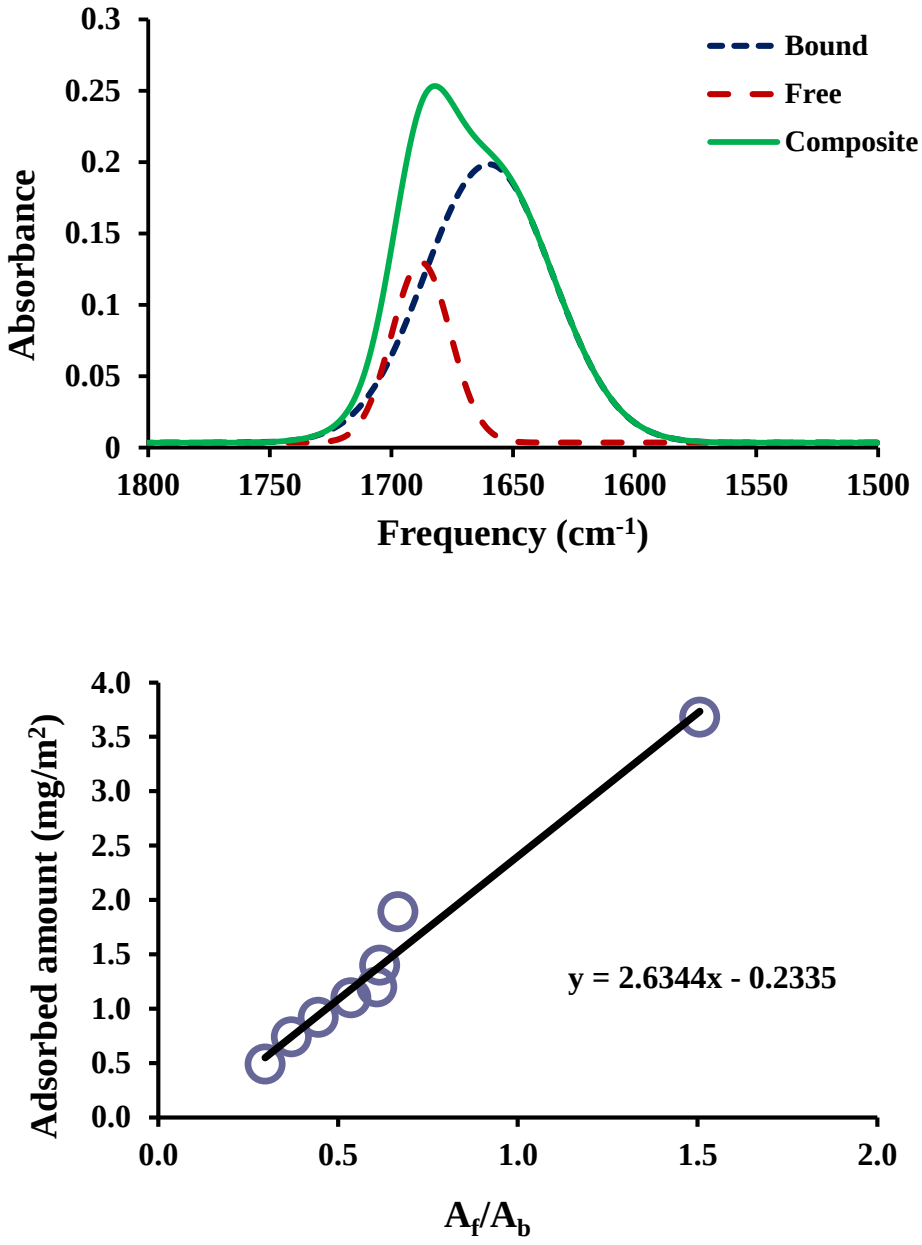

Figure 3. (a) Fitting of PVP adsorbed sample (0.49 mg/m^2) into peaks corresponding to free and bound carbonyl peaks. (b) plot of relationship between adsorbed amount and ratio of intensities relating to free to bound carbonyl groups

TMDSC derivative reversing heat flow rate curves for bulk PVP and adsorbed PVP samples were obtained. These curves are compared in Figure 4 below. From Figure

4, it is clear that bulk PVP has a glass transition at 178 ^{0}C. Some of the adsorbed samples also show glass transitions that were at higher temperatures than those seen for the bulk sample.

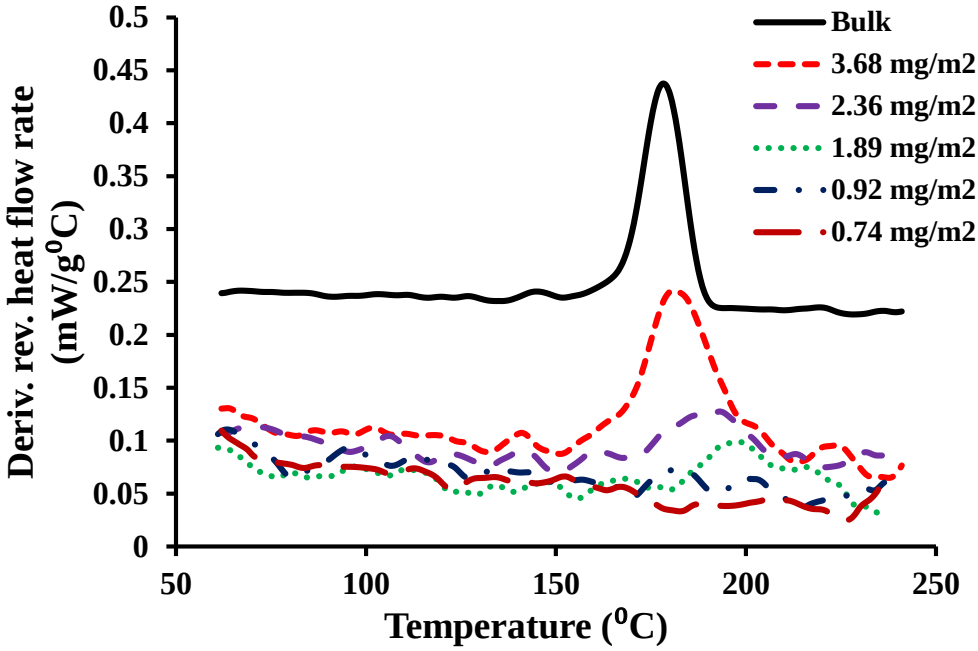

Figure 4. Derivative reversing heat flow rate curves of bulk and adsorbed PVP. The bulk curve has been scaled and vertically offset for clarity.

Discussion

Thermogravimetric analysis of bulk and adsorbed PVP samples showed two-step decompositions for all samples in Figure 1. The first and major decomposition occurred at 410 °C and the second decomposition step occurred at 525 °C. PVP is believed to decompose via the formation of an intermediate complex followed by the release of the pyrrolidone ring.[42] Figure 1 shows that adsorption of PVP onto silica resulted in a

lowering of the temperature of the first decomposition step with the second decomposition step unaffected by adsorption. This behavior could be attributed to a decrease in polymer chain flexibility and an increase in polymer chain strain.[43] This behavior is also in contrast to what has previously been observed for poly(n-alkyl methacrylate) polymers such as PMMA which has shown an increase in decomposition temperature on adsorption. This difference is due to the different mechanisms of decomposition of these polymers. The decrease in decomposition temperature showed that the surface reduces the mobility of the surface.

ATR-FTIR was also used to observe the behavior of PVP on silica. Figure 2 shows the presence of isolated silanol groups on silica; seen as a sharp intense peak at 3750 cm^{-1}. The intensity of this resonance corresponding to isolated silanol groups was seen to decrease drastically for the smallest adsorbed amount sample and to disappear altogether for the larger adsorbed amount samples. This showed that upon adsorption, these isolated silanol groups, present on the surface of fumed silica, were covered. Another area of the FTIR spectrum that was of interest was the carbonyl group region. In this region, for all the adsorbed samples, the presence of a second resonance seen as a shoulder could be seen. Figure 3 shows how the intensities of the resonances of these bound carbonyl groups were seen to increase with decreasing adsorbed amounts. This shows that as the adsorbed amount decreased, the fraction of bound carbonyl groups increased, suggesting that at smaller adsorbed amounts, the polymer was spread out on the silica surface.[32,44] In this type of configuration, at smaller adsorbed amounts, this polymer is significantly restrained.

TMDSC is a characterization technique commonly used to observe the transitions of polymers. The use of this method allows the observation of thermal transitions such as glass transition and melting and how they are affected upon adsorption. A number of studies on PMMA adsorbed on silica, for instance, showed that when PMMA is adsorbed on silica, its glass transition temperature is increased. This indicates that the polymer is less mobile when it is on the surface.[15,35] Figure 4 shows the heat flow curves of PVP in bulk and adsorbed at different amounts on silica. The bulk curve shows that PVP in bulk has a glass transition at 178 °C. From this same figure, it was seen that the smallest adsorbed amount samples did not show any thermal transitions. As the adsorbed amount increased to 1.89 mg/m^2, a glass transition was observed at an elevated temperature of about 200 °C. Larger adsorbed amount samples also showed elevated glass transitions. The largest adsorbed amount sample, showed both the presence of two thermal transitions. One which was very broad and seen at around 200 °C which was designated as 'tightly bound' and another at 183 °C correlating with "loosely bound". These results are in agreement with what has been observed from TGA and ATR-FTIR, which showed that the mobility of PVP was decreased upon adsorption on silica.

Extensive studies have been conducted on other classes of polymers adsorbed onto silica. One such class of polymers are poly(n-alkyl methacrylates) such as poly(methyl methacrylate). It is interesting to note the similarities and differences in behavior between these two polymers upon their adsorption on silica. Like PVP, PMMA adsorbs on silica via hydrogen bonding of the carbonyl groups onto silanol groups on silica. In both instances, adsorption results in increased glass transition temperatures.[35] Both polymers show behavior associated with the presence of tightly bound polymer at

very small adsorbed amounts. However for PVP, this behavior is seen at larger adsorbed amounts. Based on this, the length scale of tightly bound PVP on silica is ~1.89 mg/m2 which is significantly higher than what has been observed for other polymers which have been observed such as PLMA (0.74 mg/m^2)[45], PMMA (1.21 mg/m^2) and PVAc (0.78 mg/m^2).[17]

Conclusion

The effect of adsorption on the thermal behavior of PVP was studied using TMDSC, ATR-FTIR, and TGA. TGA measurements showed that adsorption on silica result in a decrease in the decomposition temperature of PVP. This was attributed to the increase in stiffness of the polymer chains adsorbed on the silica surface. The nature of the interaction between the polymer and the silica surface was confirmed to be hydrogen bonding between the amide carbonyl group and surface silanol groups using ATR-FTIR. This was seen from the disappearance of the isolated silanol peaks and the appearance of resonances corresponding to bound carbonyl groups. Finally, TMDSC showed that upon adsorption, the glass transition of PVP increased. Derivative heat flow curves of adsorbed PVP samples showed the presence of polymer that was ‘tightly bound’ and ‘loosely bound’. The use of these techniques showed that adsorption of PVP on silica resulted in a restriction of mobility of PVP on the silica surface due to the attractive hydrogen bonds between the polymer and surface.

Acknowledgments. The financial support of Oklahoma State University is acknowledged.

References

(1) Kabomo, M. T.; Blum, F. D.; Kulkeratiyut, S.; Kulkeratiyut, S.; Krisanangkura, P. Effects of molecular mass and surface treatment on adsorbed poly(methyl methacrylate) on silica. *J. Polym. Sci., Part B: Polym. Phys.* **2008**, *46*, 649-658.

(2) Alcoutlabi, M.; McKenna, G. B. Effects of confinement on material behaviour at the nanometre size scale. *J. Phys.: Condens. Matter* **2005**, *17*, R461-R524.

(3) Arrighi, V.; McEwen, I. J.; Qian, H.; Prieto, M. B. S. The glass transition and interfacial layer in styrene-butadiene rubber containing silica nanofiller. *Polymer* **2003**, *44*, 6259-6266.

(4) Kirst, K. U.; Kremer, F.; Litvinov, V. M. broad-band dielectric-spectroscopy on the molecular-dynamics of bulk and adsorbed poly(dimethylsiloxane). *Macromolecules* **1993**, *26*, 975-980.

(5) Miwa, Y.; Drews, A. R.; Schlick, S. Detection of the direct effect of clay on polymer dynamics: The case of spin-labeled poly(methyl acrylate)/clay nanocomposites studied by ESR, XRD, and DSC. *Macromolecules* **2006**, *39*, 3304-3311.

(6) Mammeri, F.; Rozes, L.; Le Bourhis, E.; Sanchez, C. Elaboration and mechanical characterization of nanocomposites thin films - Part II. Correlation between structure and mechanical properties of SiO2-PMMA hybrid materials. *J. Europ. Ceram. Soc.* **2006**, *26*, 267-272.

(7) Lee, D. C.; Jang, L. W. Preparation and characterization of PMMA-clay hybrid composite by emulsion polymerization. *J. Appl. Polym. Sci.* **1996**, *61*, 1117-1122.

(8) Vieweg, S.; Unger, R.; Hempel, E.; Donth, E. Kinetic structure of glass transition in polymer interfaces between filler and SBR matrix. *J. Non-Crystal. Solids* **1998**, *235*, 470-475.

(9) Sargsyan, A.; Tonoyan, A.; Davtyan, S.; Schick, C. The amount of immobilized polymer in PMMA SiO(2) nanocomposites determined from calorimetric data. *Eur. Polym. J.* **2007**, *43*, 3113-3127.

(10) Tsagaropoulos, G.; Eisenberg, A. dynamic-mechanical study of the factors affecting the 2 glass-transition behavior of filled polymers - similarities and differences with random ionomers. *Macromolecules* **1995**, *28*, 6067-6077.

(11) Blum, F. D.; Xu, G.; Liang, M.; Wade, C. G. Dynamics of Poly(vinyl acetate) in Bulk and on Silica. *Macromolecules* **1996**, *29*, 8740-8745.

(12) Lin, W.-Y.; Blum, F. D. Segmental Dynamics of Bulk and Adsorbed Poly(methyl acrylate)-d3 by Deuterium NMR: Effect of Adsorbed Amount. *Macromolecules* **1997**, *30*, 5331-5338.

(13) Fryer, D. S.; Peters, R. D.; Kim, E. J.; Tomaszewski, J. E.; de Pablo, J. J.; Nealey, P. F.; White, C. C.; Wu, W. L. Dependence of the glass transition temperature of polymer films on interfacial energy and thickness. *Macromolecules* **2001**, *34*, 5627-5634.

(14) Hartmann, L.; Gorbatschow, W.; Hauwede, J.; Kremer, F. Molecular dynamics in thin films of isotactic poly(methyl methacrylate). *Eur. Phys. J. E* **2002**, *8*, 145-154.

(15) Blum, F. D.; Young, E. N.; Smith, G.; Sitton, O. C. Thermal analysis of adsorbed poly(methyl methacrylate) on silica. *Langmuir* **2006**, *22*, 4741-4744.

(16) Mortazavian, H.; Fennell, C. J.; Blum, F. D. Structure of the Interfacial Region in Adsorbed Poly(vinyl acetate) on Silica. *Macromolecules* **2016**, *49*, 298-307.

(17) Mortazavian, H.; Fennell, C. J.; Blum, F. D. Surface Bonding Is Stronger for Poly(methyl methacrylate) than for Poly(vinyl acetate). *Macromolecules* **2016**, *49*, 4211-4219.

(18) Keddie, J. L.; Jones, R. A. L.; Cory, R. A. interface and surface effects on the glass-transition temperature in thin polymer-films. *Faraday Discuss.* **1994**, *98*, 219-230.

(19) Keddie, J. L.; Jones, R. A. L.; Cory, R. A. Size-Dependent Depression of the Glass Transition Temperature in Polymer Films. *Europhys. Lett.* **1994**, *27*, 59.

(20) Wallace, W. E.; Vanzanten, J. H.; Wu, W. L. influence of an impenetrable interface on a polymer glass-transition temperature. *Phys. Rev. E* **1995**, *52*, R3329-R3332.

(21) Griffin, P. J.; Bocharova, V.; Middleton, L. R.; Composto, R. J.; Clarke, N.; Schweizer, K. S.; Winey, K. I. Influence of the Bound Polymer Layer on Nanoparticle Diffusion in Polymer Melts. *Acs Macro Letters* **2016**, *5*, 1141-1145.

(22) Blum, F. D.; Gandhi, B. C.; Forciniti, D.; Dharani, L. R. Effect of surface segmental mobility on adhesion of acrylic soft adhesives. *Macromolecules* **2005**, *38*, 481-487.

(23) Janes, D. W.; Bilchak, C.; Durning, C. J. Decoupling energetic modifications to diffusion from free volume in polymer/nanoparticle composites. *Soft Matter* **2017**, *13*, 677-685.

(24) Priestley, R. D.; Ellison, C. J.; Broadbelt, L. J.; Torkelson, J. M. Structural Relaxation of Polymer Glasses at Surfaces, Interfaces, and In Between. *Science* **2005**, *309*, 456-459.

(25) Johnson, H. E.; Granick, S. Exchange kinetics between the adsorbed state and free solution: poly(methyl methacrylate) in carbon tetrachloride. *Macromolecules* **1990**, *23*, 3367-3374.

(26) Enriquez, E. P.; Schneider, H. M.; Granick, S. PMMA adsorption over previously adsorbed PS studied by polarized FTIR-ATR. *J. Polym. Sci. Part B:, Polym. Phys.* **1995**, *33*, 2429-2437.

(27) Berquier, J.-M.; Arribart, H. Attenuated total reflection Fourier transform infrared spectroscopy study of poly(methyl methacrylate) adsorption on a silica thin film: polymer/surface interactions. *Langmuir* **1998**, *14*, 3716-3719.

(28) Kulkeratiyut, S.; Kulkeratiyut, S.; Blum, F. D. Bound carbonyls in PMMA adsorbed on silica using transmission FTIR. *J. Polym. Sci. A.; Polym. Phys.* **2006**, *44*, 2071-2078.

(29) Blum, F. D.; Krisanangkura, P. Comparison of differential scanning calorimetry, FTIR, and NMR to measurements of adsorbed polymers. *Thermochim. Acta* **2009**, *492*, 55-60.

(30) Krisanangkura, P.; Packard, A. M.; Burgher, J.; Blum, F. D. Bound fractions of methacrylate polymers adsorbed on silica using FTIR. *J. Polym. Sci., Part B: Polym. Phys.* **2010**, *48*, 1911-1918.

(31) Madathingal, R. R.; Wunder, S. L. Effect of Particle Structure and Surface Chemistry on PMMA Adsorption to Silica Nanoparticles. *Langmuir* **2010**, *26*, 5077-5087.

(32) Fontana, B. J.; Thomas, J. R. The configuration of adsorbed alkyl methacrylate polymers by infrared and sedimentation studies. *J. Phys. Chem.* **1961**, *65*, 480-487.

(33) McBrierty, V.; Packer, K.: *Nuclear Magnetic Resonance in Solid Polymers*; Cambridge University Press: Cambridge, 1993. pp. 202-206.

(34) Porter, C. E.; Blum, F. D. Thermal characterization of PMMA thin films using modulated differential scanning calorimetry. *Macromolecules* **2000**, *33*, 7016-7020.

(35) Khatiwada, B. K.; Hetayothin, B.; Blum, F. D. Thermal properties of PMMA on silica using temperature-modulated differential scanning calorimetry. *Macromol. Symp.* **2013**, *327*, 20-28.

(36) Fleer, G.; Stuart, M. C.; Scheutjens, J.; Cosgrove, T.; Vincent, B.: *Polymers at interfaces*; Chapman & Hall: London, 1993.

(37) Coleman, M. M.; Moskala, E. J. FTIR studies of polymer blends containing the poly(hydroxy ether of bisphenol A) and poly(ε-caprolactone). *Polymer* **1983**, *24*, 251-257.

(38) Parnas, R. S.; Chaimberg, M.; Taepaisitphongse, V.; Cohen, Y. The adsorption of polyvinylpyrrolidone and polyethylene oxide onto chemically modified silica. *J. Colloid Interface Sci.* **1989**, *129*, 441-450.

(39) Cohen Stuart, M. A.; Fleer, G. J.; Bijsterbosch, B. H. The adsorption of poly(vinyl pyrrolidone) onto silica. I. Adsorbed amount. *J. Colloid Interface Sci.* **1982**, *90*, 310-320.

(40) Cohen Stuart, M. A.; Fleer, G. J.; Bijsterbosch, B. H. Adsorption of poly(vinyl pyrrolidone) on silica. II. The fraction of bound segments, measured by a variety of techniques. *J. Colloid Interface Sci.* **1982**, *90*, 321-334.

(41) Kulkeratiyut, S.; Kulkeratiyut, S.; Blum, F. D. Bound carbonyls in PMMA adsorbed on silica using transmission FTIR. *J. Polym. Sci., Part B: Polym. Phys.* **2006**, *44*, 2071-2078.

(42) Carlos, P.; Dionisio, Z.; Mercedes, P.; Senen, P.; Anna, B.; San, R. J. Study of the thermal degradation of poly(N-vinyl-2-pyrrolidone) by thermogravimetry–FTIR. *J. Appl. Polym. Sci.* **1993**, *50*, 485-493.

(43) Bogatyrev, V. M.; Borisenko, N. V.; Pokrovskii, V. A. Thermal Degradation of Polyvinylpyrrolidone on the Surface of Pyrogenic Silica. *Russian Journal of Applied Chemistry* **2001**, *74*, 839-844.

(44) Robb, I. D.; Smith, R. Adsorption of polymers at the solid-liquid interface: a comparison of the e.p.r. and i.r. techniques. *Polymer* **1977**, *18*, 500-504.

(45) Arua, U. N.; Blum, F. D. Disruptions in the crystallinity of poly(lauryl methacrylate) due to adsorption on silica. *J. Polym. Sci., Part B: Polym. Phys.* **2018**, *56*, 89-96.

APPENDICES

APPENDIX A

FULL FTIR-ATR SPECTRA OF SILICA AND ADSORBED PLMA SAMPLES

The full FTIR-ATR spectra of silica and adsorbed PLMA samples are shown in Figure A1 below.

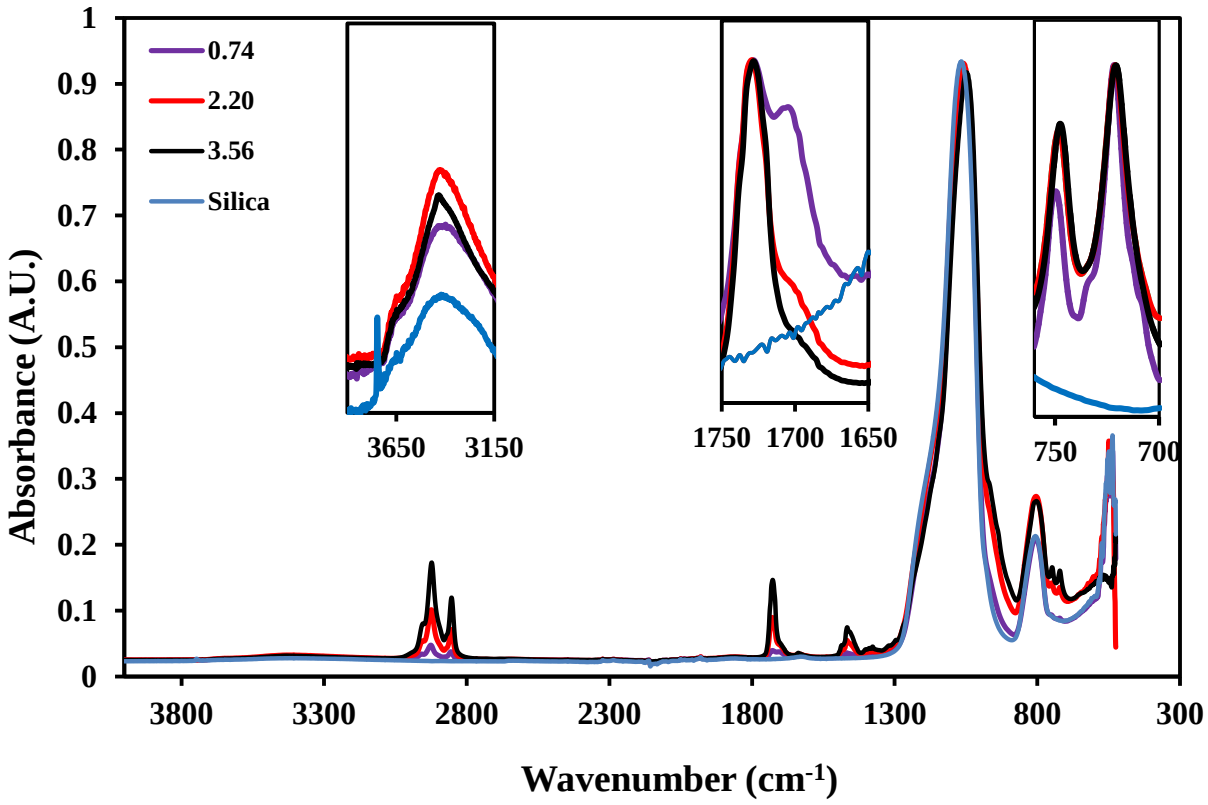

Figure A1: FTIR-ATR spectra of silica and PLMA-silica samples with the main regions of interest (1800-1600 cm^{-1} region (C=O stretching) and 900-700 cm^{-1} region (C_{β}-H out-of-plane bending and $(CH_2)_n$ in-phase rocking)) highlighted for different adsorbed

APPENDIX B

DETERMINATION OF THE RATIO OF THE MOLAR EXTINCTION COEFFICIENTS OF BOUND TO FREE CARBONYLS (*X*)

The *X* value of PLMA was determined using the model developed by Krisanangkura and coworkers.[1]

$$M_t = M_b + \left(A_f / A_b\right) X M_b$$

where M_t is the adsorbed amount of polymer, M_b is the bound amount of polymer, X is molar extinction coefficient ratio of bound to free carbonyls, A_f is the intensity of the free carbonyl band, and A_b is that of the bound carbonyl band. It should be noted that M_b is a hypothetical amount of polymer which would be needed to cover all of the surface silanols.

It was determined using ATR-FTIR for the quantitative determination of the bound fraction of carbonyls in PLMA. A plot of adsorbed amount (M_t) was plotted against the ratio of resonance intensity of free and bound carbonyl (A_f/A_b) and is shown in Figure S2.

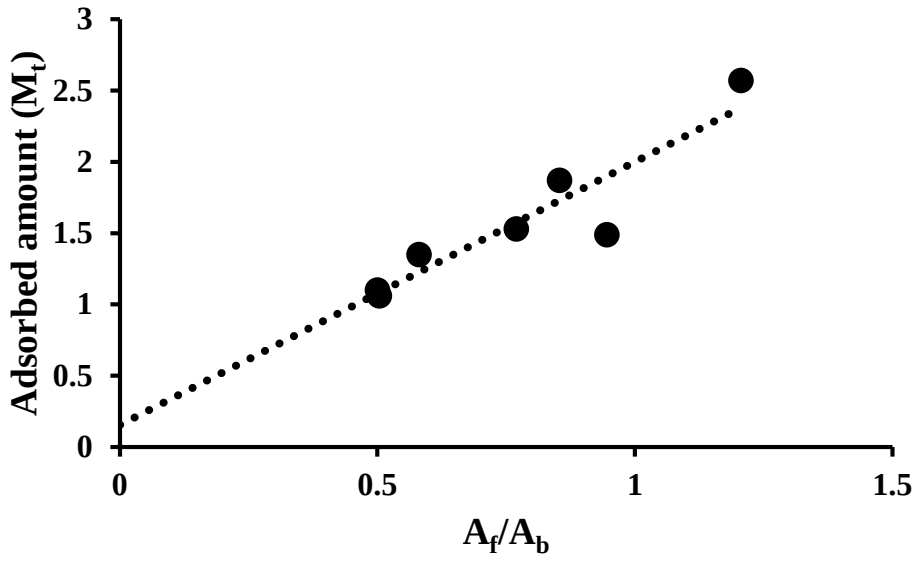

Figure B1. Plot of adsorbed amount of polymer (M_t) versus the ratios of the resonance intensities of free to bound carbonyls (A_f/A_b) based on the equation 1 above.[2]

From the above plot, and using the linear relationship above, the *X* value was found to be 11.9 ± 2.0 which was close to the value, previously reported (11.1 ± 2.9). It is interesting to note that the value of *X* for this system is the same for transmission and ATR experiments. Similarly, the value of M_b was found to be 0.174 which was close to previously reported value of 0.213 ± 0.055.

References

(1) Kulkeratiyut, S.; Kulkeratiyut, S.; Blum, F. D. Bound carbonyls in PMMA adsorbed on silica using transmission FTIR. *J. Polym. Sci., Part B: Polym. Phys.* **2006**, *44*, 2071-2078.

(2) Krisanangkura, P.; Packard, A. M.; Burgher, J.; Blum, F. D. Bound fractions of methacrylate polymers adsorbed on silica using FTIR. *J. Polym. Sci., Part B: Polym. Phys.* **2010**, *48*, 1911-1918.

APPENDIX C

HEAT FLOW CURVES SHOWING SUPER-COOLING OF BULK AND ADSORBED PLMA SAMPLES

The cooling and second heating cycles of the bulk and adsorbed polymers are shown in Figure C3. These plots show the super-cooling of adsorbed and bulk PLMA.

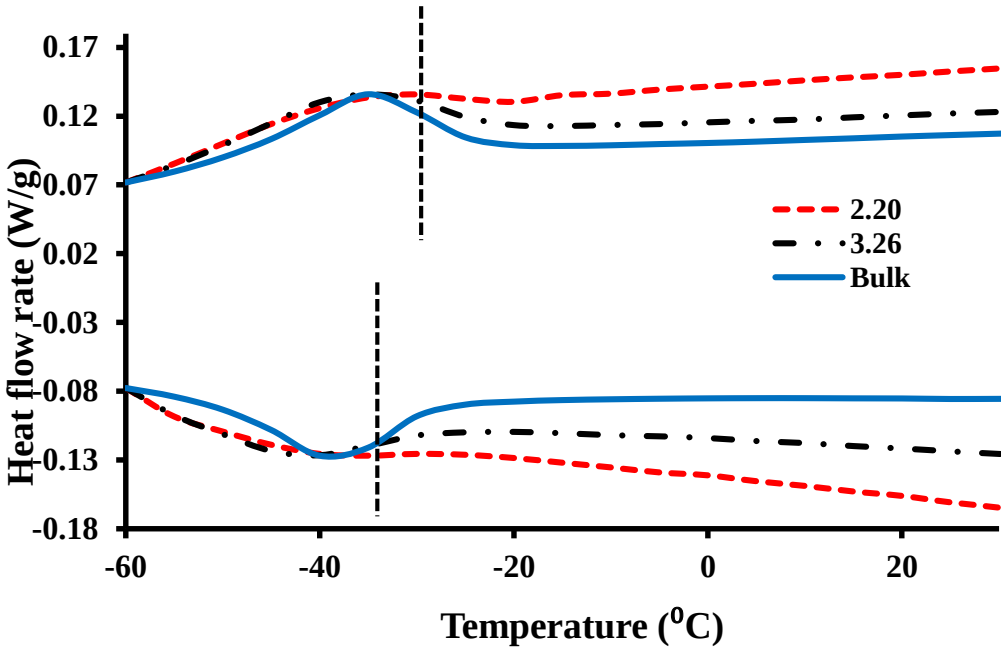

Figure C1. Heat flow curves of heating and cooling cycles of adsorbed and bulk PLMA samples (mg/m^2) showing super-cooling. The plots have been offset for clarity and the labels refer to adsorbed amounts in mg/m^2.

APPENDIX D

MATLAB CODES USED FOR THE FITTING OF SOLID STATE ^{2}H-NMR LINE SHAPES

Simulated ^{2}H-NMR line shapes were obtained with the EXPRESS program using the soccer ball model. The spectra were simulated at different jump rates. The experimental solid state ^{2}H-NMR spectra were fitted using the aforementioned simulated line shapes using MATLAB (v. 2016a). Some of the line shapes used in the fittings are shown in Figure D1 below. The codes used in MATLAB were obtained from the literature are also shown below.[1]

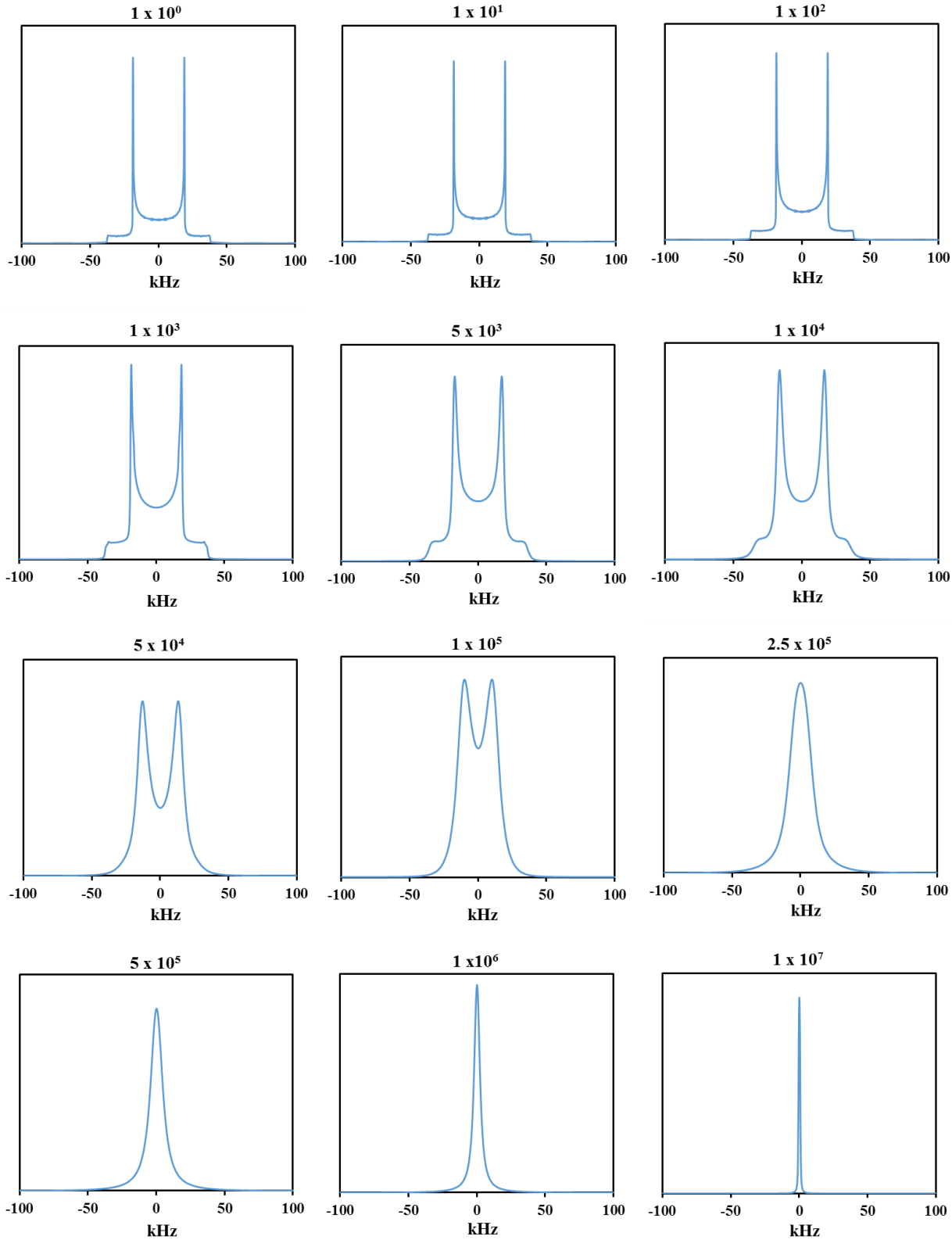
1 x 10⁰
1 x 10¹
1 x 10²
1 x 10³
5 x 10³
1 x 10⁴
5 x 10⁴
1 x 10⁵
2.5 x 10⁵
5 x 10⁵
1 x10⁶
1 x 10⁷
-100
-50
0
50
100
kHz

Figure D1. Simulated ^{2}H-NMR as a function of jump rates using the soccer ball model.

main

```
function [ ] = main( expFile, outputFile )
clearvars -except expFile outputFile
clc


tmp=ls('data/*.txt');
%tmp=dir('dat/*.txt');
%tmp=char(tmp.name);
tmp=strcat('./data/',tmp(:,:));

% Get a list of files in the data directory, and attempt to match them
to
% the experiment file provided. The result will be the best fit, a
value
% for the deviation of this fit, and a jpg file will be created which
% contains an image of the fit and the weights involved to get this
fit.


[hist, histDev] = getResult(cellstr(tmp), expFile, false, outputFile);

sketch_graph(outputFile);
```

getResult

```
function [ hist, histDev ] = getResult( dataList, expFile, displayMe,
outputFile )

% First, collect the data from the input files in dataList. Use the
% my_interp function to interpolate the data over the data
range,ensuring
% there is a value for each element in the range (currently -250 to
250).
% At the end of this loop, data is an array of dat, each of which
contains
% the full range of data.
dataRange=-150:150;
data(1).dat=[];
[data(1:length(dataList)).dat]=deal([]);
for i=1:length(dataList)
      tmp=load(char(dataList(i)));
    data(i).dat=my_interp(tmp(:,1), tmp(:,2), dataRange);
```

```
end

dataNum=length(data);

% Load and normalize the Experimental data from expFile. We sort the
% dataset by the second column, and reduce the whole array to a range
of 0
% to 1. We then interpolate the data to get a full range of -250 to 250
% and nothing else.

expB=load(expFile);
[B,idx] = sort(expB(:,2));
expB=expB(idx, :);
expB=[expB(:,1)/max(expB(:,1)), expB(:,2)];
expB=my_interp(expB(:,1),expB(:,2),dataRange);
% Starting weights are set to normalize the data sets. The weight array
% contains a weight value for each dataset, plus an additional weight
which
% will apply to all of them (similar to normalization)

weight(1:dataNum+1)=1;
for i=1:dataNum
    data(i).dat=data(i).dat./(max(data(i).dat(:)-min(data(i).dat(:))));
end
weight(1:dataNum)=1;
weight(end+1)=1/dataNum;

% Find what the starting deviation is, and set the default values.
Other
% variables used later will be initialized.

summed(1:length(dataRange))=0;
for i=1:length(dataRange)
    for j=1:dataNum
        summed(i)=summed(i)+data(j).dat(i)/weight(j);
    end
end

summed(:)=summed(:)*weight(end);
histDev=sum((summed-expB).^2);

run=1;
changeby=8;
runCnt=1;
arch=weight;
upDown=0;
upDownHist=0;

while true
    % The variable weight will be applied to the dataset. It starts
from
    % the previous 'best' weight (contained in arch), then changes one
of
    % the weights (increasing or decreasing it.
```

```
    weight=arch;
    if run<=length(weight)
        weight(run) = weight(run)*(changeby);
    else
        weight(run-length(weight)) = weight(run-
length(weight))/(changeby);

    end

    % Calculate the sum of the various datasets times their weights...
    summed(1:length(dataRange))=0;
    for i=1:length(dataRange)
        for j=1:dataNum
            summed(i)=summed(i)+data(j).dat(i)*weight(j);
        end
    end
    summed(:)=summed(:)*weight(end);

    % Determine if the deviation can be improved by raising or lowering
the
    % dataset,
    dev=.0005;

    upDown=upDownHist;
    bestDev=sum((summed-(expB+upDown)).^2);
    upDev=sum((summed-(expB+upDown+dev)).^2);

    if upDev < bestDev
        while upDev < bestDev
            bestDev=upDev;
            upDown=upDown+dev;
            upDev = sum((summed-(expB+upDown+dev)).^2);
        end
    else
        downDev=sum((summed-(expB+(upDown-dev))).^2);
        if downDev < bestDev
            while downDev < bestDev
                bestDev=downDev;
                upDown=upDown-dev;
                downDev = sum((summed-(expB+upDown-dev)).^2);
            end
        end
    end

    % Compare the new Deviation value to the best of previous deviation
    % values.
    newDev = bestDev;
    if newDev < histDev && histDev/newDev>1.000001
        % If the new deviation is better (by more than .0001%), make
this
        % deviation the best, and change the archived weights to suit.
        hist=summed;
        arch=weight;
        upDownHist=upDown;
        histDev=newDev;
```

```
        % Some users prefer to watch the deviations change to closely
match
        % the experiments. If the displayMe parameter is on, display
the
        % new best (will slow the experiment down!)
        if displayMe
            figure(2);
            %plot(dataRange, summed, dataRange, expB+upDown);
        end
        % Try to determine if changeing the next weight will improve
the
        % program.
        run=mod(run, 2*length(weight))+1;

        % runCnt is the number of iterations which have been performed
        % without showing an improvement. Reset this to 0 when there is
an
        % improvement.
        runCnt=0;
    elseif runCnt < 2*length(weight)+1
        % If there are no improvements and the program has not gone
through
        % tried to raise or lower all weights without improvement, then
        % just try to change the next weight and increment the number
of
        % null improvements.
        run=mod(run, 2*length(weight))+1;
        runCnt=runCnt+1;
    elseif changeby > 1.000002
        % If we have no improvements in a full sweep of possible
changes to
        % the program, try to change the weights by a smaller amount
(fine
        % tuning the result) to get a more exact answer. Continue this
        % until we are only changein the weights by .0002%.
        changeby=(changeby-1)*.8+1;
        runCnt=0;
    else
        % If there are no improvements and the weights are pretty
finely
        % tuned, time to quit the program.
        break
    end
end

% The following displays the results in two graphs. The top graph will
% compare the optimized fit, and the bottim will show the weights
attached
% to each dataset. The result is saved to a file specified by the user
% (preferably a .jpg file), and then closed.
clf;
figure('Visible','off');
subplot(2,1,1);
% First, plot the experimental results along with the resulting 'best
fit'
experimentalData =  expB+upDownHist;
```

```
plot(dataRange, hist, dataRange,experimentalData);

set(gca, 'YTickLabel','');
subplot(2,1,2);

T = table(dataRange',hist',experimentalData',...
    'VariableNames',...
    {'DataRange','Fit','ExperimentalData'});

writetable(T,strcat(outputFile, '.xlsx'),'Sheet',1,'Range','A1')

arch(end)=[];
groupList=[];
agg=[];

%Variables defiens for the

length_DataList = length(dataList);
average_DataListLength =length_DataList+1;

filenames = cell(average_DataListLength,1);
filenameValues = cell(average_DataListLength,1);
filenameAmount = cell(average_DataListLength,1);

slowAmounts = cell(average_DataListLength,1);
intermediateAmounts = cell(average_DataListLength,1);
fastAmounts = cell(average_DataListLength,1);

sumFileNameValue=0;
sumFileNameAmountValue=0;
sumSlow=0;
sumIntermediate=0;
sumFast=0;

% The following is dataset specific solution. The input files were a
list
% of files followed by the magnitude - fast3E+8.txt. To group the
results
% by their magnitude, the magnitude was found (based on the filename -
% fast3E+8 becomes 8), then the result was added to the aggregate data.
% This result was then plotted. Future users of this program will want
to
% modify or remove the following aggregation code.
for i=1:length_DataList

    dataChar=char(dataList(i));


tmp=str2double(dataChar(find(dataChar=='+')+1:find(dataChar=='.',1,'las
t')-1));

    fileweight = arch(i);
```

```
    if ~ismember(tmp, groupList)
        groupList(end+1)=tmp;
        agg(end+1)= fileweight
    else
        ix=find(groupList==tmp);
        agg(ix)=agg(ix)+fileweight;
    end

    [pathstr,filename,ext] = fileparts(dataChar);

    filenames{i}=filename;
    theoriticalAmount = str2double(filename);
    filenameValues{i}=theoriticalAmount;
    sumFileNameValue = sumFileNameValue+ theoriticalAmount;

    filenameAmount{i} =fileweight;
    sumFileNameAmountValue =sumFileNameAmountValue+ fileweight;

    if (1 <= theoriticalAmount) && (theoriticalAmount <= 10000)
        slowAmounts{i} =  fileweight;
        sumSlow = sumSlow+ fileweight;
    elseif (10001 <= theoriticalAmount) && (theoriticalAmount <=
1000000)
        intermediateAmounts{i} =  fileweight;
        sumIntermediate = sumIntermediate+ fileweight;
    else (1000001 < theoriticalAmount)
        fastAmounts{i} =  fileweight;
        sumFast = sumFast+ fileweight;
    end
end


filenameValues{average_DataListLength}=sumFileNameValue;
filenameAmount{average_DataListLength}=sumFileNameAmountValue;

slowAmounts{average_DataListLength} = sumSlow;
intermediateAmounts{average_DataListLength} = sumIntermediate;
fastAmounts{average_DataListLength} = sumFast;

Tablex =
table(filenameValues,filenameAmount,slowAmounts,intermediateAmounts,fas
tAmounts,...
    'VariableNames',...
    {'File','Value','Slow','Intermediate','Fast'});

Tabley = sortrows(Tablex,'File');

writetable(Tabley,strcat(outputFile, '.xlsx'),'Sheet',2,'Range','A1');


% Generating bar graph
```

```
bar(groupList,agg/sum(agg));

yaxisval= agg/sum(agg);

for i1=1:numel(yaxisval)
    text(groupList(i1),yaxisval(i1),num2str(yaxisval(i1),'%0.2f'),...
        'HorizontalAlignment','center',...
        'VerticalAlignment','bottom')
end
set(gca, 'YTickLabel','');

% Save the figure, then close open figures.
saveas(gca,   strcat(outputFile, '.jpg'));

close all
end
```

my_interp

```
function [ vals ] = my_interp( dataY, dataX, range )
%This function will fit dataY and dataX together to a range specified
by
%the input. The program will distribute dataY and dataX on a
scatterplot,
%then interpolate what the values of this scatterplot are at every
element
%in range. It does this by, for every element in range, finds the dataX
%elements immediatly before and after, then plots a straight line
between
%the dataY elements here to find what dataY is at the range position.
The
%goal is to simplify the datasets, ensuring that an element is
available
%for every position in the range, and extraneous data elements are
removed.

vals(1:length(range))=0;
[dataX, ix]=sort(dataX);
dataY=dataY(ix);
for i=1:length(vals)
    a=find(dataX<=range(i), 1, 'last' );
    b=find(dataX>range(i), 1);
    if(isempty(a))
        vals(i)=dataY(b);
elseif isempty(b)
        vals(i)=dataY(a);
    else
        ratio=( range(i)-dataX(a) ) / ( dataX(b)-dataX(a) );
        vals(i)=dataY(a)+ratio*(dataY(b)-dataY(a));
    end
end
```

sketch_graph

```
function [ ] = sketch_graph(outputFile)

    Excel = actxserver('Excel.Application');

    % Make the Excel File Visible
    set(Excel,'Visible',1);

    filename =strcat('\' , outputFile, '.xlsx');

    ResultFile = [pwd filename];

    %ResultFile = [pwd '\tmyfile.xlsx'];
    Workbook = invoke(Excel.Workbooks,'Open', ResultFile);

    resultsheet = 'Sheet1';
    try
        sheet = get(Excel.Worksheets,'Item', resultsheet);
        invoke(sheet, 'Activate');
    catch
        % If the Excel Sheet 'ExperimentSheet' is not found, throw an
error message
        errordlg([resultsheet 'not found']);
    end

    Chart = Excel.ActiveSheet.Shapes.AddChart2; %
ActiveSheet.Shapes.AddChart.Select
    %Let us Rename this chart to 'ExperimentChart'
    Chart.Name = 'ExperimentChart';

    %% Delete Default Entries
    % Let us delete all the entries in the chart generated by defalut

    ExpChart = Excel.ActiveSheet.ChartObjects('ExperimentChart');
    ExpChart.Activate;
    try
        Series = invoke(Excel.ActiveChart,'SeriesCollection',1);
        invoke(Series,'Delete');
        Series = invoke(Excel.ActiveChart,'SeriesCollection',1);
        invoke(Series,'Delete');
        Series = invoke(Excel.ActiveChart,'SeriesCollection',1);
        invoke(Series,'Delete');
    catch e
    end

    %We are left with an empty chart now.
    %Insert a Chart for Column B
    NewSeries = invoke(Excel.ActiveChart.SeriesCollection,'NewSeries');
```

```
    NewSeries.XValues = ['=' resultsheet '!A' int2str(2) ':A'
int2str(302)];
    NewSeries.Values  = ['=' resultsheet '!B' int2str(2) ':B'
int2str(302)];
    NewSeries.Name    = ['=' resultsheet '!B' int2str(1) ];

    NewSeries = invoke(Excel.ActiveChart.SeriesCollection,'NewSeries');
    NewSeries.XValues = ['=' resultsheet '!A' int2str(2) ':A'
int2str(302)];
    NewSeries.Values  = ['=' resultsheet '!C' int2str(2) ':C'
int2str(302)];
    NewSeries.Name    = ['=' resultsheet '!C' int2str(1) ];

    Excel.ActiveChart.ChartType = 'xlXYScatterLinesNoMarkers';

    %% Set the Axes

    % Set the x-axis
    Axes = invoke(Excel.ActiveChart,'Axes',1);
    set(Axes,'HasTitle',1);
    set(Axes.AxisTitle,'Caption','Data Range')

    %Give the Chart a title
    Excel.ActiveChart.HasTitle = 1;
    Excel.ActiveChart.ChartTitle.Characters.Text = 'Curve Fitting';


    %% Chart Placement
    Location  =  [  'F' int2str(2)  ];
    GetPlacement = get(Excel.ActiveSheet,'Range', Location);

    % Resize the Chart

    ExpChart.Width = 400;
    ExpChart.Height= 250;
    ExpChart.Left  = GetPlacement.Left;
    ExpChart.Top   = GetPlacement.Top;

    %% Save the Excel File

    invoke(Excel.ActiveWorkbook,'Save');
    Excel.Quit
    Excel.delete
    clear Excel

   \
```

Reference

(1) Hetayothin, B. Effect of structure and plasticizer on the glass transition of adsorbed polymer. Missouri University of Science and Technology, 2010.

APPENDIX E

GEL PERMEATION CHROMATOGRAPHS OF SYNTHESIZED PMMA

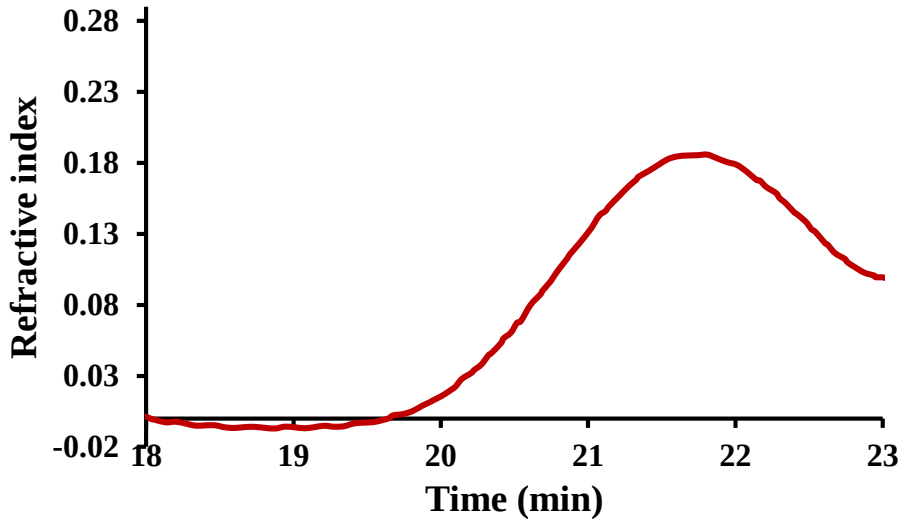

Figure E1. GPC chromatograph of synthesized PMMA sample P1 (4.99 kg/mol)

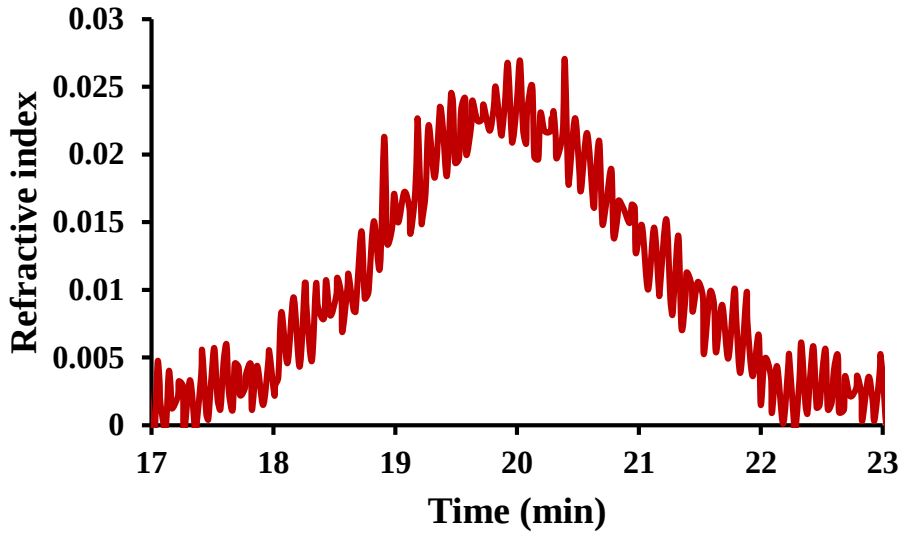

Figure E2. GPC chromatograph of synthesized PMMA sample P2 (20.4 kg/mol)

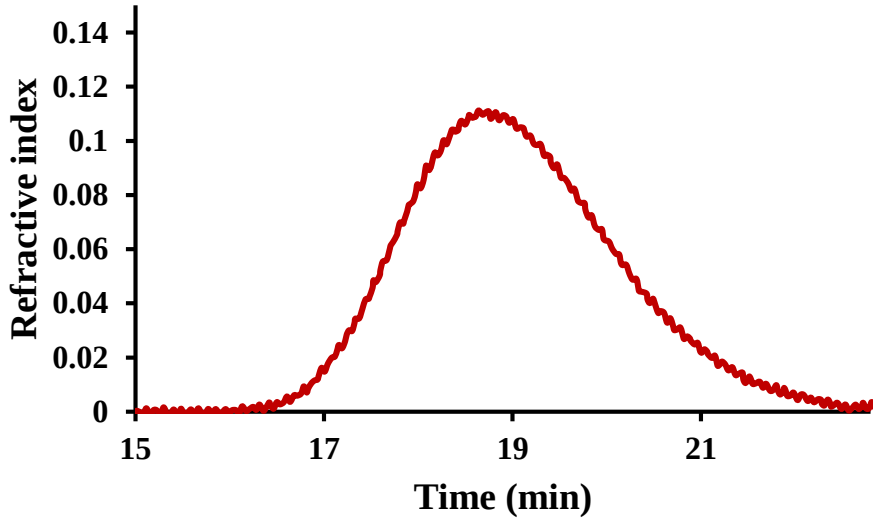

Figure E3. GPC chromatograph of synthesized PMMA sample P3 (38.8 kg/mol)

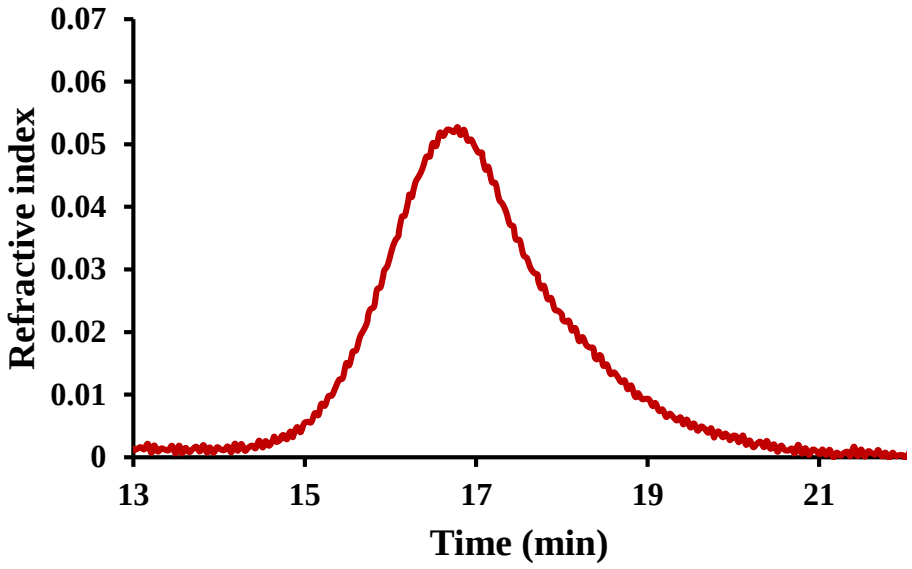

Figure E4. GPC chromatograph of synthesized PMMA sample P4 (181 kg/mol)

Table E1. Summary of molecular masses of synthesized PMMA

Sample	Number average M_n (g/mol)	Weight average M_w (g/mol)	Polydispersity index
P1	4994	7743	1.55
P2	20392	39894	1.96
P3	38747	81259	2.10
P4	181000	395000	2.18

APPENDIX F

^{1}H-NMR SPECTRA OF SYNTHESIZED PMMA

The tacticities of the polymers synthesized were determined using ^{1}H-NMR spectroscopy.

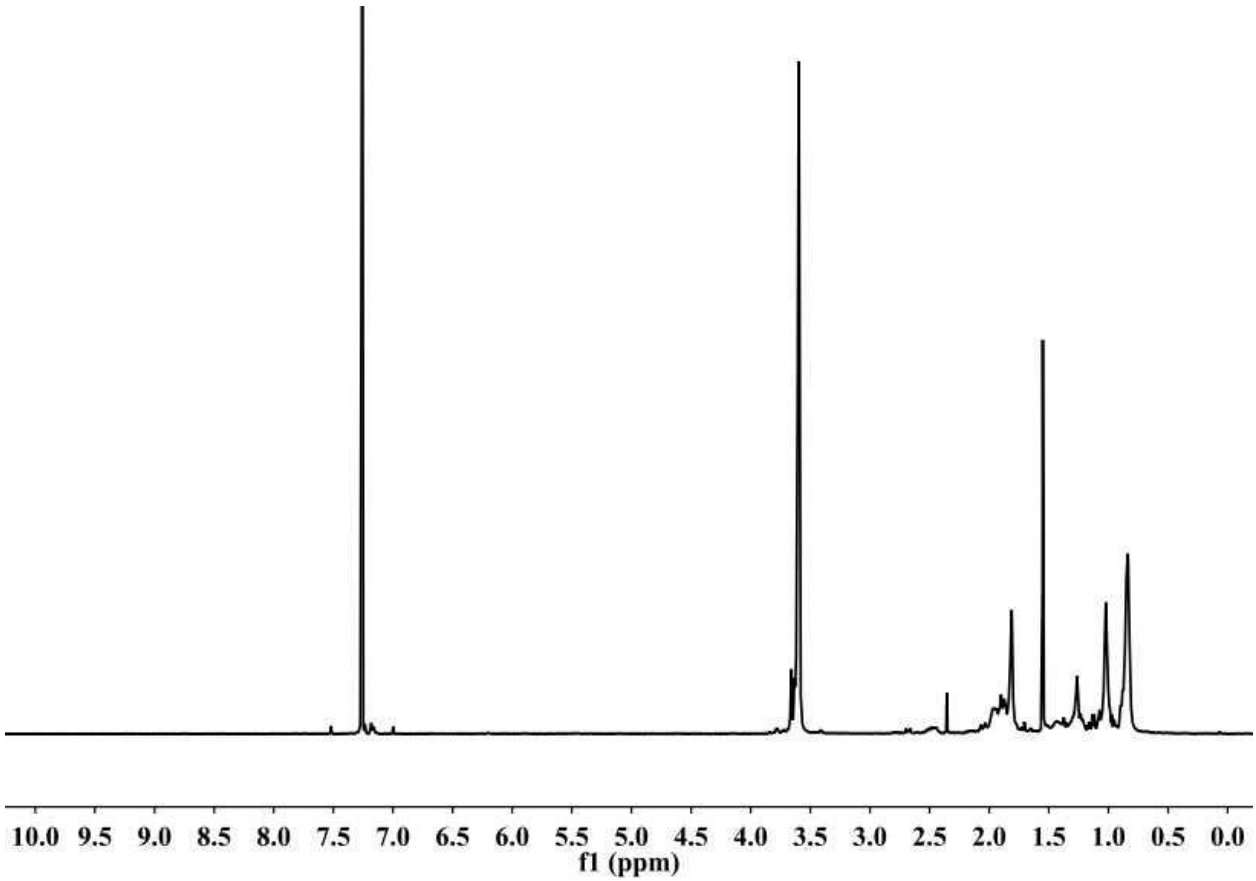

Figure F1. ^{1}H-NMR spectrum of sample **P1** (4.99 kg/mol) in $CDCl_3$.

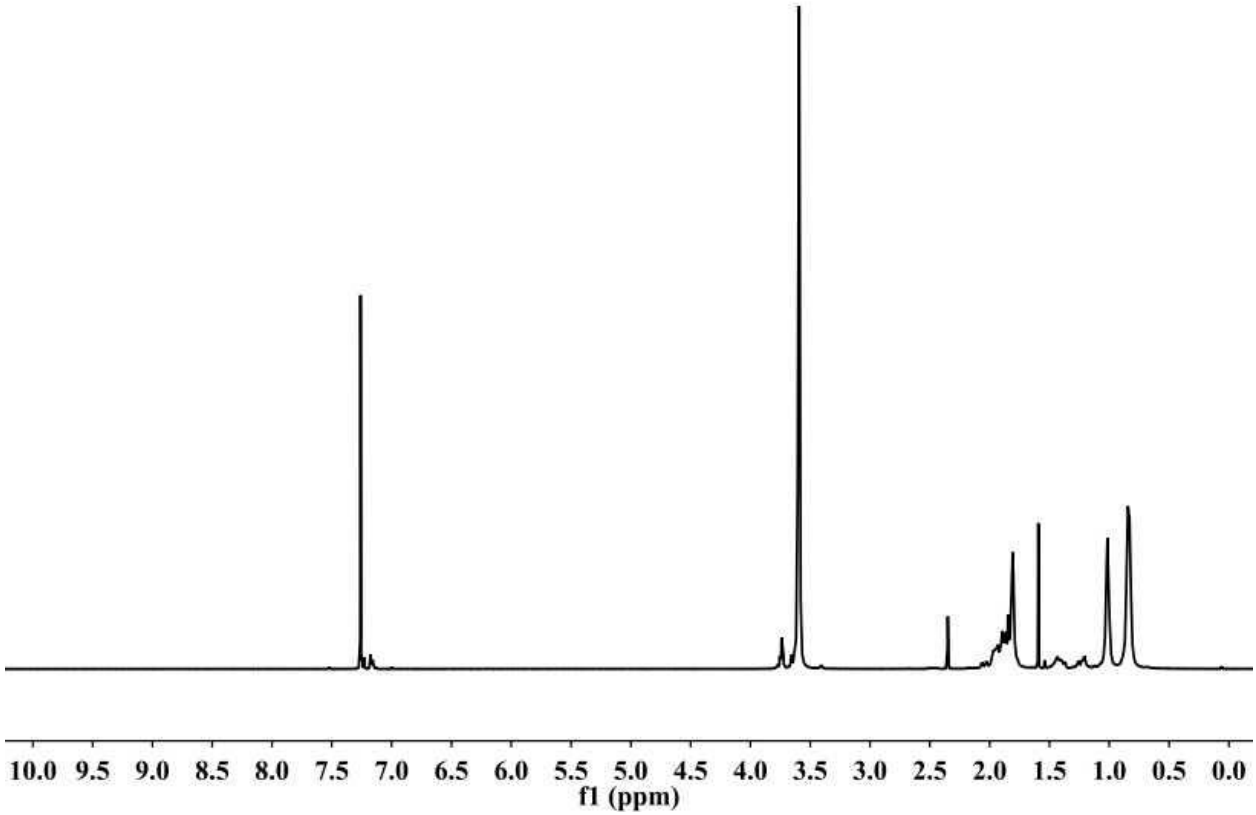

Figure F2. ^{1}H-NMR spectrum of sample **P2** (20.4 kg/mol) in $CDCl_3$.

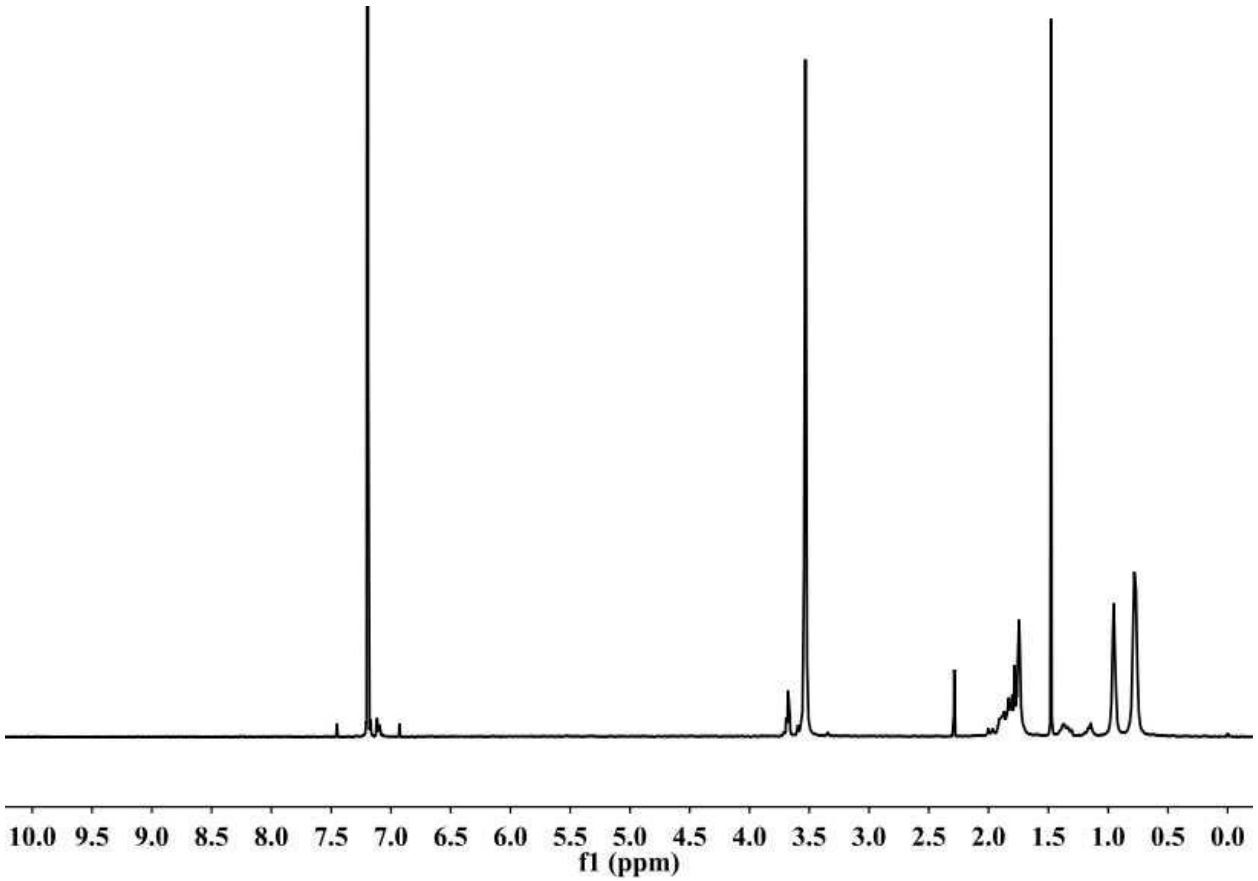

Figure F3. ^{1}H-NMR spectrum of sample **P3** (38.8 kg/mol) in $CDCl_3$.

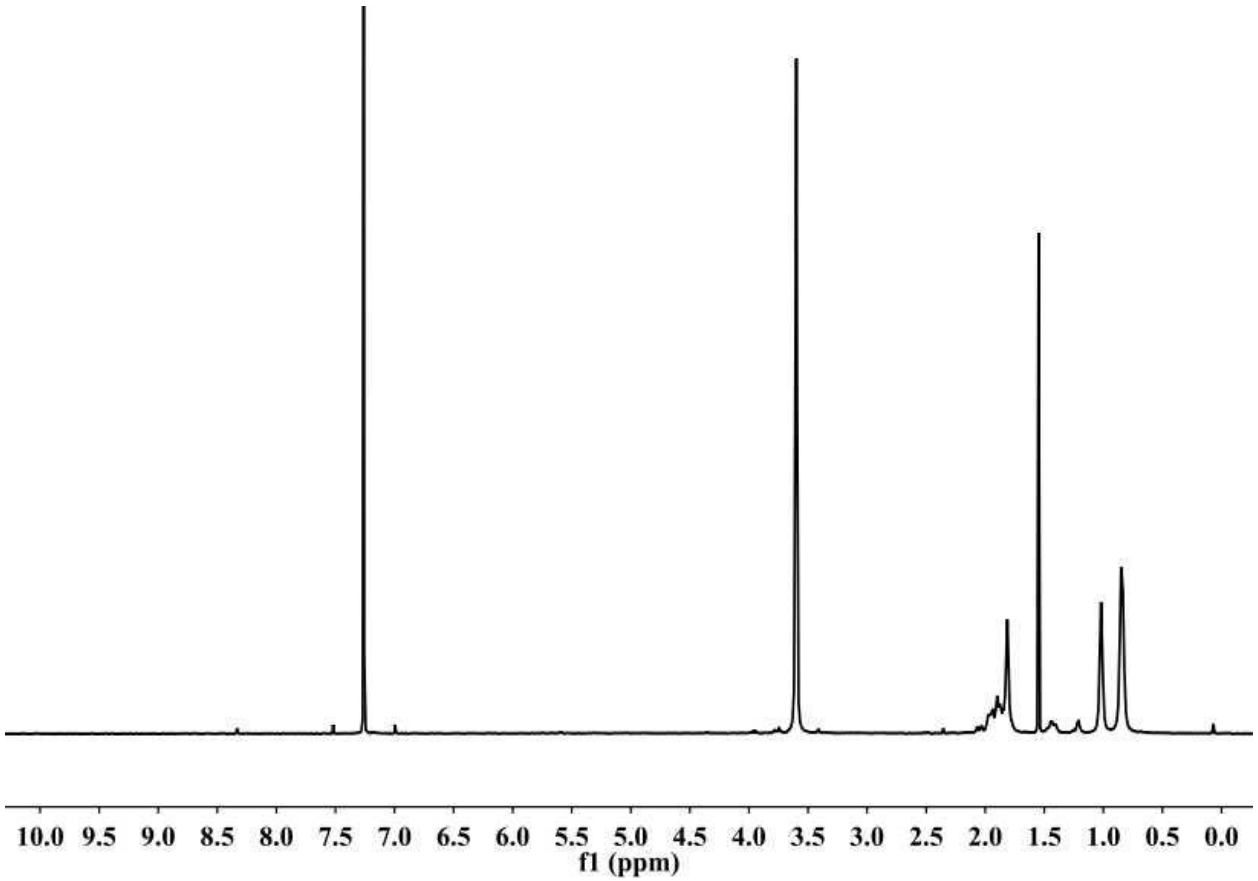

Figure F4. ^{1}H-NMR spectrum of sample **P4** (181 kg/mol) in $CDCl_3$.

APPENDIX G

EFFECT OF WATER ON THE BEHAVIOR OF PVP ADSORBED ON SILICA

PVP is a very hygroscopic polymer. Under normal lab conditions, it can absorb up to 10% of its mass in moisture. The presence of water at these high amounts has a large effect on the measurements made on PVP. One example of where water has the biggest impact is in FTIR-ATR measurements. This is illustrated in the figures below.

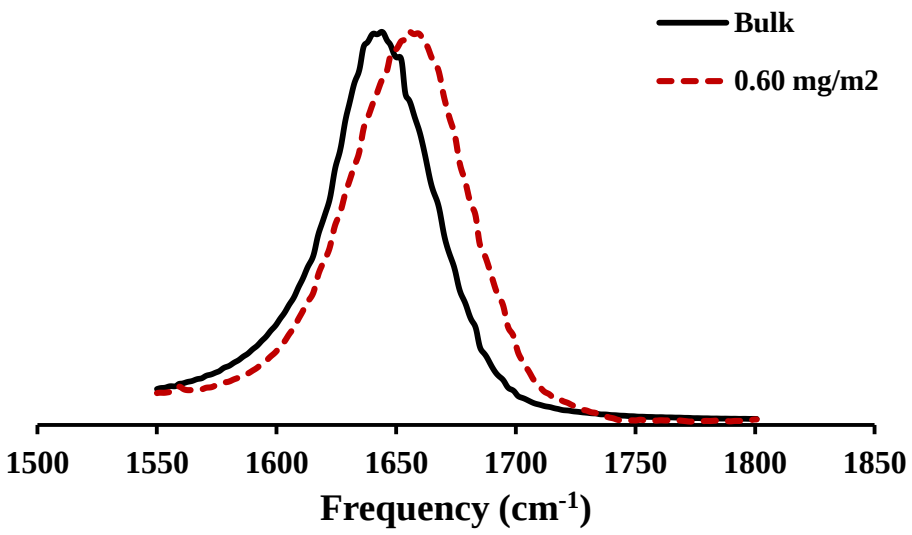

Figure G1. FTIR-ATR spectra of bulk PVP and PVP adsorbed on silica (at 0.76 mg/m^2) before drying

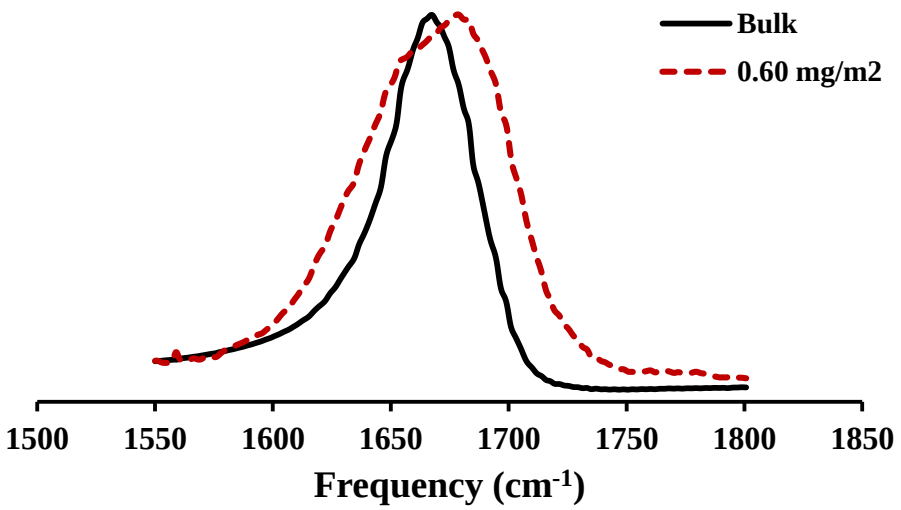

Figure G2. FTIR-ATR spectra of bulk PVP and PVP adsorbed on silica (at 0.76 mg/m^2) after drying.

The difference between the two figures shows the effect of drying on FTIR measurements. Prior to drying adsorption resulted in only a slight shift of the frequency of the carbonyl peak. After drying, a clear shoulder was observed for the adsorbed polymer sample. This showed the presence of bound carbonyl groups similar to what has been observed for the n-alkyl methacrylate polymers.

VITA

Ugo Nnenna Arua

Candidate for the Degree of

Doctor of Philosophy

Thesis: THE STRUCTURE AND DYNAMICS OF POLYMERS ADSORBED ONTO SILICA

Major Field: Chemistry

Biographical:

Education:

Completed the requirements for the Doctor of Philosophy in Chemistry at Oklahoma State University, Stillwater, Oklahoma in July, 2018.

Completed the requirements for the Bachelor of Science in Chemistry at the University of Botswana, Gaborone, Botswana in 2010.

Experience:

Instructor for CHEM 1014, Department of Chemistry, Oklahoma State University, Stillwater, Oklahoma, 2018.

Teaching and research assistant, Department of Chemistry, Stillwater, Oklahoma State University, Stillwater, Oklahoma, 2012 – 2017.

Professional Memberships:

American Chemistry Society